Durham E-Theses

Diffraction dissociation in elementary particle reactions

P. J. Walters

DIFFRACTION DISSOCIATION IN

ELEMENTARY PARTICLE REACTIONS

$P = \frac{1}{2}(p + p')$

$\Delta = (p - p')$

FIG 49

FIG 50

DIFFRACTION DISSOCIATION IN
ELEMENTARY PARTICLE REACTIONS

THESIS SUBMITTED TO

THE UNIVERSITY OF DURHAM

BY

PATRICK J. WALTERS, B.Sc. (DURHAM)

FOR THE DEGREE OF DOCTOR OF PHILOSOPHY

DEPARTMENT OF PHYSICS

DURHAM UNIVERSITY

DATE: MARCH 1974

CONTENTS

Acknowledgement

I would like to thank Fred Gault for invaluable help and advice at all stages of this work and also for collaboration on various aspects of it. My thanks also to Alison Thomson for collaboration on the quark model work and also for many helpful suggestions.

The support of an S.R.C. research studentship is also acknowledged.

Abstract

We extend the results for asymptotic s-channel vertices in terms of covariant couplings to high spin fermion and boson production. The formalism is applied to diffraction, considered as proceeding by pomeron exchange. It is found that the pomeron couples in a similar manner to a vector object. In particular the hypothesis is made that the pomeron coupling to the $N \rightarrow N^*$ vertex is γ_β. This is supported by fits to the $N \rightarrow N^*$ ($\frac{3}{2}^-$, 1520; $\frac{5}{2}^+$, 1688) data. The behaviour of the pomeron as a vector object is understood in the quark model and it is seen that most of the fermion data can be described in an $SU(6)_W$ quark model. The breakdown of the approach for boson diffraction dissociation is noted, as spin orbit terms are needed to reproduce the data.

A relativistic quark model is presented for mesons with spin $\frac{1}{2}$ quarks which is closely related to the non-relativistic harmonic oscillator model. The conventional quark model spectrum is reproduced with particles lying on straight Regge trajectories, although the masses predicted for the PC = +| states are large. The most interesting feature of the wave-functions is the natural inclusion of spin-orbit terms which is suggestive of the "current" quark approach. The comparison of the model predictions with the data is encouraging and they include meson decay widths for emission of a pseudoscalar or a photon. Diffraction dissociation is also considered in the model and the

inclusion of spin-orbit interaction rectifies some of the difficulties of the $SU(6)_W$ model applied to meson dissociation.

1. A survey of some topics related to diffraction scattering and quark models

1.1 Introduction

The aim of this chapter is to survey some of the background material to diffraction scattering and quark models, which are the main subjects of this thesis.

Diffraction scattering exists in particle physics in analogy to optical diffraction because particles have wave properties. Just as in the optical case, the main features of the scattering may be deduced without invoking any detailed dynamics. For instance, if the notion of diffraction is to have any meaning, it must be possible to relate the total cross-section and the diffractive slope. Also simple arguments predict which states may be produced diffractively as well as the helicity structure of the amplitudes. Finally the observation of approximate energy independence for diffractive cross-sections is easily made plausible in this view.

It might be expected that the above predictions, which are in impressive agreement with data, would emerge as a matter of course from more sophisticated theories, but this is not the case. The characteristic procedure of present dynamical, but nevertheless partial theories, is to relate diffraction to other processes without automatically incorporating any physical concept of diffraction. Most notable in this respect is Regge

theory where diffraction is unhappily united with particle exchange processes. Clearly the correct method is to build up the diffractive amplitude from models of the inelastic production processes. This is the procedure of the multiperipheral class of models, however the approximation scheme is unrealistic. The most promising approach is the vector meson field theory of Cheng and Wu and it is interesting that it is this theory which is most closely related to the naive diffraction picture.

Given the hypothesis that hadrons are built up from three basic constituents, the quarks, then the SU(3), spin, parity and G parity spectrum of hadrons is reproduced. This success is made all the more incredible by the fact that no free quarks have ever been observed. It is still possible to hope that quarks exist but have very high masses, certainly larger than 4 GeV, but even this is unlikely because one of the quarks is stable and so should be detected in cosmic rays if quarks can be produced at all. Consequently quarks must be considered in some way inseparable from hadrons and at least in this sense fictitious.

Presumable quark model results will emerge from some future bootstrap scheme, but in the meantime the quark model may be used to abstract results, without of course extracting so much as to imply physical quarks. The most magnificent success of this approach is the Gell-Mann current commutation relations

and the associated chiral $SU(3) \otimes SU(3)$ charge algebra.

It is interesting to spectulate on which bootstrap scheme is likely to accommodate the quark model results. The basic bootstrap idea is to assume that there exists a unique set of particles, the physical ones, which are consistent with unitarity, analyticity, Lorentz invariance and crossing. The conventional approach to this hypothesis is to consider a limited sector of the particle spectrum and attempt, iteratively to produce consistency. Clearly any finite scheme like this is inadequate because of the large and probably infinite numbers of particles in the actual spectrum, all of which are in some sense equally significant. The only reasonable way of including democracy is to assume all the particles from the beginning in some approximation to the physical spectrum and to test whether a solution of this form can be built consistent with the general principles. This is the approach of the dual models where the first approximation is to treat all particles as stable, or equivalently to postulate straight Regge trajectories. With this assumption a finite set of models, the dual models, can be constructed satisfying all the general conditions for a physical theory except unitarity. The spectrum resulting from these models is very interesting because although it fails to include $SU(3)$ symmetry, the spin, parity and G parity properties are the same as the quark model. Of course there are many

defects of the model including anomalous space time
dimensions; however, given the spectrum success it
is encouraging to hope that the successful quark
model results may emerge in dual models.

This conclusion is reinforced by the fact
that present dual models already have a parton
interpretation, and thus quarks and bootstrap pictures
may be complementary ideas in a future theory.

1.2 Diffraction scattering and the optical analogy

To obtain a general idea of the type of cross-
sections typical of diffraction we begin by considering
the most extreme case where hadrons are assumed to act
like completely absorbing black discs.   In the impact
parameter representation the scattering amplitude for
elastic spinless scattering is given by

$$T(q) = \frac{4\sqrt{s}\,q}{i} \int db \; e^{-i q \cdot b} \, t(b) \qquad (1.1)$$

where $t(b) = e^{i\chi(b)} - 1$

b is the impact parameter, q the momentum of the
outgoing particle and $\chi(b)$ is the eikonal.   The
condition for complete absorption within a radius R
and no absorption outside is

$$t(b) = \begin{cases} -1 & b < R \\ 0 & b > R. \end{cases} \qquad (1.2)$$

Substituting condition (1-2) into equation (1-1) gives
the result

$$T(q) = i\sqrt{s}\,q \int_0^R b\,db \int_{-\pi}^{+\pi} d\phi \; e^{-iq b \sin\theta \cos\phi} = 8\pi i\sqrt{s}\,R\,\frac{J_1(qR\sin\theta)}{\sin\theta} \qquad (1.3)$$

The differential cross-section is then given by

$$\frac{d\sigma}{dt} = \pi R^4 \left[\frac{J_1(qR\sin\theta)}{qR\sin\theta} \right]^2 \qquad (1.4)$$

which may be re-written at small momentum transfer in the form

$$\left.\frac{d\sigma}{dt}\right|_{-t \ll 1} \simeq \pi R^4 \exp\left(\frac{tR^2}{4}\right) \qquad (1.5)$$

If we take the hadron radius to be given by the pion Compton wavelength $R \sim \frac{1}{m_\pi} \sim 7$ nat. units then we correctly estimate the diffractive slope to be approximately 10 nat. units. Of course this model predicts oscillations in the differential cross-sections and the wrong relationship between the elastic and inelastic cross-sections $(\sigma_{inel} = 2\sigma_{el})$ but these details depend strongly on the sharpness of the absorption edge.

The simple shadow scattering picture also predicts s-channel helicity conservation (S.C.H.C.) for elastic scattering. To prove this we need only show that free propagation of a wave conserves s-channel helicity. Clearly the total angular momentum J is a constant of the motion (i.e. $[\underline{J}, H_{free}] = 0$) and hence we can deduce that $\underline{q} \cdot \underline{J} = \underline{q} \cdot \underline{S}$ (as $\underline{q} \cdot \underline{L} = \underline{q} \cdot (\underline{r} \wedge \underline{q}) = 0$) is a constant and this is just the s-channel helicity. Of course other components of J are preserved, we could for instance choose J_z , but here the orbital and spin angular momentum components mix. We now proceed to check this result in detail for diffraction of a spinor object.

The problem is to solve the free Dirac
equation subject to boundary conditions appropriate
for a diffractive system as shown in fig. 1.   This
is most easily accomplished using the Green' function
technique, the Green's function for a spinor object
being given by

$$S_p^\pm(x, x') = (p_0 \gamma_0 + i \nabla \cdot \gamma + m) G_p^\pm(x, x') \qquad (1.6).$$

where $G_p^\pm(x, x')$.   is the scalar Green's function, which
is given by

$$G_p^\pm(x, x') = -\frac{1}{4\pi} \frac{e^{\pm i p |x - x'|}}{|x - x'|}$$

The Green's function satisfies the equation

$$(p_0 \gamma_0 - i \nabla \cdot \gamma - m) S_p^\pm(x, x') = - I_4 \delta^3(x - x') \qquad (1.7).$$

From the free Dirac equation and the equation for the
Green's function we obtain the integral equation (1-8)
for the wave-function $\psi(x)$.

$$\psi(x) = -i \int_V dx' \, \nabla' \left(\overline{S}_p^{(-)}(x, x') \, \gamma \, \psi(x') \right) \qquad (1.8).$$

with $\overline{S}_p^{(-)}(x, x') = \gamma_0 \, S_p^{(-)\dagger}(x, x') \, \gamma_0$

Using Gauss' theorem, equation (1-8) may be re-written
as an integral over the surface S shown in fig. 1.

$$\psi(x) = -i \int_S dS_n \, \overline{S}_p^{(-)}(x, x') \, \gamma \cdot \hat{n} \, \psi(x') \qquad (1.9).$$

where $\hat{n}$ is a unit vector normal to surface S.   Taking

the limit as $x \to \infty$ equation (1-9) reduces
to the form

$$\psi(x) \xrightarrow[x \to \infty]{} -i \frac{e^{ipx}}{x} \int_S dS_n \, e^{-ip'\cdot x'} (p_0 \gamma_0 - p' \cdot \underline{\gamma} + m) \underline{\gamma} \cdot \hat{n} \, \psi(x') \quad (1.10)$$

The integral over the hemisphere at infinity vanishes
so we need only consider the surface $z = 0$ where the
absorption takes place.   If the absorption doesn't
affect the helicity then the wave-function on the
surface is proportional to the incident wave $u_\lambda(p) e^{ipz}$.
where λ is the initial helicity, which may be taken for
definiteness to be $+\frac{1}{2}$.   Then from equation (1-10) we
obtain the result

$$\psi(x) \propto (p_0 \gamma_0 - p' \cdot \underline{\gamma} + m) \gamma_z \begin{pmatrix} 1 \\ 0 \\ \frac{p}{E+m} \\ 0 \end{pmatrix} = 2p\cos\frac{\theta}{2} \begin{pmatrix} \cos\frac{\theta}{2} \\ \sin\frac{\theta}{2} \\ \frac{p}{E+m}\left(\cos\frac{\theta}{2} \\ \sin\frac{\theta}{2}\right) \end{pmatrix} \quad (1.11)$$

which is just a spinor with helicity in the direction of
the outgoing momentum and hence we have S.C.H.C.   The
result is also easily proved for diffraction of electro-
magnetic waves. [1]. It is remarkable that this naive
prediction is strongly supported by the experimental
evidence available on elastic processes.

The success of this argument for S.C.H.C.
depends on the assumption that the absorption does not
alter the helicity.   In optics this will be false if the
diffraction system has polarization properties (other
than circular).   Thus consider light of a definite

polarization state (say right-hand circular)
incident upon the diffraction system, then the
preferential absorption of one of the perpendicular
polarization states of which the incident wave is
composed, will produce some left-handed helicity
photons as in equation (1-12) below

$$|R \cdot H\rangle = \frac{1}{\sqrt{2}} \left(|\perp\rangle + |\shortparallel\rangle \right) \xrightarrow[\substack{\text{Diff} \\ \text{system}}]{\substack{\text{Action} \\ \text{of}}} \left(\eta_\perp |\perp\rangle + \eta_\shortparallel |\shortparallel\rangle \right)$$

$$= \alpha |R \cdot H\rangle + \beta |L \cdot H\rangle \qquad (1.12)$$

$|R \cdot H\rangle \ (|L \cdot H\rangle)$ is a right- (left-) handed
helicity state and $|\perp\rangle$ and $|\shortparallel\rangle$ are states with
polarization perpendicular to the incident direction
and perpendicular to each other. Clearly the same
reasoning will apply to spinor diffraction. Hence
if a spinor object is incident upon the diffraction
system with helicity along the direction of motion
(say the z direction), then with preferential
absorption negative helicity states may be produced.

$$|z\rangle = \frac{1}{\sqrt{2}} \left(|x\rangle - i|y\rangle \right) \xrightarrow[\text{absorp.}]{\text{After}} \frac{1}{\sqrt{2}} \left(\eta_x |x\rangle - i \eta_y |y\rangle \right)$$

$$= \alpha |z\rangle + \beta |-z\rangle \qquad (1.13)$$

with

$$\alpha = \left(\eta_x + \eta_y \right)/2 . \qquad \beta = \left(\eta_x - \eta_y \right)/2$$

$|x\rangle$, $|y\rangle$ and $|z\rangle$ are states with spin in the x, y
and z directions respectively. For pure s-channel
helicity conservation the absorption in the x and y
directions must be the same. However, it is impossible

to make the amplitude pure helicity flip because the
absorption is always positive and hence the non-flip
amplitude is bigger than or equal to the flip
amplitude.   For targets without spin (like π) such
preferential absorption is impossible because there is
no physical variable to define a special direction.
In the case of spinning targets S.C.H.C. will again
hold because the system will have rotational symmetry
about the incident direction.

From the preceeding discussion it is clear
that for diffraction of a complex system, made up of
several degenerate components, unequal absorption of
the constituent components will produce new states by
diffraction.   It is through this mechanism that
diffractive particle production can occur [2] because
physical hadrons are made up of many virtual states.
Of course the virtual states are not strictly
degenerate with the physical hadron and so have finite
lifetimes, however at very high energy the lifetime of
the virtual states may be considered to be essentially
infinite because the energy differences are so small.
Hence as in the optical analogy, if the absorption of
the various "constituent" states differ, then the
outgoing wave will be contaminated by particles other
than the incident one.   Scattering produced in this
manner is called diffraction dissociation and sometime
after this prediction was published, a number of
production processes displaying diffractive features
were experimentally observed.

Clearly the internal quantum numbers $(I, Y, B, Q, G, \text{etc.})$ of the virtual states composing the hadron will be the same as the hadron itself and hence the dissociated state will have the same internal quantum numbers as the initial particle. This prediction is strongly confirmed by experiment although some controversy still surrounds the G-parity selection rule.

The simplest example of diffraction dissociation is vector meson photoproduction. Here the photon is considered to make a virtual transition to a vector meson in accordance with vector dominance.

$$|\gamma\rangle_{ph} = |\gamma\rangle_{bare} + \frac{m_\rho^2 e}{f_\rho} |\rho\rangle_{bare} + other vector mesons \qquad (1.14)$$

As the vector mesons interact strongly with hadronic matter, while the bare photon interaction is approximately a hundred times smaller, the process proceeds as in vector meson elastic scattering except the incident vector meson is transverse and off shell. Clearly S.C.H.C. is expected just as in elastic scattering and this is confirmed by experiment [3]

Now consider the nucleon diffractive production processes. As in the previous example the physical nucleon is analysed into its bare constituents.

$$|N\rangle_{ph} = |N\rangle_{bare} + \epsilon_{\pi N} |\pi N\rangle_{bare} + \epsilon_{\pi\pi N} |\pi\pi N\rangle + \cdots \epsilon_{K\Lambda} |K\Lambda\rangle_{bare} + \cdots \qquad (1.15)$$

By parity and angular momentum conservation the πN state will be in a P_{11} configuration and hence the dissociation $N \rightarrow P_{11}$ will be quasi-elastic in much the same way as $\gamma \rightarrow \rho$. Consequently we predict the process

will have all the characteristics of elastic
scattering namely S.C.H.C. and differential cross-
sections displaying a sharp forward peak with slope
similar to elastic scattering.   In fact the slope is
anomalously high (see table 1) and this may be due to
the absorptivities of the N and πN states differing in
the peripheral region but being identical and total in
the central region.   Experiments have not been
performed with polarized targets and so S.C.H.C.
cannot be definitely confirmed although it is
suggested by the sharp forward peak of the differential
cross-section.

Production of other N^* states requires a change
in the relative orbital angular momentum and hence these
processes are in a different category to the strict
quasi-elastic scattering occuring for N $\rightarrow$ P_{11} .   In
the $j = \ell + \frac{1}{2}$ partial wave, changes in orbital angular
momentum produce the states D_{13}, F_{15} G_{17}, etc. while in
the $j = \ell - \frac{1}{2}$ partial wave the states D_{11}, F_{13} and G_{15} can
also be produced.   The states D_{13}, F_{15}, G_{17}, etc. are
the states experimentally observed, however the
existence of the D_{11}, F_{13}, G_{15} ... sequence of states is
more questionable.   Because of the change in orbital
angular momentum accompanying the absorption in these
processes, S.C.H.C. is no longer expected and more s-
channel helicity amplitudes will be populated, thus
giving less sharp diffraction peaks.   In fact the
hypothesis of orbital production makes definite
predictions for the spin structure which are in accord
with data.   (See Ch. 3).   A further point is that,
all other things being equal the loss in orbital angular

momentum in the production of these states implies
that these processes are less peripheral than the
quasi-elastic processes and hence have smaller slopes.
Of course processes producing more final states as in
$N \rightarrow N\pi\pi$ are possible but we will not consider these
in detail as they are essentially similar to the
simple case already discussed, and instead move on to
considerations of meson dissociation.

The pion dissociation $\pi \rightarrow 2\pi$ is forbidden
by G parity and hence the lowest mass pion dissociation
states occur in the 3π system. Quasi-elastic
scattering requires the final state to be a heavy pion
(0^{-+}) for which the only reasonable candidate is the
disputed $E(1420)$ resonance. To produce higher spin
objects orbital angular momentum must be lost, and then
the states A_1 (1^{++}), A_3 (2^{-+}), 3^{++} etc. can be
produced exactly in accord with the experimental
observations. Finally we note that this mechanism
does not commit itself to assuming that the A_1, A_3, etc.
are resonances and this question depends upon the
dynamics of the 3π system.

A surprising experimental observation is that
not only are all diffractive slopes approximately the
same, but also a large class of non diffractive reactions
have comparable slopes and this suggests a common
production mechanism. Hence attempts have been made to
explain non diffractive phenomenon along diffractive or

absorptive guidelines and also the opposite, namely
to understand diffractive phenomena in a similar
manner to the non-diffractive.   The most naive model
of non-diffractive processes is single particle exchange,
but this is ruled out on a number of grounds, one of
which is the experimental point that the slopes do not
in fact depend strongly on the mass of the exchange,
with the exception of pion exchange.   This and many
other objections can be overcome by supposing the
exchange to be composite and it is then a Reggeon.
We will now proceed to give a brief account of this
point of view explaining how diffractive phenomena are
incorporated.

1.3   The Regge classification scheme

High energy two body processes can be
classified according to the internal quantum number
exchange between beam and target and this is
empirically correlated with the energy dependence of
the cross-section as in table 2. [4]   For diffractive
scattering there is no internal quantum number exchange
and the cross-section becomes nearly independent of
energy for high energies.

It is not necessary to connect the quantum
number exchange with particles [5] though this is both
suggestive and productive.   It will be shown in
chapter 3 that the identification of particle and
quantum number exchange leads to a natural explanation
of the energy dependences in table 2 with the exception
of diffraction.   Further evidence in support of this

hypothesis is the fact that when exchanges are allowed the cross-section has forward "peaks" but when no exchange is possible then there is no forward peaks and the cross-section is about a hundred times smaller than the comparable exchange process.

The exchange deemed responsible for diffraction is called the Pomeranchuk or pomeron and it carries vacuum quantum numbers, but doesn't appear to correspond to any known particles which suggests that the pomeron isn't a simple Regge pole but rather something more complicated. Further evidence for the special nature of the pomeron trajectory is that the slope is rather small approximately $1/2$ GeV^{-2} compared with a universal slope of about 1 GeV^{-2} for all other trajectories as shown in fig. 2. As the pomeron trajectory passes through or near the point $t = 0$ $J = 1$ it is very tempting to identify the pomeron with a fixed $J = 1$ pole, which is known to give constant asymtotic cross-sections, however this conjecture must be rejected for several reasons. First of all such a pole is incompatible with t-channel unitarity and secondly it would not be absorptive and hence contradicts the belief that elastic scattering is essentially a diffractive phenomenon. Finally a particle pole on the pomeron trajectory at $J = 1$ would have the wrong parity to belong to the vacuum. It can be seen that the pomeron is a somewhat mysterious entity and we will proceed in the next section to consideration of models for production processes which will illuminate the pomeron structure.

1.4 Models for diffraction scattering

Hadron elastic and total cross-sections are
of the order of magnitude $(1/m_\pi)^2 \sim 20$ mb and this
suggests a picture whereby the main contribution to
the cross-section comes from the outer or peripheral
pions, the central core of the hadron, which contains
multi-particle virtual states, contributing a much
smaller amount to the cross-section.   We also observe
that the width of the elastic peak is of the order of
the pseudoscalar meson mass squared.   Of course the
mathematical reason for this result is the relationship
between the cross-section and the elastic slope.
Physically however we may imagine that when the momentum
transfer becomes comparable with the pion mass, then
there is a high probability of producing a pion in the
final state.   Briefly restated, the reason for the sharp
two body diffractive slopes is that high momentum
transfer breaks up the hadron and so the two body cross-
section is small in this momentum transfer region.
This gives the reason why all two body slopes are
approximately the same, and the individual momentum
transfers in multi-particle processes are similarly
restricted.

The previous considerations suggest that at
high energy multi-particle processes will be dominantly
multi-peripheral, with resonances in the low sub-energy
channels, and hence in general tree diagrams as in fig.3
are appropriate.   It is not clear which exchanges are
dominantly responsible for these inelastic production

processes, though if the cross-section is not to
vanish with increasing energy then the exchange must
be the pomeron.   Experiment indicates the main process
is vector meson Regge exchange.

We begin by considering the historically
earliest multi-peripheral model due to Amati, Fubini
and Stanghellini (A.F.S.) [6] where the exchange was
considered to be the elementary pion and the emitted
particles were vector mesons as single pion
emission is forbidden by G-parity.   To make use of
this picture of production processes in elasitic
scattering we consider the unitarity equation,
separating the elastic and inelastic intermediate
states as in fig. 4 and substituting tree graphs for
the inelastic amplitudes as illustrated in fig. 5.   Of
course it is impossible to sum explicitly over all these
graphs, though for the restricted class of ladder
diagrams this may be achieved and this approximation
is the multi-peripheral model.   We may also consider
the hypothesis that the sum over all possible graphs
generate a Regge pole or composite exchange.   This is
plausible because the Bethe Salpeter wave function for
say two pions bound by vector mesons, will include a
sum over all possible graphs and not simply those of
the ladder approximation.   Accepting this conjecture
and identifying A_{inel} with the imaginary part of a Regge
pole, we are able to understand why the pomeron behaves
as though it were a Reggeon.   However, the trajectory
is only predicted in the ladder approximation.

In this model the unitarity equation can be
solved exactly and this reveals a number of defects.
As the amplitude is dominated by A_{inel} this form is
substituted into the elastic unitarity integral and
generates a cut, the A.F.S. cut as shown in fig. 6.
If the Regge pole is considered to consist purely of
ladder diagrams then it has been shown by Mandelstam [7]
to be cancelled by other diagrams, but this objection
is spurious if the Regge pole includes other non ladder
terms.   Also the A.F.S. cut interferes constructively
with the pole whereas destructive interference is
favoured by experiment.

In the multi-Regge model the main ideas of
the A.F.S. approach are retained but the exchanges are
composite rather than elementary.   Furthermore only
ladder diagrams are retained in A_{inel} and this is, of
course, false, so the model can then only be valid in
a limited region of phase space and even then only to
the extent that it is valid to neglect the crossed
diagrams.   One attempt to surmount this limitation is
by appealing to duality, whereby the s-channel resonances
can be accounted for in an average way by Regge exchanges.
However, in the case of pomeron exchange this duality
argument breaks down, also for a pomeron with unit
intercept multi-pomeron exchange is impossible because
the Froissart bound is exceeded.

If only one pomeron exchange is allowed as in
fig. 7 then this corresponds to the two fireball model
where production processes are associated with two jets
arising from the break-up of the projectile and target

respectively. The exact manner of break-up is left unspecified and may even be of a multi-peripheral type provided pomeron exchange is excluded, however the model is clearly suggestive of the diffraction dissociation picture of Good and Walker. It is interesting to observe that very little of A_{inel} is made up of the known quasi-two body diffractive processes and hence it is clear that multi-particle states are very important. It is also tempting to assume that the cross-section for states produced by orbital change is small and consequently only low spin fireballs are produced which will, therefore, decay almost isotropically in its rest frame, but this assumption is certainly in conflict with experimental data.

As noted earlier the main defect of the multi-peripheral model was the neglect of the crossed diagrams. Cheng and Wu [3] calculate the elastic amplitude from the basic ladder diagrams including all possible twists as shown in fig. 7 and this set of diagrams is called a tower. The resulting tower amplitude might be expected to be a moving pole, however the result diverges like a fixed power.

$$T \sim \frac{s^{1+\alpha g^4}}{(\ln s)^2} \qquad (1-15)$$

where α is a positive constant dependent on the type of particle involved (e.g. scalar or spinor) and g is the coupling constant. This result cannot be correct because, like multi-pomeron exchange in the multi-

peripheral model the Froissart bound is violated.
Cheng and Wu conjecture that this problem might be
solved if s-channel unitarity is included by iterating
the towers in the s-channel as in fig. 8.   The result
is effectively equivalent to an eikonal formula with
the tower amplitude playing the role of the potential.
The total cross-section is then predicted to grow like
$(\log s)^2$ which is as fast as is allowed by the Froissart
bound.   This result is most interesting because
hadronic total cross-sections do indeed appear to rise
with energy in the prescribed manner.   We also note
that these results can be obtained in a much less
complicated manner in the droplet formalism of Yang [9]
and this approach is effectively an extension of the
ideas of Good and Walker.

1.5   The internal structure of hadrons

i)   Dual models

The simplest approach to the dual model is
to consider the hadron to be composed of an infinite
number of partons.   Consideration of two body scattering
by formation of resonances in this picture leads to the
Veneziano model [10].   Because the parton-parton
coupling constant is large and the number of diagrams to
a given order increases rapidly with order the most
significant diagrams are those with a very large number
of interactions.   Furthermore only planar diagrams
are considered because of the small probability of
partons passing one another without interaction
(see fig. 9) and hence the set of resonant intermediate
states can be replaced by planar fishnet diagrams of high

order as in fig. 10(a).   The most important feature
to notice about fig. 10 is that because of the
infinite numbers of partons there is a symmetry
between the s- and t-channels and this is the duality
principle.   (See fig. 10(b) and 10(c)).   If scalar
partons are assumed and the diagrams are treated
statistically then the simple Veneziano model is
reproduced.

Taking the continuous limit for the fishnet
diagrams, the diagram in fig. 11 is obtained, and it is
found that the flow of momentum is analogous to the heat
flow in a conducting plate [11].   Using this analogy it
is easy to construct the Veneziano amplitude for any
given diagram and for instance the result for the box
diagram is symbolically indicated in fig. 12.   More
examples of these diagrams will be given in a later
chapter, in particular with reference to the pomeron.

Before leaving the subject of dual models we
will outline the free Hamiltonian for hadrons in the
dual models and the method of Ramond.   In the ordinary
Veneziano model the Hamiltonian is given by an infinite
set of covariant oscillators as in equation (1-16)

$$H = \sum_{n=1}^{\infty} n\, a_{n\mu}^{+} a_n^{\mu} + p_0^2 = \frac{1}{2} \sum_{n=1}^{\infty} \left(p_n^2 + n^2 q_n^2 \right) + p_0^2 \qquad (1.16)$$

p_0 is the centre of mass momentum and (p_n, q_n)
are internal momenta and positions, q_n^{+}, q_n are the
corresponding harmonic oscillator creation and
annihilation operators.   Ramond assumes the existence

of an internal time τ conjugate to H and also a corresponding Heisenberg equation of motion for any operator f as in equation 1-17

$$[H, f] = i \frac{df}{d\tau} \qquad (1.17)$$

From equation 1-17 it follows that the creation operator is a simple exponential function of time as below

$$a_n^+(\tau) = a_n^+ e^{in\tau} \qquad (1.18)$$

From equations 1-17 and 1-18 we can define a set of hadronic field operators in terms of the creation and annihilation operators $a_n^+(\tau)$ and $a_n(\tau)$ for instance the momentum operator given in equation 1-19

$$P^\mu(\tau) = p_0^\mu + \sum_1^\infty p_n^\mu = p_0^\mu + \frac{1}{\sqrt{2}} \sum_{n=1}^\infty \sqrt{n} \left(a_n e^{-in\tau} + a_n^+ e^{in\tau} \right) \qquad (1.19)$$

Any observable of the system is the time average of the corresponding field operator over a complete cycle of the internal time from $\tau = -\pi$ to $\tau = \pi$ as below.

$$\mathcal{O} = \langle \mathcal{O}(\tau) \rangle = \frac{1}{2\pi} \int_{-\pi}^{+\pi} d\tau \, \mathcal{O}(\tau) \qquad (1.20)$$

For example the external momentum p_0 is the time average of the field momentum $P(\tau)^\mu$. Ramond [12] now uses this relation to go from the free equation for the external hadron to the internal field equation. For example if the free external motion is governed by the Klein Gordon equation

$$(p_0^2 - m_0^2) \varphi(x) = 0 \qquad (1.21)$$

then the corresponding internal field equation is given by the replacement $p_0^2 \longrightarrow \langle : P^\mu(\tau) P_\mu(\tau): \rangle$ and the full equation is shown below.

$$\left(\langle : P^\mu(\tau) P_\mu(\tau): \rangle - m_0^2 \right) |\phi\rangle = 0 \qquad (1 \cdot 22)$$

with

$$L_0 \equiv \langle : P^2: \rangle = p_0^2 + \sum_{n=1}^{\infty} n\, a_n^\dagger a_n$$

We can now identify the equation (1-23) for the mass squared operator as the original Veneziano model

$$m^2 = m_0^2 + \sum_{n=1}^{\infty} n\, a_n^\dagger a_n \qquad (1 \cdot 23)$$

The time like states have negative normalization and must be eliminated. This is achieved by subsidiary conditions generalized from the simple gauge relations 1-24 for pure vector particles.

$$0 = p_\mu\, a_n^\mu \,|\,Physical\ state\rangle = \langle P^\mu(\tau)\rangle \langle e^{in\tau} P_\mu(\tau)\rangle |Phy\rangle \qquad (1 \cdot 24)$$

on replacing $\langle P^\mu \rangle \langle e^{in\tau} P_\mu \rangle$ by $\langle e^{in\tau}: P^\mu P_\mu: \rangle$ we obtain the Virasoro gauge conditions [13] 1-25

$$L_n |Phy\rangle = \langle e^{in\tau}: P^\mu(\tau) P_\mu(\tau): \rangle |Phy\rangle = 0 \qquad (1 \cdot 25)$$

In the special case of a tachyon ground state $m_0^2 = -1$ it can be shown [14] that all "ghost" or negative normalization states are eliminated. The tachyon state can be removed by increasing the dimension of space but we will pursue this no further and instead consider the fermion dual model [12].

　　　To obtain the field equation corresponding to the Dirac equation a generalization of the Dirac matrices $\Gamma_\mu(\tau)$ is required such that

$$\langle \Gamma_\mu(\tau) \rangle = \gamma_\mu \qquad (1 \cdot 26)$$

From the anti-commutation relations obeyed by the Dirac matrices, we expect "equal time" anti-commutation relations for the generalized matrices $\Gamma_\mu'(\tau)$ as in equation 1-27

$$\{ \Gamma_\mu'(\tau), \Gamma_\gamma'(\tau')\} = 2\, g_{\mu\nu}\, (2\pi)\, \delta(\tau-\tau') \qquad (1.27)$$

Finally we also require the adjoint matrix to obey the condition 1-28

$$\Gamma_\mu^{+}(\tau) = \gamma_0\, \Gamma_\mu'(\tau)\gamma_0 \qquad (1.28)$$

If we assume expansion 1-29

$$\Gamma^{\prime\nu}(\tau) = \gamma^\nu + \sqrt{2}\, i\, \gamma_5 \sum_{n=1}^{\infty} \left(b_n^{+\nu} e^{in\tau} + b_n^\nu e^{-in\tau} \right) \qquad (1.29)$$

then $\Gamma^{\prime\nu}(\tau)$ has the required properties provided the b's obey the anti-commutation relations 1-30 and all other anti-commutators vanish.

$$\{ b_{n\mu}^{+}, b_{m\nu} \} = g_{\mu\nu}\, \delta_{mn} \qquad (1.30)$$

If the a_n's are also assumed to commute with the b_n's we obtain the generalized Dirac equation 1-31 on replacing $\gamma \cdot p$ by $\langle P_\mu(\tau)\Gamma^{\prime\nu}(\tau) \rangle$

$$\left(F_0 - m_0 \right) |\psi\rangle = 0 \qquad (1.31)$$

with

$$F_0 = \langle P_\mu(\tau)\Gamma^{\prime\nu}(\tau) \rangle = \not{p}_0 + i\, \gamma_5 \sum_{n=1}^{\infty} \sqrt{n}\, \left(a_n^{+} b_n + b_n^{+} a_n \right)$$

The corresponding mass operator and mass squared operators are

$$m = m_0 + i \gamma_5 \sum_{n=1}^{\infty} \sqrt{n} \left(a_n^+ b_n + b_n^+ a_n \right) \qquad (1.32)$$

and

$$m^2 = m_0^2 + \sum_{n=1}^{\infty} n \left(a_n^+ a_n + b_n^+ b_n \right) \qquad (1.33)$$

The b_n^+ operators are clearly to be interpreted as spin excitation operators just as the a_n^+ are orbital excitation operators. As in the boson dual model there are gauge conditions; however, as we are mainly interested in displaying the form of the fermion dual model, we will leave our account at this point.

ii) The quark models

The three quarks u, d, s which form the fundamental triplet representation $\underline{3}$ of SU(3) have quantum numbers as shown in figure 13. The hadron SU(3) spectrum is now explained by assuming mesons are composed of a quark-antiquark pair and baryons three quarks. Then the SU(3) multiplet assignments are as below

Mesons $\quad \underline{3} \otimes \underline{3}^* = \underline{8} \oplus \underline{1}$

Baryons $\underline{3} \otimes \underline{3} \otimes \underline{3} = \underline{10} \oplus \underline{8} \oplus \underline{8} \oplus \underline{1}$

It is possible to incorporate the spins and parities of the states by including the orbital and spin angular momenta of the quarks assuming that the quarks are spinor objects. The group $SU(6) \subset SU(2) \otimes SU(3)$ is the most natural generalization of SU(3) and this

includes the spin of the quarks in a non-relativistic manner. If the spin and the orbital angular momentum are assumed to be independent, then a very crude classification is obtained from the group $U(6) \otimes U(6^*) \otimes O(3)$ where $O(3)$ accounts for the orbital angular momentum of the quarks.

The main difficulty with this symmetry, other than the fact that spin-orbit coupling is not negligible, is its non-relativistic character. The problem is that angular momentum is not a relativistic invariant, however, if the Lorentz boosts are confined to the direction of the angular momentum projections, say the z direction, then the values of these projections remain invariant. Clearly it is possible to form a relativistic sub-group of $U(6) \otimes U(6^*) \otimes O(3)$ which is valid for co-linear processes. To construct this group a set of SU(2) spin operators commuting with Lorentz transformations in the z-direction are required. These are given by [16]

$$W_x = i \gamma_0 \gamma_x \gamma_z = \gamma_0 \sigma_x \qquad W_x^* = - \gamma_0 \sigma_x$$

$$W_y = i \gamma_0 \gamma_y \gamma_z = \gamma_0 \sigma_y \qquad W_y^* = - \gamma_0 \sigma_y \qquad (1.34)$$

$$W_z = i \gamma_x \gamma_y = \sigma_z \qquad W_z^* = \sigma_z.$$

It is clear that $\gamma_x \gamma_y$ is invariant under a Lorentz boost in the z-direction, while the operators W_x and W_y have the matrix γ_o multiplying the usual SU(2) operators so as to compensate the change in γ_z on a Lorentz boost. The novel feature of these operators is the negative sign for the anti-quark operators W_x^* and W_y^* and this has the consequence that the meson wave-functions differ from the ordinary SU(6) wave-functions. The only orbital angular momentum operator to remain invariant under Lorentz boosts in the z-direction is L_z and so the reduced group is $U(6)_W \otimes O(2)$.

If the quark model is to be combined with the dual model then an infinite sea of quark anti-quark pairs in an SU(3) singlet state are required besides the ordinary valence quarks. One consequence of this is that the valence quark centre of mass is no longer fixed thus giving an extra degree of freedom which may be exploited to enforce anti-symmetric statistics [17]. This solves one of the major difficulties of the simple quark model, where although quarks are spinor objects they are obliged to obey symmetric statistics [18]. If the quarks have harmonic oscillator interactions as in the Veneziano model then because of the infinite number of degrees of freedom we may write single particle oscillator wave-functions for each quark. If the spin is incorporated using the SU(6) scheme then the quark equation is

$$m_i^2 \phi_i = -(p_i^2 + \omega^2 x_i^2) \phi_i = 2\omega(-a_i^\dagger a_i + \text{constant}) \phi_i \qquad (1.35)$$

where x_i and p_i are the Jacobi position and momentum co-ordinates of the ith quark and m_i its contribution to the hadron mass. It is interesting to attempt to incorporate the quark spin in a more dynamical manner as in the Ramond dual model. We then require an equation for the mass operator as shown below

$$m_i \psi_i = \sqrt{2\omega} \left(\alpha_-^i a_i^\dagger + \alpha_+^i a_i \right) \psi_i = \left(\not{p}_i + V_i(x_i) \right) \psi_i \qquad (1.36)$$

In writing equation 1-36 we have set $\alpha_{+\mu} + \alpha_{-\mu} = \gamma_\mu$ so as to reproduce the momentum term $\not{p}_i$ correctly. We now demand that the equation for the mass squared m_i^2 return to a form as close as possible to equation 1-35, and consequently must not contain terms quadratic in the creation or destruction operators. This criterion is satisfied if

$$\alpha_{+\mu} \, \alpha_{+\nu} = \alpha_{-\mu} \, \alpha_{-\nu} = 0 \qquad (1.37)$$

Condition 1-37 is solved by the operators defined below

$$\alpha_{\pm\mu} = \tfrac{1}{2} \left(1 \pm \gamma_5 \right) \gamma_\mu \qquad (1.38)$$

The quark spinors of the new equation are no longer of the $SU(6)_W$ type because the equation is fully relativistic and also contains spin-orbit interaction. The presence of the spin-orbit term is most easily seen in the squared equation displayed below

$$m_i^2 \psi_i = -2\omega \left(a_\mu^\dagger a^\mu + i \gamma_5 \sigma_{\mu\nu} a^\mu a^\nu + constant \right) \psi_i \qquad (1.39).$$

This simplistic formulation of a dual quark model is of course not to be taken seriously because, among other things, it is not parity invariant, however it illustrates some concepts to be used in a later chapter.

Finally we consider the quark model in the formulation of current algebra. First of all the axial and vector currents are constructed from the quark fields $q(x)$ and the corresponding charges Q_{S_i} and Q_i defined as shown

$$V_i(x) = \bar{q}(x) \gamma_\mu \frac{\lambda_i}{2} q(x) \quad , \quad Q_i = \int V_{0i}(\underline{x},t) \, d\underline{x}$$

$$A_i(x) = \bar{q}(x) \gamma_5 \gamma_\mu \frac{\lambda_i}{2} q(x) \quad , \quad Q_{S_i} = \int A_{0i}(\underline{x},t) \, d\underline{x} \tag{1.39}$$

If the quark fields are assumed to obey equal time (anti) commutation relations as in free field theory then the following charge commutation relations are obtained [19]

$$[Q_i, Q_j] = i f_{ijk} Q_k \quad , \quad [Q_i, Q_{S_j}] = i f_{ijk} Q_{Sk} \quad , \quad [Q_{S_i}, Q_{S_j}] = i f_{ijk} Q_k \tag{1.40}$$

where f_{ijk} are the SU(3) structure constants. This algebra can be reduced into two separate SU(3) sub-algebra's by defining new charges $Q_{\pm i} = \frac{1}{2}(Q_i \pm Q_{S_i})$ when commutation relations 1-40 become

$$[Q_{+i}, Q_{-j}] = 0 \quad , \quad [Q_{\pm i}, Q_{\pm j}] = i f_{ijk} Q_{\pm k} \tag{1.41}$$

which correspond to an SU(3) $\otimes$ SU(3) algebra. It is possible that the charge commutation relations remain exact even in an interacting quark theory and consequently this algebra has a rather different status

to the approximate $U(6) \otimes U(6) \otimes U(3)$ symmetry.
Despite this fundamental difference these algebras are
related, and this will now be investigated.

Because current algebra is fully relativistic
we anticipate that the related classification group will
also be relativistic and hence must be $U(6)_W$. In
$U(6)_W$ the z direction is given preference and this is
achieved in current algebra by considering the current
matrix elements in a frame with infinite momentum in
the z direction. (I.M.F.) The x and y components of
the currents are unaffected by the boost into the I.M.F.,
while the z and t components become infinite and equal.
Clearly in calculating experimental quantities only the
current components which are infinite will give finite
contributions and hence the other components may be
neglected. Consequently there are 18 significant
current components and corresponding charges namely,
Q_i , Q_{5i} $i = 0, 1, 2, \cdots , 8$. As a $U(6)$ algebra has
36 generators this is insufficient and further charges
are required. These extra charges are obtained from
the tensor currents $\tau_{i\mu\nu} = \bar{q}(x) \sigma_{\mu\nu} \frac{\lambda_i}{2} q(x)$ which arise
naturally in current algebra from commuting currents with
their divergences. The tensor currents of significance
in the I.M.F. are $\tau_{ixz} = \tau_{ixo}$ and $\tau_{iyz} = \tau_{iyo}$ which
are infinite while the other components are finite or zero.
Evidently the scalar and pseudo-scalar currents are
irrelevant. Thus we may define 18 more charges in this
frame τ_{ix} and τ_{iy} $i = 0, 1, 2, \cdots 8$.

$$T_{ix(y)}(t) = \int d\underline{x} \, \tau_{ix(y)o}(\underline{x}, t) \qquad (1.42)$$

giving 36 "good" charges in all and these charges can
be shown to form a $U(6)_{\not{t}}$ algebra.   Although this
algebra is isomorphic to the "constituent" quark
classification algebra $U(6)_W$ it is not equal to it.
If these groups were equal then for the quarks of current
alggebra the spin would completely decouple from the
internal motion as in $U(6)_W \otimes O(2)$ and this is refuted
by a variety of experimental results, for instance the
non-zero anomalous magnetic momenta of the neutron and
proton.   Presumably, however, there exists a trans-
formation between one algebra and the other.   This
idea is made more graphic by introducing two types of
quarks the "current" quarks of the "exact" $U(6)_{current}$
and the "constituent" quarks of the approximate $U(6)_W$
The problem is then reformulated as a transformation
between the current quarks and the constituent quarks.

The simplest model in which to consider this
transformation is the free quark model, but even in the
I.M.F. this is not in general a good approximation.
The free Dirac equation for a quark in the rest frame
of the hadron is

$$(\not{q} - m_q) \psi = 0 \qquad\qquad (1.43)$$

where q is the momentum relative to the centre of mass.
Now on transforming to the I.M.F. $q_z \to 0$ and $q_o \to \omega_\perp$
and the equation becomes

$$\omega_\perp \psi = (\underline{\alpha} \cdot \underline{q}_\perp + \gamma_o m) \psi \qquad\qquad (1.44)$$

with $\omega_\perp = \sqrt{q_\perp^2 + m_q^2}$

Note that we have multiplied equation 1-43 by γ_0
as well as transforming to the I.M.F. to obtain equation
1-44 so that the elements of this equation are now just
the terms in the U(6) current algebra (i.e. $\gamma_0, \gamma_0\gamma_\lambda, \gamma_c\gamma_y$)
Now the constituent quark algebra is generated by
$(\gamma_0\sigma_x, \gamma_c\sigma_y, \sigma_z)$ which are semi-diagonal and
consequently if equation 1-44 is "diagonalized" by a
Foldy-Wouthuysen transformation S we will be able to
connect the current and constituent quarks [20]
S is given by

$$S = exp\left(\underset{\sim}{\sigma}\cdot\underset{\sim}{q}_\perp \theta\right) \quad with \quad tan\, 2q_\perp \theta = \frac{q_\perp}{m} \qquad (1\cdot45)$$

Thus the relation between constituent and current quarks
is given by

$$\psi_{current} = S^{-1}\psi_{constituent} \qquad (1\cdot46)$$

The most important effect of this transformation is to
introduce a spin-orbit term $\underset{\sim}{\sigma}\cdot\underset{\sim}{q}_\perp$ into the current quark
spinor. It is interesting to find the corresponding
transformation in equation 1-36 which in the I.M.F.
becomes

$$\gamma_0 m\psi_\infty = \left(\underset{\sim}{\alpha}\cdot\underset{\sim}{q}_\perp - i\omega\gamma_5\underset{\sim}{\alpha}\cdot\underset{\sim}{x}_\perp\right)\psi_\infty \qquad (1\cdot47)$$

This equation is exactly soluble, however it is
sufficient for our purposes to display the ground state
solution.

$$\psi_\infty^0 \propto \begin{pmatrix} |0\rangle_z + \underset{\sim}{\sigma}\cdot\underset{\sim}{a}_\perp^\dagger|0\rangle_z \\ |0\rangle_z - \underset{\sim}{\sigma}\cdot\underset{\sim}{a}_\perp^\dagger|0\rangle_z \end{pmatrix} = \begin{pmatrix} 1 & \underset{\sim}{\sigma}\cdot\underset{\sim}{a}_\perp^\dagger \\ -\underset{\sim}{\sigma}\cdot\underset{\sim}{a}_\perp^\dagger & 1 \end{pmatrix}\begin{pmatrix} |0\rangle_z \\ |0\rangle_z \end{pmatrix}$$

$$= \begin{pmatrix} 1 + \underset{\sim}{\sigma}\cdot\underset{\sim}{a}_\perp^\dagger & 1 - \underset{\sim}{\sigma}\cdot\underset{\sim}{a}_\perp^\dagger \\ -(1 - \underset{\sim}{\sigma}\cdot\underset{\sim}{a}_\perp^\dagger) & 1 + \underset{\sim}{\sigma}\cdot\underset{\sim}{a}_\perp^\dagger \end{pmatrix}\begin{pmatrix} |0\rangle_z \\ 0 \end{pmatrix} \qquad (1\cdot48)$$

$|0\rangle_2$ is a two dimensional harmonic oscillator ground state embedded in a Pauli spinor. The second equation rather than the third is the most relevant because here we take the non-parity invariant part of the solution into the constituent quark spinor and we may guess that the correct parity invariant solution is obtained by replacing the "neutrino" type spinor by the Pauli $SU(6)_W$ spinor. The transformation is now of the same form as the free quark transformation and it might be hoped that even in the more general interacting case a transformation of a similar form to equation 1-45 will be appropriate. Indeed this Melosh transformation [20] model does improve a number of quark model predictions. Despite this success, formulation of relativistic quark models in terms of this transformation is of very little use especially as it encourages the unphysical assumption of single particle quark wave-functions. The proper use of this transformation is as a simple algebraic formulation of the $SU(6)$ representation mixing.

2. The properties and mechanism of
   diffraction dissociation

2.1 Introduction

One of the basic problems in particle physics is to understand the general collision $AB \rightarrow C_1 C_2 \cdots C_n$. Experiment gives two very important hints. The first is the small transverse momenta characteristic of all the outgoing particles and this is opposed to the model where A and B stop each other in the centre of mass because then transverse and longitudonal momenta are treated symmetrically. The second is the rather slow growth in multiplicity with increasing energy, perhaps like logs and thus very little of the available kinetic energy is transformed into matter. Both these points argue in favour of a picture whereby the projectile and target pass through each other becoming excited and fragment, but nevertheless retain most of the kinetic energy of the parent state. The angular distributions for the breakup of the target and projectile respectively become asymptotically independent of energy and hence are diffractive. (See fig. 14). This hypothesis is called limiting fragmentation [21].

Of course there are also other contributions to the cross-section from particles moving slowly in the centre of mass which are not obviously correlated with either the target or projectile. These may result from very massive fragmentation states or alternatively arise from non diffractive sources and as yet experiment has

not decisively settled this issue.   Clearly an
important question to be resolved is the mechanism
of diffractive fragmentation and the aim of this
chapter is to discuss this question in the context of
the low mass fragmentation states presenting some of
the relevant experimental evidence.

2.2   The dependence of diffractive cross-sections
      on fragmentation mass and the problem of
      isolating the quasi two body contribution

The dependence of the diffractive cross-
sections on the fragmentation mass M_x is obtained in the
inclusive experiment $AB \rightarrow AX$ where X represents the
fragments from the breakup of B.   Indeed most of the
diffractive data is obtained from "missing mass"
experiments of this sort where only the parameters of
the outgoing particle A are measured and from this the
cross-section is determined as a function of "missing
mass" M_x and momentum transfer.   A typical mass spectrum
is shown in fig. 15 and it will be noticed that it is by
no means resonance dominated even for low mass.   Both
the cross-section "bumps" and the background appear to
become asymptotically energy independent as in limiting
fragmentation although it has been suggested [22] that
either the background or the resonances disappear
asymptotically.

The issue is further complicated by the fact
that not all the cross-section bumps correspond to
genuine resonances.   The evidence for this assertion is

very strong [23]. The most important fact indicating
this conclusion is that many of the diffractive cross-
section bumps are not found in other production or
formation experiments, for example A_1, A_3, Q , L, and
perhaps the $N^*(\frac{1}{2}^+, 1410)$ and $N^*(\frac{5}{2}^+, 1710)$.   The
$N^*(\frac{1}{2}^+, 1410)$ may be identified with the Roper resonance
P_{11} (1470) while the $N^*(\frac{5}{2}^+, 1710)$ probably corresponds to
the F_{15} (1688) although the mass discrepancies are
disturbing.   Furthermore some of these mass bumps are
very broad, for example the A_1 has a width of
approximately 400 MeV, and they do not fit the simple
Breit-Wigner resonance form.   Finally the decay
products of these "resonances" are surprisingly near the
threshold.   Morrison has designated such "mass
enhancements" D resonances [23].   Of course there are
also some genuine resonances produced diffractively, for
instance the $N^*(\frac{3}{2}^-, 1520)$ or D_{13} and probably
$N^*(\frac{5}{2}^+, 1688)$.

2.3 Possible mechanisms for diffraction dissociation

a)   Diffractive resonance excitation

The simplest view of diffraction dissociation
is of resonance excitation and subsequent decay as in
fig. 16.   Certainly some diffractive production is of
this type;   however, as noted previously there is a large
background as well as kinematic mass enhancements which
superficially appear to be resonances.   Clearly this
model is totally inadequate to explain the mass spectrum,
even the resonance part alone because of the non Breit-
Wigner form of the D "resonances".   Furthermore if the

D-resonances are genuine resonance states then they
should occur in other production processes. For
example the charge exchange (C.E.X.) cross-section
for $N^{*0}(5/2^+, 1688)$ is approximately 10 μb (at 15 GeV)
and as the $N^*(1/2^+, 1410)$ has a similar diffractive
cross-section we expect comparable C.E.X. cross-sections,
whereas in fact no signal is observed at all. Similar
reasoning applies to the A_1 and Q mesons where again
C.E.X. cross-sections of the order of 10 μb are expected
but are not detected. The possibility remains that
Reggeons do not couple to the D states but this is
ruled out by the existence of cross-over phenomena.
Despite all these difficulties it seems probable that
there is some direct resonance contribution even for the
disputed D states. The reason for this is that these
states are expected in the quark model classification and
simple calculations in this model, which only allows
resonance excitation, underestimate the relevant cross-
sections. Furthermore we will present arguments in
section 2.3(c) which indicate that resonance dominance
is possible but that the number of resonances is
considerably more than previously expected. Finally
we also note that if there are competing mechanisms then
interference effects are expected and this will produce
non Breit-Wigner resonance forms as in rho meson
production.

b) The Deck mechanism and the multi-
peripheral picture

The rough qualitative features of the
diffractive fragmentation mass spectra, namely a
large background with peaks closely following the
various production thresholds, may be qualitatively
understood in analogy to non diffractive production.
The fragmentation $B \rightarrow X$ is similar to non diffractive
production with the mass M_X taking the place of the
centre of mass energy $\sqrt{s}$ Empirically non diffractive
production processes rise rapidly above the threshold
to a peak or peaks and then fall with increasing energy
perhaps like $1/\sqrt{s}$. Hence if this picture is applied
to the fragmentation process then the main features of
the data are produced with no special emphasis given to
the resonances in preference to the background;
however, the picture lacks a detailed mechanism and is
not quantitative.   It is, of course, possible to test
this picture by comparison with the corresponding
production data, for example the photo-production
$\gamma B \rightarrow X$ inelastic cross-section.

A specific model in which the D-resonances
may be understood is the peripheral or Deck mechanism
shown in fig. 17 where the D resonance is identified
with a kinematic bump in the cross-section for the out-
going π, R state.   It is important that the exchange is
a pion because then the states R and π emerge predominantly
in the same direction due to the pion peak and there is
the possibility of simulating resonance behaviour.

Explicit calculation predicts the A_1, A_3, and L

peaks in reasonable agreement with experiment.

(See table 3 and fig. 18). Despite this success the

model is theoretically defective because the $\rho_{\pi\pi}$ vertex

has been assumed to be independent of the off shell

pion mass and this is wrong. When the pomeron

becomes massless it will act in a similar manner to a

photon and if the pion exchange is also massless then

the $\rho_{\pi\pi}$ vertex vanishes on angular momentum grounds

in exactly the same way as the $\gamma_{\pi\pi}$ vertex vanishes in

the forward direction. In practice these dips don't

seem to occur; for instance in the process $\gamma p \rightarrow \pi^+ n$

pion exchange vanishes in the forward direction but is

compensated by s and u channel nucleon exchange Born

terms required to preserve gauge invariance. Similarly

in the $\pi \rightarrow 3\pi$ dissociation the full gauge invariant set

of diagrams shown in fig. 19 maintain the pion peak

except of course when the resonance R has spin zero.

Although this refinement destroys some of the simplicity

of the Deck model it leaves all the results of the naive

calculation unaltered. We also note that because the

D peak occurs near the πR threshold the outgoing

πR state will be in a relative S wave and hence the

effective spin of the D resonance will be the same as

the R state and the parity opposite.

The model must also explain why Deck mass

enhancements cannot be produced non diffractively, for

instance in C.E.X. Clearly the Deck model cross-

section is determined by the size of the $\pi A \rightarrow \pi A$

forward peak rather than the total cross-section and the

relevant non diffractive processes have forward dips thus suppressing the corresponding Deck cross-section. For example the $\pi p \to A_1^0 p$ C.E.X. cross-section is calculated from the relative size of the forward peaks for $\pi^- p \to \pi^- p$ and $\pi^- p \to \pi^0 n$ and this results in a $\pi^- p \to A_1^0 n$ cross-section of approximately $1 \mu b$ compared with $10 \mu b$ in the resonance excitation picture. Cross-sections of this size will be unobserved and consequently we understand why the D-resonances are peculiar to diffraction.

Consider the $B \pi R$ coupling in the case where B is a pseudoscalar. Clearly it vanishes unless R is of natural parity and hence the outgoing D resonance must have unnatural parity. In the case where B is a nucleon the state R can have either natural or unnatural parity. However the ratio of the natural parity coupling to the unnatural parity is $\sim (m_R + m_N)/(m_R - m_N) \sim 10$ and hence the production of natural parity R states is suppressed. Consequently the emerging D state will have the same naturality as the incident nucleon. In general the Deck mechanism predicts the rule that there should be no change in naturality at a diffractive vertex. This anzatz, which was first discovered empirically by Morrison [25] is in agreement with experiment, although there is some dispute over its validity particularly in the boson sector. We point out that none of the baryon states listed in table 3 can have appreciable Deck cross-sections, either because the $N \pi R$ vertex has unnatural parity or the outgoing πR state has relative orbital

angular momentum other than zero and hence is relatively suppressed. For this reason it seems probable that the cross-section bumps in nucleon dissociation correspond to genuine resonances.

The Deck model also predicts the diffractive helicity structure. Consider the fragmentation of a pseudoscalar meson in the t-channel where the incident and outgoing particle R both move in the same direction. The pion exchange evidently can not change the helicity and hence T.C.H.C. is predicted for the R and consequently for the D. There is considerable evidence in favour of this prediction particularly for A_1 and Q production [26, 27]. We can also consider the nucleon dissociation and in exactly the same manner predict T.C.H.C. Here again the prediction is consistent with experiment [28, 29] but the amplitude $T^t_{\frac{1}{2}',-\frac{1}{2}}$ is also admissible. [See table 1].

The Deck mechanism alone however fails to explain the cross-over phenomena. The most transparent case is $K^0 \to Q^0$ and $\bar{K}^0 \to \bar{Q}^0$ which will be unaffected by normalization problems. The crossovers should be determined by the πN crossovers and hence the $Q^0 p$ cross-section should be larger at smaller t and steeper than $\bar{Q}^0 p$ just as the $\pi^- p$ compared with $\pi^+ p$ [30]. This is opposite to the data and hence there is at least one other effect over and above the Deck phenomenon. Finally we note that the Deck mechanism and its predictions are completely compatible with the Good Walker picture discussed in Chapter 1.

c)   Intermediate or hybrid picture

          arising from dual models

          Diffractive fragmentation is similar to

inelastic production processes.   In the Deck model

multiperipheral processes are taken to dominate, but

this cannot be a complete picture.   A better approach

is to substitute a complete model for the inelastic

processes treating the fragmentation as a collision

$PB \rightarrow X$, where P is a pomeron.   If the pomeron is

treated like a scalar particle, then the Veneziano model

may be used to predict the mass spectra in each of the

channels for boson dissociation [32].   These models

meet with considerable success especially considering

the fact that they are compared with data in a far more

detailed manner than any of the previous pictures.

          One general point arising from the dual models

is that the multiperipheral and resonance mechanisms are

both equivalent [31] provided all the resonances are

included.

3. A phenomenological analysis of diffraction dissociation reactions

3.1 Introduction

In this chapter we study the diffractive data from a phenomenological point of view adopting the resonance excitation mechanism. As mentioned in the previous chapter this mechanism alone is inadequate, particularly for boson dissociation where mass enhancement effects dominate over simple resonance production. For this reason we restrict the detailed data fits to $N^*(3/2^-, 1520)$ and $N^*(5/2^+, 1688)$ which are well established resonances. This, however, is not very much of a restriction as the differential cross-sections for boson dissociations are so simple that fitting is superfluous especially as it is known from density matrix measurements that only one t-channel helicity amplitude is populated. The cross-sections for fermion dissociation [33, 29, 39] $N \to N^*(1/2^+, 1470, 3/2^-, 1520, 5/2^+, 1688, 7/2^-, 2190)$ show much more structure. The $N \to N^*(1/2^+, 1470)$ is sharply peaked in the forward direction and is easily fitted with the S.C.H.C. amplitude alone and here the main problem is to understand the anomalously large slope. The $N \to N^*(3/2^-, 1520)$ cross-sections display a forward dip and hence is inconsistent with S.C.H.C. unless there is some coincidental dynamical reason for the dip and we investigate both these possibilities. Similarly the $N \to N^*(5/2^+, 1688)$ is incompatible with S.C.H.C. as the cross-section shows evidence of a plateau in the

small t region although one can dispute this. [29, 39]
Furthermore the density matrices for the $N^*(5/2^+, 1688)$
decay have been measured [28] and they indicate that
the only non zero amplitudes are $T^t_{\frac{1}{2}, \pm\frac{1}{2}}$.

In fitting data we assume diffraction proceeds
by pomeron exchange and neglect meson exchange effects
and the possibility of cuts. The reason for these
simplifying assumptions was that our main concern in
data analysis was to study the helicity properties of
diffractive vertices rather than produce detailed data
fits. This is interesting because it is known that
S.C.H.C. is conserved at the NN and $\gamma\rho$ vertices while
T.C.H.C. is favoured at the $\pi \rightarrow A_1$ and $K \rightarrow Q$
vertices and is consistent with the data for the
$N \rightarrow N^*(5/2^+, 1688)$ transition. As explained in
the previous chapter the Deck effect predicts the
results for boson dissociation and clearly it is
important to understand the helicity regularities also
observed in resonance excitation processes.

Suppose some unified explanation of these
regularities does exist on the basis of some dynamical
theory (e.g. the quark model) then simplicity would be
expected in the covariant couplings rather than helicity
amplitudes. Considerations of this sort motivated us
to adopt the covariant approach to Regge physics.
Furthermore covariant formalism obviates the need for
crossing and any apriori lorentz frame preference.

3.2 The covariant approach to Regge physics

A Regge exchange is conceived of as the exchange of a composite object, which will have a number of excited states lying on a trajectory together with lower daughter trajectories as shown in fig. 20 [34].

Consider some two body scattering process where the particles involved are taken to be spinless for simplicity. At high energy and small momentum transfer the cross-section will be determined by the exchange of the lightest particles with the allowed quantum numbers. It might be expected that good approximation to the scattering amplitude is simply the exchange of the lightest particle alone as in equation 1 where the exchange has spin J.

$$T_J \sim g_J^2(t) \, \frac{P_J(P \cdot Q)}{m_J^2 - t} \underset{s \to \infty}{\sim} g_J^2(t) \frac{(-\nu)^J}{m_J^2 - t} \qquad (3.1)$$

where g_J is the coupling constant and P_J is the Legendre polynomial with $\cos\theta$ replaced by $P \cdot Q$ This result cannot be correct for a number of reasons the most important of which is that the cross-section has the dependence $\sigma \sim \nu^{2J-2}$ and hence for J = 1 the cross-section is constant and the $J > 1$ the cross-section rises in violation of the Froissart bound. These difficulties are resolved by noting that the exchange is composite and so instead of taking the value of the spin at the lowest mass pole we should interpolate back along the trajectory where the effective spin is much smaller. For instance at t = 0 the effective spin of the vector meson trajectories is $\sim 1/2$ and hence $\sigma \sim S^{-1}$ in accord with table 2 and indeed all the results in table 2

follow in a similar manner except for diffraction
where there are no known poles from which to
extrapolate the pomeron trajectory. As the daughter
trajectories are lower in the J plane than the leading
particles their contribution to the cross-section falls
off more rapidly with energy and hence they can be
neglected. (Actually in dual models the degeneracy of
the daughters grows exponentially and hence they make
important contributions to the amplitude). Consequently
a good approximation to the scattering amplitude is the
exchange of the whole set of particles on the leading
trajectory as in equation 2 below

$$T \simeq \sum_{J} \frac{g_J^2(t)(-\nu)^J}{t - m_J^2} \qquad (3.2)$$

All the particles on the leading trajectory will have
the same naturality (e.g. the quark model) however it is
also useful to define trajectories of a definite parity
as parity is a good quantum number and this is achieved
by introducing a factor $(1 \pm (-)^J)/2$. The series in
equation 2 can be approximately summed using the
Sommerfeld-Watson transform trick to give the usual Regge
result (equation 3) provided the residue $\beta(t)$ which
interpolates the couplings $g_J(t)$ has reasonable analytic
properties.

$$T_{Regge} \simeq \beta^2(t) \frac{(1 \pm e^{-i\pi\alpha(t)})}{2 \sin \pi\alpha(t)} \nu^{\alpha(t)} \qquad (3.3)$$

The factor $\dfrac{1 \pm e^{-i\pi\alpha(t)}}{2\sin\pi\alpha(t)}$ is the Regge propogator

where $\alpha(t)$ is the trajectory function with $\text{Re}\,\alpha(m_J^2) = J$.

The covariant approach to Regge physics extends the preceeding results to scattering involving external spins by using the propogators and couplings for high spin particles [35].

High spin objects are described by Rarita Schwinger wave functions. Consider for instance the wave function for a spin J boson, this will be built up from J spin one wave functions $\in_\mu$ (such that $q\cdot\in = 0$). The product $\in_{\mu_1}^{m_1} \cdots\cdots \in_{\mu_J}^{m_J}$ will contain all the spins from J = 0 up to J, the irreducible representations having definite spin. The irreducible representation with spin J is totally symmetric and traceless $T_{\mu_1\cdots\mu_J}^{J\,m_J}$. Fermion wave functions are obtained by combining a boson wave function with a Dirac spinor.

The vertex for a spin S_1 particle making a transition to a spin S_2 object coupling to a spin J exchange is given by the expression

$$V(S_1, S_2; J m_J) = \overline{\psi}_{\nu_1\cdots\nu_{S_1}}^{S_2 m_2}\;\overline{\psi}_{\alpha_1\cdots\alpha_J}^{J\,m_J}\;\widetilde{G}_{\gamma_1\cdots\nu_{S_2}\gamma_1\cdots\alpha_J\mu_1\cdots\mu_{S_1}}\;\psi_{\mu_1\cdots\mu_{S_1}}^{S_1 m_1} \qquad (3\cdot4)$$

Assuming S_1 and S_2 are intergers. If they are half-intergers the labels μ and ν just extend to $S_i - \tfrac{1}{2}$. $\widetilde{G}$ is the coupling and examples of how this is deduced are given in appendices 2 and 3. Because the maximum total spin of the particles 1 and 2 is $S_1 + S_2$ only the first $S_1 + S_2$ of the internal α labels can couple to the spin and the remainder will have orbital couplings as in spinless scattering. The coupling

can therefore by written as below

$$\tilde{G}_{\nu_1 \cdots \nu_{s_1} \alpha_1 \cdots \alpha_J \mu_1 \cdots \mu_{s_1}} = G_{\nu_1 \cdots \nu_{s_1} \alpha_1 \cdots \alpha_{s_1+s_2} \mu_1 \cdots \mu_{s_1}} \varphi_{\alpha_{s_1+s_2 \tau_1}} \cdots \varphi_{\alpha_J} \qquad (3.5)$$

where G is the reduced coupling. The effect of $s_1 + s_2 > J$
J will be explained in the subsequent sections.

The scattering amplitude for spin J exchange
is now written as

$$T^J = \sum_{m_J} V(s_1 s_2; J, m_J) \frac{1}{t - m_J^2} V(s_3, s_4; J, m_J)$$

$$= \overline{\psi}^{s_2} G(s_2 s_1) \psi^{s_1} \varphi_{\alpha_{s_1+s_2} \cdots} \cdots \varphi_{\alpha_J} \sum_{m_J} \frac{\psi^{m_J}_{\alpha_1 \cdots \alpha_J} \overline{\psi}^{m_J}_{\beta_1 \cdots \beta_J}}{t - m_J^2}$$

$$\varphi_{\beta_J} \cdots \varphi_{\beta_{s_3+s_4+1}} \overline{\psi}^{s_4} G(s_4, s_3) \psi^{s_3} \qquad (3.6)$$

where some of the indices have been suppressed. As
$$\sum_m \epsilon_\mu^m \epsilon_\nu^{m*} = -g_{\mu\nu} + \frac{\Delta_\mu \Delta_\nu}{m_J^2} \qquad \text{and at high energy}$$
$P \cdot \varphi \gg P \cdot \Delta \varphi \Delta / m_J^2$ we conclude that the asymptotic
form for $\sum_{m_J} \psi^{m_J}_{\alpha_1 \cdots \alpha_J} \overline{\psi}^{m_J}_{\beta_1 \cdots \beta_J} \sim g_{\alpha_1 \beta_1} g_{\alpha_2 \beta_2} \cdots g_{\alpha_J \beta_J}$
Therefore if $s_1 + s_2 \geq s_3 + s_4$ we have

$$T^J \simeq \overline{\psi}^{s_2} G_{\alpha_1 \cdots \alpha_{s_1+s_2}}(s_1, s_2) \psi^{s_1} \frac{\nu^{J-(s_1+s_2)}}{t - m_J^2} \varphi_{\alpha_{s_1+s_2}} \cdots \varphi_{\alpha_{s_3+s_4+1}} \qquad (3.7)$$

$$\overline{\psi}^{s_4} G_{\alpha_{s_3+s_4} \cdots \alpha_1}(s_3, s_4) \psi^{s_3}$$

If we now sum over the spin of the exchange we obtain
the Regge pole exchange

$$T_{Regge} \simeq \overline{\psi}^{s_2} G(s_2, s_1) \psi^{s_1} \xi_\pm \frac{\nu^{\alpha(t)-(s_1+s_2)}}{\sin \pi \alpha(t)} \varphi_{\alpha_{s_1+s_2}} \cdots \varphi_{\alpha_{s_3+s_4+1}}$$

$$\overline{\psi}^{s_4} G(s_4, s_3) \psi^{s_3} \qquad (3.8)$$

where the factor $\xi_{\pm} = (1 \pm e^{-i\pi\alpha(t)})/2$ is called

the signature factor and this comes from including the

term $(1 \pm (-)^T)/2$ in the sum so that the exchange

has definite parity. The spin content of the

amplitudes is contained in the vertices $\bar{\psi}^{s_2} G \psi^{s_1}$ and

in the next section we calculate the asymptotic s-channel

helicity vertices for the processes relevant for

diffraction dissociation namely $0 \to J$, $1 \to 1$ and

$\frac{1}{2} \to J$. The vertex may be written asymptotically in the

form [36].

$$\bar{\psi}^{s_2\lambda_2}_{\nu_1\cdots\nu_{s_2}} G_{\nu_1\cdots\nu_{s_2}\alpha_1\cdots\alpha_{s_1+s_2}\mu_1\cdots\mu_{s_4}} \psi^{s\lambda_1}_{\mu_1\cdots\mu_{s_1}} \sim (-t)^{\lambda_2-\lambda_1} V_{\lambda_1\lambda_2} Q_{\alpha_1}\cdots Q_{\alpha_{s_1+s_2}} \quad (3.9)$$

where we have extracted the basic t dependence of the

vertex demanded by angular momentum conservation and kept

only the terms corresponding to the highest energy

dependence in the amplitude. $V_{\lambda_1\lambda_2}$ is the s-channel

helicity vertex where λ_1 and λ_2 are the initial and

final helicities respectively.

3.3 S-channel helicity vertices and boson dissociation

The s-channel helicity vertices for bosons

where calculated from the couplings listed in table 4

using the information given in appendix 3 and the results

are presented in table 5. [37] . Referring to table 5 it

can be seen that for $0 \to J$ transitions S.C.H.C.

corresponds to the coupling $g_{s_{+1}} g_{\mu_1\alpha_1}\cdots g_{\mu_{s_2}\alpha_{s_2}}$ which

couples the external spin to the internal exchange spin

with the minimum amount of orbital coupling. The

reason for this is that the vertex $\sim Q_{\alpha_1}\cdots Q_{\alpha_{s_2}}$ and

the only spin wave function with this property are

$\epsilon^c_\mu \sim Q_\mu/\mu'$ hence for the coupling $g_{s_{+1}} g_{\mu_1\alpha_1}\cdots g_{\mu_{s_2}\alpha_{s_2}}$

the final wave function must have helicity zero.

T.C.H.C. on the other hand corresponds to a pure

orbital coupling $g_1 \varphi_{\alpha_1} \cdots \varphi_{\mu_{S_2}} \varphi_{\mu_1} \cdots \varphi_{\mu_{S_2}}$ and hence

the t-channel helicity remains unaffected.

Mathematically this result can be seen as follows, in

the t-channel centre of mass the initial and final

bosons approach each other in a straight line and if

T.C.H.C. is to be violated at least one term in the

final state Rarita Schwinger wave function must be $\epsilon'^{\pm}_{\mu}$

and as $\epsilon^{\pm} \cdot \varphi = 0$ the pure momentum coupling

conserves T.C.H.C.

We also note that for $0 \to J$ transitions

S.C.H.C. is impossible for abnormal vertices and as

the pomeron has natural parity, S.C.H.C. implies

Morrisons rule for these processes. This result

follows directly from parity which for the vertices is

$$V^{\pm}_{\lambda_1, \lambda_2} = \pm (-)^{\lambda_1 - \lambda_2} V^{\pm}_{-\lambda_1, -\lambda_2} \qquad (3.10)$$

as the initial spin is zero $\lambda_1 = 0$ and for S.C.H.C.

$\lambda_2 = 0$ hence the abnormal vertex V^-_{oo} must vanish.

Of course T.C.H.C. also implies Morrisons rule for

identical reasons.

The vertices for the normal parity transition

$1^- \to 1^-$ are included because of its relevance via

vector dominance to the process $\gamma \to \rho$ which is

experimentally accessible. The coupling conserving

S.C.H. for $\rho \to \rho'$ scattering is $g_{\mu\nu} \varphi_{\alpha_1} \varphi_{\alpha_2} -$

$2 (g_{\mu\alpha_1} \varphi_\nu \varphi_{\alpha_2} + g_{\nu\alpha_1} \varphi_\mu \varphi_{\alpha_2})$ which is rather more complicated

than the simple results for $0 \longrightarrow J$ transitions. The

S.C.H.C. coupling for the process $\gamma \to \rho$ is obtained

from the above coupling by applying gauge invariance
and is given by $g'_{\mu\nu} Q_{\alpha_1} Q_{\alpha_2} - 2g_{\mu\alpha_1}(Q_\mu Q_{\alpha_2} - k\cdot Q\, g_{\mu\alpha_2})$
where k is the momentum of the photon and $g'_{\mu\nu} = (k\cdot Q\, g_{\mu\nu}$
$- Q_\mu k_\nu)$ Finally we consider the consequences of the
exchange spin J being less than the external spin.
If the exchange spin is such that a non zero coupling
implies an unphysical value for the orbital angular
momentum then it is a nonsense coupling.   For
example in $\rho \to \rho'$ vertex the coupling $g_{\mu\alpha_1} g_{\nu\alpha_2}$
is nonsense for J = 1 because this implies that $L = -1$
(see appendix 3) which is unphysical.   Alternatively
a coupling is nonsense for an exchange spin J   if such
a spin cannot couple because it has too few spin labels
to saturate the coupling.   If J_0 is a nonsense point
for some coupling and this spin also corresponds to a
particle pole then clearly the residue must vanish at
this point.   Suppose for instance the pomeron is
associated with a spin 2^+ particle then for $0 \to S$
transitions for $S \geq 3$ the pomeron cannot both
couple and conserve S.C.H. since the pomeron coupling
$g_{\mu_1\alpha_1} g_{\mu_2\alpha_2} \cdots g_{\mu_S\alpha_S}$ is nonsense for $J < $ S and hence
must vanish.

3.4   Fermion helicity vertices

The couplings given in table 6 for $\frac{1}{2} \to S$
vertices are easily deduced.   In appendix 2 the $\frac{1}{2},\frac{1}{2}$,
J coupling is derived.   All the higher spin transitions
$\frac{1}{2} \to S$ follow trivially from this result and the boson
couplings of table 4 because in the Rarita Schwinger
formalism the $\frac{1}{2} \to S$ vertex is simply reducable to
$C^\pm(\frac{1}{2},\frac{1}{2}) \otimes C^\tau(0, S-\frac{1}{2})$ as can be seen by comparing

tables 4 and 6.

Using the results of appendices 2 and 3 the s-channel vertices in table 7 are easily obtained. Notice that the γ_β coupling preserves S.C.H. in the $\frac{1}{2} \rightarrow \frac{1}{2}$ transition while for the $0 \rightarrow S - \frac{1}{2}$ transition S.C.H. is preserved by the coupling $g_{\mu\alpha} \cdots$ and hence the coupling to preserve S.C.H. for the transition is $g_{2s+1} \gamma_{\beta_1} g_{\mu_1 \beta_2} \cdots g_{\mu_{s-\frac{1}{2}} \beta_{s+\frac{1}{2}}}$. This is readily verified from the tables. Similarly as the ρ_β coupling preserves T.C.H. for $\frac{1}{2} \rightarrow \frac{1}{2}$ transition in the case $\frac{1}{2} \rightarrow S$ the T.C.H.C. coupling is $g_1 \rho_{\beta_1} \cdots \rho_{\beta_{s+\frac{1}{2}}} \rho_{\mu_1} \cdots \rho_{\mu_{s-\frac{1}{2}}}$. Referring to table 7 it can be seen that the T.C.H.C. coupling populates all the s-channel helicity vertices, conversely the S.C.H.C. coupling populates all the t-channel helicity vertices. Clearly the coupling $(g_1 \rho_{\beta_1} + g_2 \gamma_{\beta_1}) \rho_{\mu_1} \cdots \rho_{\mu_{s-\frac{1}{2}}} \rho_{\beta_2} \cdots \rho_{\beta_{s+\frac{1}{2}}}$ is the most general coupling to populate only the t-channel helicity vertices $V^t_{\frac{1}{2} \frac{1}{2}}$ and $V^t_{\frac{1}{2} -\frac{1}{2}}$.

Nonsense couplings are defined in exactly the same way as for bosons, namely a coupling is nonsense for exchange spin J_0 if a spin J_0 particle cannot produce the coupling because it has too many spin labels. (Orbital couplings ρ_β are of course irrelevant). Just as in the boson case if the pomeron is associated with a 2^+ particle (f dominance) then it cannot conserve S.C.H. for $S > \frac{5}{2}$ because the coupling is nonsense and must vanish.

Suppose J_0 is a nonsense point corresponding to some coupling function g_n then if the exchange has a pole at J_0 then the coupling must vanish at $\alpha = J_0$ and even if there is no pole then the coupling may vanish but need not. The behaviour of the coupling at nonsense points is called the nonsense mechanism and is restricted by the demand that the amplitude be analytic at these points. The other vertex may be sense or nonsense and hence we demand that the products $g_n g_n'$ and $g_n g_s$ be analytic. The common nonsense mechanisms are displayed in table 8 [36].

In the case of pomeron exchange we are interested in the behaviour of the couplings for $J_0 = 1$ $(\alpha_P - 1 = \alpha_P' t)$ which corresponds to the point $t = 0$. If diffractive scattering is to exhibit a forward peak in the cross-section, the strong fixed pole (S.F.P.) mechanism is the only possibility. However, the $N \rightarrow N^*(3/2^-, 1520), N^*(5/2^+, 1688)$ cross-sections do not have forward peaks and this could be due to other nonsense mechanisms as the S.C.H.C. coupling is nonsense at $J_0 = 1$ for both the $\frac{1}{2}^+ \rightarrow \frac{3}{2}^-$ and $\frac{1}{2}^+ \rightarrow \frac{5}{2}^+$ vertices. Of course, the density matrix results for the $N^*(5/2^+, 1688)$ decay indicate that these results are due to the presence of other amplitudes than the S.C.H.C. one rather than nonsense mechanisms.

3.5 Morrisons rule and covariant couplings

For pion dissociations it was found that Morrisons rule was a consequence of both T.C.H.C. and S.C.H.C. Considering the substitution rule $V^+_{\lambda_1,\lambda_2}(g; m_+, m_-) \rightarrow V^-_{\lambda_1,\lambda_2}(f; -m_-, m_+)(-)^{s_i - \lambda_2}$ for fermion vertices we can see that the boson result does not carry over to fermions. T.C.H.C. for instance implies that the abnormal amplitude is smaller than the normal amplitude by a factor $\sim m_-/m_+$ provided $g \sim f$ (which will be true in most constituent models). In the case of S.C.H.C. the normal and abnormal amplitudes will be of the same order. (again if $g \sim f$) This is unfortunate because Morrisons rule in fermion dissociation is consistent with the data and hence we must conclude that g is not of the same order as f or that there are accidental cancellations, for instance $m_- f_1 - f_2 \approx 0$. .

We now consider an argument which suggests that $f \sim t$ and so the abnormal production is suppressed in the forward direction and is hence unobserved [38].

The spin sum for the spin J propogator $\sum_{m_J} \psi^{m_J} \bar{\psi}^{m_J}$ is composed of terms like $\sum_m \epsilon^m_\alpha \epsilon^{*m}_\beta = -g_{\alpha\beta} + \Delta_\alpha \Delta_\beta / m_J^2$. When this is summed over J to obtain the Regge propogator $m_J^2 \rightarrow t$ and hence $\Delta_\alpha \Delta_\beta / m_J^2 \rightarrow \Delta_\alpha \Delta_\beta / t$. The contribution of factors like $\Delta_\alpha \Delta_\beta / t$ to the amplitude will be a power of ν lower than the leading term and so it is usually neglected, however it contains a $1/t$ singularity which

must be cancelled. If the factor $\Delta_\alpha \Delta_\beta / t$ is contracted with momentum couplings, as $p \cdot \Delta \sim m^2 - m'^2$ it will vanish for equal mass scattering and it is assumed to be cancelled by daughters in the unequal mass case. Now if we consider contracting Δ_β with the coupling γ_β $(\gamma_5 \gamma_\beta)$ then using the Dirac equation we obtain $\not{\Delta} \sim m_-$ for the normal vertex and $\gamma_5 \not{\Delta} \sim m_+$ for the abnormal vertex, and so for equal mass scattering the contribution of $\Delta_\alpha \Delta_\beta / t$ to the normal vertex vanishes but does not for the abnormal vertex. As this factor can occur in a leading order contribution to an invariant amplitude, for instance the A_1 contribution to $\gamma N \to \pi N$ and $N N$ scattering [40, 41], cancellations from daughters do not occur. Consequently f must develop a zero at t = 0 and hence we expect $f \sim t$ even in the unequal mass case. Consequently $\frac{d\sigma}{dt}\big|_{t=0} = 0$ at t = 0 for unnatural parity production in agreement with Morrisons rule. We have therefore proved that S.C.H.C. and indeed any γ_β coupling is consistent with this modified Morrisons rule.

3.6 <u>Preliminary discussion to the data fits</u>

As there are 6 independent couplings for $\pi N \to \pi N^*(5/2^+, 1688)$ and as we do not wish our data analysis to be just random fitting we must start with some physical considerations. Our view was that because the pomeron has a small slope and unit intercept we expect that it will simulate the behaviour of a vector

object.   Of course this does not have the
implication that we believe the pomeron to be a
vector particle especially in view of the fact that
J = 1 does not correspond to a pole on the pomeron
trajectory but simply for small t the exchange will
have unit angular momentum.   Hence the coupling will
be of the form $g_1 P_\beta + g_2 \gamma_\beta$.   This alone is
sufficient to fit the density matrices of Lambsa et
al [28] because the only t-channel amplitudes produced
by this coupling are $T^t_{\frac{1}{2} r \frac{1}{2}}$.   In elastic
scattering the γ_β coupling alone corresponds to
S.C.H.C. and hence we suggest that the generalization
of S.C.H.C. to inelastic nucleon diffraction is γ_β
or reduced gamma coupling (R.G.C.).   Notice that this
hypothesis has the advantage over S.C.H.C. that for
an f dominated pomeron the coupling does not vanish
for $S_F > 5/2$.   In the fits to the data we also
consider the possibilities of more general gamma
couplings, T.C.H.C. and S.C.H.C.   General fits have
too much freedom to be of any value.   A variety of
possible nonsense mechanisms were also considered as
a possible explanation for the small t structure in
$N \to N^*(3/2^-, 1520)$ and $N \to N^*(5/2^+, 1688)$.

3.7 Data fits

As previously mentioned we assume pomeron
dominance and fit the differential cross-section
data [33] for $\pi N \to \pi N^*(3/2^-, 1520), \pi N^*(5/2^+, 1688)$
and the density matrix data [28] for $N^*(5/2^+, 1688)$.

The s-channel amplitudes are paramarlized in the form

$$T^s_{\lambda_1 \lambda_2} \sim (-t')^{|\lambda_2 - \lambda_1|} V_{\lambda_1 \lambda_2} \, g_{\pi \pi \rho} \, \xi_+ \, \nu^{\alpha \rho(t)} \qquad (3.11)$$

where $\xi_+ = (1 + e^{-i\pi\alpha\rho})/2$, $t' = t - t_0$ and $V_{\lambda_1 \lambda_2}$
is the appropriate helicity vertex given in table 7.
The differential cross-section and the density matrices
are given by

$$\frac{d\sigma}{dt} = \frac{1}{2} \frac{1}{64\pi s p^2} \sum |T^s_{\lambda_1 \lambda_2}|^2 \qquad (3.12)$$

and

$$\rho_{\lambda \lambda'} = \sum_{\lambda'} T_{\lambda_1 \lambda} \, T^*_{\lambda_1 \lambda'} \Big/ 2 \sum_{\lambda_1 \lambda_2} |T_{\lambda_1 \lambda_2}|^2 \qquad (3.13)$$

An exponential t' dependence is included in the residues
along with the appropriate nonsense factor $N(\alpha_P)$
thus $g_{\pi\pi\rho} g_i = G_i e^{At'} N_i (\alpha_P)$. As the maximum $|t_0| \approx 0.0004$
we take $t' \approx t$.

The first point to note is that

$$\rho_{\frac{1}{2}\frac{1}{2}} = (|T_{\frac{1}{2}\frac{1}{2}}|^2 + |T_{\frac{1}{2}-\frac{1}{2}}|^2)/2\sum|T|^2 \qquad (3.14)$$

and it is clear that both T.C.H.C. (g_1) and $g_2 \gamma_\beta$
couplings give $\rho_{\frac{1}{2}\frac{1}{2}}$ = 0.5 in the Gottfried-Jackson
frame. To distinguish between these two couplings,
or a linear combination of the two, requires more
accurate forward direction data than is presently
available. The presence of two t-channel helicity
amplitudes for R.G.C. suggests that there will be a
slight fall off in the small t region in the
differential cross-section while T.C.H.C. predicts no
such fall off.

In fitting $\pi N \to \pi N^*(5/2^+, 1688)$ we find
that R.G.C. and T.C.H.C. are compatible with all the
data while S.C.H.C. with a S.F.P. nonsense mechanism
is compatible only with the differential cross-section.
As there is so little forward structure in $d\sigma/dt$
there is no point in fitting with a linear combination
of g_1 and g_2 especially as we note from table 9 that
$M_+ G_1 \approx G_2$. In fig. 22 we present a representative
best fit and also a fit using the Gell-Mann nonsense
mechanism. The factor $N(\alpha_\rho) \approx \alpha_\rho - 1$ introduced
into each coupling by the G.M. mechanism causes a
forward turn over and the data is consistently under
fitted in this region. The sense choosing fit with
γ - coupling approximates the T.C.H.C. and R.G.C. fits
as one might expect.

In fitting $\pi N \to \pi N^*(3/2^-, 1520)$ the
dominant influence is the forward turn over but even
here the couplings with G.M. nonsense factors underfit
the data in this region. The addition of multi-
pomeron cuts might improve the G.M. fit, but the effect
of such cuts would have to be inordinately strong to
bring our fit into line with the data. The T.C.H.C.,
R.G.C. and S.C.H.C. (with S.F.P.) fail to fit the turn
over and the best fit is achieved by gamma coupling
choosing either S.F.P. or sense. A linear combination
of g_1 and g_2 gives a moderately good fit (table 10).

Density matrix data and predictions in the
helicity frame are given in fig. 24. For the $N^*(5/2^+, 1688)$
only S.C.H.C. fails to fit the data and we feel that this

rules it out as a viable hypothesis. There is no density matrix data for the $N^X(\tfrac{3}{2}^-, 1520)$ and we present predictions, the most interesting being that for gamma coupling. It is clear from fig. 24b that $\rho_{\frac{1}{2}\frac{1}{2}}$ data with better that 10% error would serve to distinguish between R.G.C. and gamma coupling.

4.   Some attempts to unify diffractive scattering
      by using the idea of constituents

4.1 Introduction

If a hadron is composed of constituents then hadron-hadron scattering is reduced to scattering of the constituents.   For diffractive scattering the simplest assumption is that all diffraction is the result of elastic scattering among the constituents.   The most general formulation of this idea is the model of Chou and Yang (C.Y.) [42] which is flexible enough to include tightly bound systems of a few objects as in the quark model or many and perhaps indefinite numbers of internal degrees of freedom as in parton and dual models.

A specific example of the C.Y. model is to assume the constituents to be quarks.   Unfortunately however the non-relativistic quark model extended to diffraction dissociation by using Glauber theory, as in the C.Y. model, predicts zero-cross-section in the forward direction for all processes except elastic scattering [43, 44].

Carlitz, Frautschi and Zweig (C.F.Z.) [45] present a quark model in which the general systematics of diffraction dissociation are predicted.   The idea here is to extend the conservation of internal quantum numbers at diffractive vertices to the quantum numbers of the quark model.   The most interesting feature of this model is that it allows for a Hierarchy of strengths in diffraction dissociation due to the various symmetry breaking terms and this meets with considerable success for fermion dissociation.

Finally, Freund, Jones and Rivers (F.J.R.) [46] and Carlitz Green and Zee (C.G.Z.) [47] use the idea of duality to build a model for the pomeron coupling. This model can be extended and made more definite by the use of exchange degeneracy (E.X.D.) arguments and then it becomes the Kislinger model [48] which is closely related to the C.Y. model.   Unfortunately this model suffers from the same defect of the naive quark model in that it predicts forward cross-section dips for all diffractive processes except elastic scattering.

In this chapter we will describe and criticise the various constituent models of diffractive scattering.

4.2 The droplet model

Hadrons consist of a number of constituents, at least in the minimal sense of the virtual particles in field theory, and so a collision can be decomposed into the scattering of the constituents.   Physically the scattering is easiest to view in position space and at asymptotic energies because of lorentz contraction, the transverse impact distance is the only relevant parameter (See Fig. 25)

Consider a constituent of impact parameter b_{A_i} in A colliding with a constituent in B at impact parameter b_{B_j} then the S matrix is

$$S(b + b_{A_i} - b_{B_j}) = e^{-F_{ij}} \qquad (4-1)$$

At high energies the long range forces due to particle exchange become unimportant because the interaction time becomes essentially instantaneous.   Hence asymptotically unless particles A_i and B_i are in line i.e. $b + b_{A_i} - b_{B_j} \approx 0$

there will be no interaction i.e. $S(\underline{b} + \underline{b}_{A_i} - \underline{b}_{B_j}) = 1$ and we expect $F_{ij} \sim \delta^2(\underline{b} + \underline{b}_{A_i} - \underline{b}_{B_j})$. The full scattering matrix is the product of the individual scattering matrices

$$S(\underline{b}) = \prod_{ij} S(\underline{b} + \underline{b}_{A_i} - \underline{b}_{B_j}) = exp[-\sum_{ij} F_{ij}]$$

$$= exp[-\int \rho_A(\underline{x}_A) \rho_B(\underline{x}_B) F(\underline{b} + \underline{b}_A - \underline{b}_B) d\underline{x}_A d\underline{x}_B] \quad (4.2)$$

where $\rho_A(\underline{x}_A)$ and $\rho_B(\underline{x}_B)$ are the probability densities of constituents being at $\underline{x}_A$ in A and $\underline{x}_B$ in B respectively. The densities of constituents is presumably related to the charge density and from this hypothesis follow a number of interesting results for elastic scattering the most important of which is the Feynman-Wu-Yang conjecture [49] that

$$\frac{d\sigma}{dt}(AB \to AB) \sim \left(\frac{d\sigma}{dt}\right)_{t=0} |F_A(t)|^2 |F_B(t)|^2 \quad (4.3)$$

where F_A and F_B are the electric form factors for A and B respectively. Experimentally this relation compares with the data very favourably. (See ref. 4, ch. 5).

To extend this formalism to include diffraction excitation [42] ρ_A and ρ_B must be considered as q-numbers rather than c-numbers and consequently obey commutation rules like $\psi^+\psi$ where ψ is some (Fermi) field. Of course there may be many types of field and indeed to include all physical particles at least three fields are necessary for instance the u, d and s quark fields. However, as the number of different types of

field does not affect the results this complication is
ignored.   The s-matrix is now an operator and so
inelastic transitions can be calculated by taking matrix
elements.   When this formalism is applied to nucleus
nucleus scattering the model reduces to Glauber theory.

Chou and Yang take the fields in A to be
independent of the fields in B   (i.e. $[\mathcal{S}_A, \mathcal{S}_B] = 0$)
because there is little momentum transfer between
colliding beams of high energy.   Consequently the
collision just leads to a re-arrangement of the stuff in
the projectile and target.   The predictions for elastic
scattering are essentially similar to the c-number
theory provided the "blackness" of each hadron does not
fluctuate much as the constituents move around.

Now consider the diffraction excitation process
$AB \rightarrow A^* B^*$ where the stuff in A re-arranges itself to
become A^* and similarly for B and B^* .   The scattering
amplitude is

$$-T(t) = \text{Limiting amp as } s \rightarrow \infty = \int d^2 b \, e^{-i \vec{q} \cdot \vec{b}} \langle A^* B^* | S - 1 | AB \rangle$$

$$\overset{\text{Def.}}{=} [\langle A^* B^* | S - 1 | AB \rangle] = [\langle A^* B^* | S | AB \rangle] \qquad (4.4)$$

Just as for elastic scattering finite cross-sections at
infinite energy are expected for some processes dependent
on the nature of A^* and B^* and these are the diffraction
excitation reactions.   Chou and Yang derive a number of
selection rules which we quote.

i)   Because S depends only on space co-ordinates,
in the process $AB \rightarrow A^* B$, A and A^* (also B and B^*) must
have the same charge, G parity, Isospin, I_z, Strangeness
and baryon number.

ii)   Spin parity selection rule; for the diffraction excitation process AB → A*B*, A and A* (also B and B*) cannot both be spinless and have the opposite parity.

iii)   The differential cross-section will have a forward dip if the product of the parities is negative

$$\frac{d\sigma}{dt}(AB \to A^*B^*)\Big|_{t=0} = (1 + P_A P_B P_{A^*} P_{B^*}) A \qquad (4.5)$$

iv)   There is no left-right asymmetry as $s \to \infty$ in diffractive inelastic scattering off a transversely polarized target.

Also since $\psi_{B^*}^{+} \psi_{A^*} \psi_B \psi_A$ has a fluctuating phase for diffraction excitation processes it is expected that diffraction excitation will have a smaller cross-section than elastic scattering. Furthermore the phase fluctuations will be more rapid for higher excited states and so the cross-section will fall as the masses of A^* and B^* increase.   Hence it can be seen that although as s increases more and more channels become open, the two body cross-section need not grow without bound.

The predictions of the C.Y. model are summarized in table 11, where the states listed are the quark model predictions, not all of which are well established.   It can be seen that the C.Y. predictions for forward dips are consistent with the fermion data presently available. Elastic NN and N → $N^*(\frac{1}{2}^+, 1470)$ cross-sections both have strong forward peaks and the N → $N^*(\frac{3}{2}^-, 1520)$ a forward dip as predicted.   In table 11 there are a number of states listed which are not seen and this could be due to the relative suppression resulting from the forward cross-section dip; notice for instance that the N → $N^*(\frac{3}{2}^-, 1520)$

cross-section is a factor three smaller than the
$N \rightarrow N^*(\frac{1}{2}^+, 1470)$ cross-section. The only other
process for which the data is clear is the $N \rightarrow N^*$
$(\frac{5}{2}^+, 1688)$ for which no dip is predicted in accord
with the data which may however show a forward plateau
although this has been disputed. Notice also that the
values of the cross-section decrease with higher
excitation mass as anticipated.

The predictions for the boson data are more
difficult to test because the extent to which the data
is quasi-two body is ambiguous. For pion dissociations
the A_1, A_2 and A_3 are all predicted to occur, the A_1 and
A_2 with forward dips. The A_1 data doesn't appear to
exhibit any forward dip, however the direct resonance
production is obscrued by mass enhancement effects.
There is at present considerable controversy as to
whether the A_2 is diffractively produced or not. If the
A_2 is diffractively produced it will be a resonance
excitation process as it is forbidden by the Deck
mechanism and we note that like the A_1 it will be
relatively suppressed in the C.Y. model because of the
cross-section dip at $t = 0$. The predictions for
$K \rightarrow K^*$ are similar.

We also note that it is possible to produce
some resonances in double dissociation with forward
peaks when the single dissociation cross-sections both
dip at $t = 0$, for instance the $NN \rightarrow N^*(\frac{3}{2}^-, 1520)$
$N^*(\frac{3}{2}^-, 1520)$ cross-section can have a forward peak even
though $NN \rightarrow NN^*(\frac{3}{2}^-, 1520)$ cross-section dips at $t=0$.

Finally it is also clear that the C.Y. model will predict a generalized Feynman-Wu-Yang expression for the differential cross-sections in terms of the transition form factors $F_{AA^*}(t)$, $F_{BB^*}(t)$.

$$\frac{d\sigma}{dt}(AB \to A^*B^*) = \frac{d\sigma}{dt}\Big|_{t=0} |F_{AA^*}(t)|^2 |F_{BB^*}(t)|^2 \qquad (4.6)$$

4.3 A difficulty of the non-relativistic quark model

In the non-relativistic quark model the single scattering approximation to Glauber theory predicts a forward zero in the amplitude. To prove this we expand the s-matrix operator in equation (4) of the C.Y. model to first order.

$$T(\underset{\sim}{q}) = \sum_{ij} \int d^2\underset{\sim}{b}\, e^{-i\underset{\sim}{q}\cdot\underset{\sim}{b}} \langle A^*|\rho(b_i)|A\rangle \langle B^*|\rho(b_j)|B\rangle$$
$$\delta^2(\underset{\sim}{b}+\underset{\sim}{b}_i-b_j)\, d^2\underset{\sim}{b}_i\, d^2\underset{\sim}{b}_j$$
$$= \sum_{ij} \int d^2\underset{\sim}{b}\, e^{-i\underset{\sim}{q}\cdot\underset{\sim}{b}} \langle A^*|\rho(\underset{\sim}{b}_i)|A\rangle \langle B^*|\rho(\underset{\sim}{b}+\underset{\sim}{b}_i)|B\rangle\, d^2\underset{\sim}{b}_i \qquad (4.7)$$

where the summation is over the quarks i in A and j in B. Putting $\underset{\sim}{q}\cdot\underset{\sim}{b}=0$ for forward scattering and making a transformation at variable we obtain

$$T(\underset{\sim}{Q}) = \sum_{ij} \int d^2\underset{\sim}{b}_i\, d^2\underset{\sim}{b}_j\, \langle A^*|\rho(b_i)|A\rangle \langle B^*|\rho(b_j)|B\rangle \qquad (4.8)$$

Now if A is say a baryon and $i=3$ we have

$$\langle A^*|\rho(b_3)|A\rangle = \int d\underset{\sim}{r}_1\, d\underset{\sim}{r}_2\, dz_3\, \psi_{A^*}^*(c_1,c_2,c_3)\, \psi_A(c_1,c_2,c_3)$$
$$\delta^3(c_1+c_2+c_3) \qquad (4.9)$$

In the limit $s \to \infty$ conservation of energy implies $q_{A^*} = q_A$ and so clearly equation 8 is just the orthonormality equation for the wave-functions ψ_{A^*} and ψ_A and similarly ψ_{B^*} and ψ_B; hence $T(\underline{Q}) = 0$ unless $A^* = A$ and $B^* = B$.

Parry [50] suggests that this embarrassing result will be removed in a relativistic theory; the point is that when $m_{A^*} \mp m_A$ the lorentz contraction effects on the initial and final wave-functions will be different and so orthogonality is lifted.

Byers and Frautschi [51] and Le Yaouanc et al [52] suggest that the difficulty can be removed within the context of a non-relativistic theory by working in a frame in which the composite system moves slowly both initially and finally. Such a system is the Briet frame and here the momentum transfer corresponding to forward scattering does not vanish (also $\underline{q} \cdot \underline{b} \neq 0$) and hence the single scattering amplitude does not vanish for forward scattering.

J.S. Bell [53] has generalized the non-relativistic quark model for diffraction excitation to a relativistic theory in the light plane formalism and suggests that neither of the proposed methods of resolving the forward zero in the single scattering approximation are valid.

4.4 The Carlitz, Frautschi, Zweig (C.F.Z.) quark model

As explained in the previous section the naive application of the quark model to diffraction excitation predicts cross-sections with forward dips which is contrary to experiment. It is hoped that this difficulty may be

removed but in the meantime ignoring the problem we may
nevertheless predict the general systematics of diffraction
in the quark model.   The paradigm model of this type is
due to Carlitz-Frautschi and Zweig [45].

C.F.Z. extend the empirical result that there
is no change in I, B, Q, B, G at a diffractive vertex to
the conservation of the internal quantum numbers of the
quark model.   They present two arguments for this
hypothesis

i)   If a compound state results from elastic
scattering of its components then no internal
quantum numbers change.

ii)   If the diffraction dissociation amplitude
is built up by unitarity from a coherent sum
over intermediate states

$$\mathfrak{I}_m \, T(AB \to A^*B^*) = \sum_X T(AB \to X) \, \rho_X \, T(X \to A^*B^*) \qquad (4 \cdot 10)$$

maximum coherence occurs when the quantum numbers
of the final state are as close as possible to the
quantum numbers of the initial state.

C.F.Z. use the non-relativistic SU(6)
classification and for a particular SU(3) multiplet there
is no change in quark spin or generalized charge conjugation
G .   A summary of the predictions is presented in table 11.
Consider first the N $\longrightarrow$ N* reactions;   only $\underline{56} \longrightarrow \underline{56}$
transitions are allowed in first order, thus
N $\longrightarrow$ N*($\frac{1}{2}^+$, 1470), N*($\frac{5}{2}^+$, 1688) are allowed.   Of course
there are SU(6) symmetry breaking terms and hence the
$\underline{56} \to \underline{70}$ transitions N $\longrightarrow$ N*($\frac{3}{2}^-$, 1520), N ($\frac{7}{2}^-$, 2190) do
occur but are relatively suppressed.   Notice that the

differential structure for allowed reactions is different from that for the forbidden reactions and appears to conform to the predictions of the C.Y. model. Indeed referring to table 11 it can be seen that the C.Y. model predicts a dip for all C.F.Z. forbidden reactions. Furthermore we note that the forward cross-sections for forbidden reactions are $\sim 10\%$ of the allowed results (see table 12) as expected from $SU(6)$ breaking terms but the total cross-section values for forbidden reactions are only about a factor 3 less than the allowed values which suggest a mechanism other then $SU(6)$ breaking.

Now consider the boson dissociations for which the only first order allowed processes are $\pi \to A_3$ and $K \to L$. The transitions $\pi \to A_1 A_2$ and $K \to K^*(1240) Q$ are both forbidden by quark spin conservation. Although the $\pi \to A_1$ and $K \to Q$ transitions have cross-sections $\sim \frac{1}{10} \sigma_{el}$ the prediction of the C.F.Z. model is not necessarily wrong because these processes may be almost entirely due to mass enhancement effects. Evidently Morrisons rule is not obeyed in general although for πK projectiles all the first order allowed transitions are consistent with this anzatz. This is because if the quark spin remains zero then the spin of the produced hadron is the same as the orbital angular momentum L of the quarks and thus the final parity

$$P_f = - (-)^L = (-)^{J+1} \quad \text{and hence} \quad \Delta P = (-)^J \quad \text{which}$$

is Morrisons rule. However, when the quark spin changes as in the transitions $\pi \to A_1, A_2$ there is no general consistency with Morrisons rule.

The main defect of the C.F.Z. model is that the spin is treated on exactly the same basis as other internal variables and yet it is not a relativistic invariant; hence the C.F.Z. model will be frame dependent. This defect can be remedied by using the relativistic $SU(6)_W \otimes O_t(2)$ vertex symmetry. As this group is relativistically invariant for colinear processes we treat the problem in the t-channel centre of mass where the particles at a vertex all move in a straight line. Clearly all the predictions of the C.F.Z. model remain the same except now in addition we predict T.C.H.C. Of course, this cannot be entirely correct because the $N \rightarrow N$ transition conserves S.C.H. This result may also be included by allowing quark spin flip which is the most general vertex interaction. (Of course we maintain $L_Z = 0$ for the $O_t(2)$ symmetry). Clearly we still predict the correct helicity structure for $N \rightarrow N^*(3/2^-, 1520)$, $N^*(5/2^+, 1688)$ namely the amplitudes $T^t_{\frac{1}{2},\pm\frac{1}{2}}$ as both states have quark spin $\frac{1}{2}$. Furthermore if the relative values of the flip and non-flip values are adjusted to give S.C.H.C. then the flip amplitude is proportional to $\sqrt{-t}$ and hence we correctly predict a forward dip for the $\underline{56} \rightarrow \underline{70}$ transition $N \rightarrow N^*(3/2^-, 1520)$. Thus this modified C.F.Z. model reproduces all the fermion data and this is essentially the approach of Le Yaouanc et al [54], although they work in a non-relativistic framework.

We now consider the modified C.F.Z. model applied to bosons. Of course the successful prediction of T.C.H.C. for $\pi \rightarrow A_3$ and $K \rightarrow L$ are still maintained.

However we now also allow $\pi \rightarrow A_1, A_2$ and $K \rightarrow K^*(1420), \varphi$ in first order but predict T.C.H. flip ($T^t_{c,\pm 1}$) rather than T.C.H.C. and also forward dips in the cross-section as in the C.Y. model, both of which are contrary to the date. To obtain the correct result for $\pi \rightarrow A_1$ etc. we must introduce a substantial amount of spin orbit interaction and a model with this property is presented in Ch. 7

4.5 The twisted loop dual quark model

The twisted loop quark model of F.J.R. [46] and C.G.Z. [47] is based on the two component duality ideas of Freund and Harari [55]. In this picture the high energy two body scattering amplitude A can be decomposed into two parts, one A_P due to diffraction and the other A_R corresponding to Regge exchanges. According to the Freund-Harari hypothesis the Regge contribution is built up from s-channel resonances while the diffractive amplitude corresponds to non-resonant intermediate states.

These ideas may be pictorially represented in the quark model [56]. In a scattering process quark lines are drawn for all the external particles and they are connected in valid duality diagrams such that the quark lines do not change their nature and $q\bar{q}$ pairs in the same hadron do not annihilate. (Presumably $q\bar{q}$ pair annihilation in the same hadron correspond to weak and electromagnetic processes $q\bar{q} \rightarrow$ leptons).

Figs. 26, 27, 28, 29 and 30 display a number of valid quark duality diagrams, together with the corresponding Veneziano representations. Fig. 26 and 27 are the only valid diagrams corresponding to single

particle exchange for meson meson scattering.   Fig. 26
will evidently contribute to A_R but fig. 27 cannot
because there are no s-channel poles.   To construct
higher order diagrams the simple one particle exchange
diagrams are iterated using s-channel unitarity and the
results correspond to figs. 28, 29 and 30.   Notice that
diagrams 28 and 29 both have s-channel poles and so
contribute to A_R.   Fig. 30 is interesting because it
corresponds to a two particle s-channel intermediate state
which contributes to the background.   Furthermore as there
is no net exchange of quarks the t-channel singularity has
vacuum quantum numbers and hence the diagram is a suitable
candidate for the pomeron singularity.   In the Fubini
Veneziano model this diagram can be computed and is in
general a cut, but for space-time dimensions 26 it
becomes a pole.   Despite the unphysical nature of this
result it is possible to extract some phenomenological
information from the diagrams alone ignoring the detailed
mathematical correspondence and such a program corresponds
to the twisted loop quark model of F.J.R. and C.G.Z.

Using the duality transformations as in fig. 30
it can be seen that the pomeron coupling is dominated by
resonances.   The internal loop connecting the upper and
lower vertices may be regarded as a vacuum fluctuation and
hence we may deduce that the pomeron has vacuum quantum
numbers i.e. SU(3) singlet with natural parity and
$G = +1$.   As the only well known resonances with these
properties are the f and f' it is assumed that the
pomeron couples via f and f' in the SU(3) singlet
combination f_1 .

The model can also include symmetry breaking in the sense that the f and f' trajectories are not degenerate, the f' being heavier and hence lower. For this reason the f and the f' cannot cancel one another and hence diffraction dissociation is allowed for any process for which either the f or the f' couple to both vertices, but of course we are mainly interested in the first order allowed processes. For boson dissociations the only significant restriction is generalized charge conjugation G , as in the C.F.Z. model and thus in this model $\pi \rightarrow A_1, A_2, A_3$ are all allowed. The $N \rightarrow N^*$ transitions are not very interesting because all the reactions listed in table 11 are allowed. The helicity properties of the pomeron coupling are, of course, predicted to be the same as these for the f, f' couplings.

For further predictions the model must be made more quantitative [47]. Referring to fig. 30 it can be seen that the J-plane amplitude may be written in the form

$$\mathcal{I}_m T(J,t) = \sum_{ij} \frac{\beta_{iAA^*}(t)}{J - \alpha_i(t)} \; B_{ij}(J,t) \; \frac{\beta_{jBB^*}(t)}{J - \alpha_j(t)} \qquad (4.11)$$

$1/(J - \alpha_i(t))$ is the propogator for particle i where i and j are labels for the vacuum quantum number exchanges, β_{iAA^*} is the coupling of i to the AA^* vertex and $B_{ij}(J,t)$ represents the pomeron singularity. The Fubini Veneziano model for the pomeron takes this form.

It is not our intention in this survey to give an exhaustive account of the predictions following from equation 11, however we mention that the ratio of the $K\rho$ to $\pi\rho$ cross-sections are predicted with impressive accuracy. One further interesting feature of equation 11 is that if the ρ is exchange degenerate with the f then the vertices will, by vector dominance resemble the electromagnetic coupling and hence the model is linked with the C.Y. approach. The extreme form of this idea is the Kislinger model [48] where the pomeron is replaced by an SU(3) singlet conserved vector current. Though this idea makes the predictive power of the model much higher it is wrong because it implies that all normal parity vertices vanish in the forward direction, (this result is easily proved in covariant formalism) which is contrary to data. Hence we conclude that the idea of identifying the pomeron with a conserved vector current is wrong although it may be correct to assume the pomeron couples like a vector particle.

5. Some approaches to relativistic quark models

5.1 Introduction

In this chapter we consider some attempts to incorporate relativity in the "constituent" quark model. Such a generalization is certainly necessary so as to include high energy scattering phenomena (c.f. Chapter 4 section 3) and also because the internal quark velocities are not small compared with the speed of light, particularly for mesons. Furthermore a relativistic version of the model is needed to provide a more adequate theoretical basis for quarks.

If quarks are fundamental particles then the starting point should be field theory. The most natural model is to consider quarks to be bound by a neutral vector "gluon" field and this view has proved successful in formulating both the current commutation relations [19] and light cone algebra [57]. However, if this picture is taken seriously rather than just a framework from which to abstract algebraic results then it leads to difficulties. The mass spectrum emerging from this model can be predicted by considering the bound state problem in the Bethe Salpeter equation (with the Ladder approximation) and it bears no relation to the physical mass spectrum [58]. Indeed any model for which the "potential" is singular at the origin will not lead to rising Regge trajectories with approximately even spacing [59]. Neglecting spin complications exactly linear Regge trajectories are obtained from harmonic oscillator quark quark interactions. Clearly such an interaction is unphysical. This is not

only because the harmonic oscillator has infinite range, as potentials like $- A \exp(-b^2 r^2)$ would also give approximately linear trajectories for the low lying states, but rather because the physical origin of this interaction is obscure. Of course this problem is not confined to the quark model as it is difficult to find any dynamical explanation whatsoever for linear rising trajectories although one suggestion [60] is that trajectories continue to rise due to the effects of coupling to higher multiplicity intermediate states. However, we will simply accept linearly rising trajectories as a fundamental fact and this attitude conforms to the dual model philosophy.

In formulating relativistic quark models it is important to maintain a close relation with the non-relativistic model so that the successful predictions of this model are not destroyed. The most direct approach is to construct covariant wave-functions by boosting the non-relativistic results, and this is quite simple because in the $SU(6)$ quark model the spin is decoupled from the potential. However, it is difficult to understand this result in a relativistic theory and indeed the evidence favours a considerable spin-orbit interaction at least for mesons. [Chapter 1 section 5 ii]

The most straight-forward extension of the non-relativistic quark model is to assume the potential to be a covariant oscillator in a scalar equation and to incorporate quark spin by using boosted spinors. This is the approach of Feynman Kislinger and Ravndal (F.K.R.) [61] the results of which are about as good as the non-

relativistic model but now there are fewer free parameters. The main defect of this approach is that spin is not treated dynamically.

Clearly a more adequate starting point is the Bethe Salpeter equation for spinor quarks. However, in a model of this sort, the calculational simplicity of the F.K.R. approach is lost. The most interesting model of this type is due to Bohm, Joos and Kramner (B.J.K.) [62] where the Bethe Salpeter equation for a quark antiquark pair bound by the most general covariant oscillator potential is solved perturbatively from analytic solutions for the mass zero equation.

5.2 Covariant wave-functions and the Bethe Salpeter equation

A covariant wave-function describing a bound state of n particles $\psi(1,2,\cdots n)$ transforms under a Lorentz boost Λ as a tensor product of one particle states.

$$\psi(1,2,\cdots n) \xrightarrow{\Lambda} S_1(\Lambda) S_2(\Lambda) \cdots S_n(\Lambda) \psi(1,2,\cdots n) \qquad (5.1)$$

where $S_i(\Lambda)$ is the Lorentz boost for the ith particle. Our main interest is in the two particle fermion anti-fermion bound state which is described by a wave-function $\psi_{\alpha\beta}$ where α is the spinor index and β the antispinor index. $\psi_{\alpha\beta}$ can be treated as a 4 x 4 matrix and if it is expanded in terms of invariants formed from the Dirac bilinear covariants $\Gamma = (1, \gamma_5, \gamma_\mu, \gamma_5\gamma_\mu, \sigma_{\mu\nu})$ then it will automatically have the correct Lorentz transformation properties.

We now consider the equation for the covariant wave-function due to Bethe and Salpeter [63]. The two particle Bethe Salpeter wave-function is diagramatically represented on the left-hand side of fig. 31. (Of course the inclusion of the propagators is purely for convenience). The binding is due to the repeated action of a basic irreducible potential V composed of all graphs which do not separate into two graphs when the constituent particle lines are cut. (As these graphs are already included, see figs. 32 and 33). Because the potential acts an infinite number of times one further interaction will leave it unaltered and hence we have the Bethe Salpeter equation shown in fig. 31. Clearly it is easy to generalize this equation to bound states of several particles and fig. 34 shows the equation for a three particle bound state.

We now consider the special case of a fermion-anti-fermion bound state; the Bethe Salpeter equation in momentum space is

$$\psi_{P_{\alpha\beta}}(q) = \lambda \frac{1}{(\frac{\not{P}}{2} + \not{q} - m_q)_{\alpha\gamma}} \frac{1}{(\frac{\not{P}}{2} - \not{q} + m_q)_{\beta\delta}} \int \frac{d^4 k}{(2\pi)^4} V_{\gamma\delta}(P; k, q)_{\sigma\kappa} \psi_{P_{\sigma\kappa}}(k)$$

$$(5.2)$$

where the repeated indices are summed over and $\not{A}_i = A_\mu \gamma_i^\mu$. In position space this equation is in general an integro-differential equation, however when the potential just depends on the exchange momentum i.e. $V(P; k, q) = V(k - q)$ then the equation 2 becomes a differential equation (equation 5.3) in position space and this is the ladder approximation.

$$\left(\frac{\not{P}}{2} + i \not{\partial} - m_q\right) \psi_P(x) \left(\frac{\not{P}}{2} - i \overleftarrow{\not{\partial}} + m_q\right) = \lambda V(x) \psi_P(x) \qquad (5.3)$$

x is the co-ordinate conjugate to q.

The Bethe Salpeter equation is homogeneous and hence the wave-function normalization is undetermined. The simplest procedure is to normalize to the charge on the constituents as in fig. 35. For spinor - anti-spinor constituents the result is

$$\langle \psi_p | \frac{j^A(q=0)}{\varrho_A} | \psi_p \rangle = \int \frac{d^4k}{(2\pi)^4} Tr \left[\bar{\psi}_p(k) \gamma_\mu \psi_p(k) (\frac{\not{P}}{2} + \not{k} + m_q) \right]$$

$$\equiv 2 P_\mu \qquad\qquad (5.4)$$

where the factor $(\frac{\not{P}}{2} + \not{k} + m_q)$ is to cancel the extra propogator which would otherwise be included and ϱ_A is the charge on the particle A and $\bar{\psi} = \gamma_0 \psi^\dagger \gamma_0$.

5.3 Relativistic wave-functions from physical considerations

The most general form for the pseudoscalar ground state meson (0^{-+}) is [64]

$$\chi_p = \gamma_5 (A + B\not{P} + q \cdot P C \not{q} + D \sigma_{\mu\nu} q^\mu P^\nu) \qquad (5.5)$$

where A,B, C and D are even functions of $q \cdot P$. If it is assumed that the ground state is a pure S-wave as in the non-relativistic quark model then equation 5 reduces to $\qquad \chi_p = \gamma_5 (A + B\not{P}) \qquad\qquad (5.6)$

Similarly for vector mesons, neglecting all but the S-wave states (and therefore any spin orbit interaction) we obtain $\qquad \chi_v = \not{\in} (A' + B'\not{P}) \qquad\qquad (5.7)$

where $\in_\mu$ is a spin one wave-function.

If we wish to approximate the non-relativistic model then in the rest frame the wave-function should act like the product of a spinor and anti-spinor at rest. Boosting this into the general frame we obtain the results [64, 65].

$$\chi_\rho = \gamma_5 \left(1 - \frac{\not{P}}{m_\rho}\right) \varphi_\rho(q^2)$$

$$\chi_V = \not{\epsilon} \left(1 - \frac{\not{P}}{m_V}\right) \varphi_V(q^2)$$

(5.8)

This is the approach of the boosted symmetry schemes $(U(6,6))$ however such wave-functions correspond to weak binding.

If the quarks are regarded as real objects with a large mass $M_q \gg M_{meson}$ then the binding energy $\sim 2M_q$ and the "individual quarks" have effectively zero energy. Hence we expect the amplitude for the "negative energy" part of the wave-function to be of the same order as the "positive energy" component. For the forms given in equations 6 and 7 there are only two possibilities of this type and these are

$$\chi_\rho = \gamma_5 \left(1 + O\left(\tfrac{1}{m_q}\right)\not{P}\right) \varphi_\rho(q^2)$$

$$\chi_V = \not{\epsilon} \left(1 + O\left(\tfrac{1}{m_{q_V}}\right)\not{P}\right) \varphi_V(q^2)$$

(5.9)

$$\chi_\rho = \gamma_5 \left(\not{P} + O\left(\tfrac{m^2}{m_q}\right)\right) \varphi_\rho(q^2)$$

$$\chi_V = \not{\epsilon} \left(\not{P} + O\left(\tfrac{m^2}{m_q}\right)\right) \varphi_V(q^2)$$

(5.10)

Equations 8, 9 and 10 are the three possible forms
for the Bethe Salpeter wave-functions of the pseudo-
scalar and vector mesons considered by Llewellyn-
Smith [64]. Similarly it is simple to deduce the
expected form for the higher orbital states provided
orbital mixing and spin orbit terms are neglected.

We now proceed to discuss the expected form of
the Baryon wave-functions. This is important because
the solution of the Bethe Salpeter equation for baryons
is evidently much more difficult than for mesons. We
will just consider the orbital momentum zero states as
for mesons. Clearly the nucleon $\sim u \chi_\rho C^{-1}$ and
the $\Delta \sim u \chi_V C^{-1}$ where u is some spinor and C the
charge conjugation matrix. In the case of the boosted
non-relativistic wave-functions the results are simple
and are [65]

$$\psi_N = \left[\gamma_5 \left(1 - \frac{\not{p}}{m_N}\right)_{ab} C^{-1} u_c(p)(q_a q_b - q_b q_a)q_c + \begin{smallmatrix} cyclic\ perms \\ a,b,c \end{smallmatrix} \right] \psi_N(q^2)$$

$$\psi_\Delta = \sum_{m\lambda} C_{3/2}^{m\lambda} \left[\not{\epsilon}^m \left(1 - \frac{\not{p}}{m_\Delta}\right)C^{-1} u_c^\lambda(p)(q_a q_b + q_b q_a)q_c + \begin{smallmatrix} cyclic \\ perms \end{smallmatrix} \right] \psi_\Delta(q^2)$$

$$(5.11)$$

where $u(p)$ is a free spinor of momentum p and mass $m_N (m_\Delta)$
q_a, q_b, q_c are the SU(3) quark wave-functions
and $C_{3/2}^{m\lambda}$ are the Clebsch Gordon co-efficients for
projecting spin $3/2$ out of $1/2 \otimes 1$

In the strong binding limit just as for
mesons the wave-function will be made up of a combination
of pure "positive energy spinors" and pure "negative

energy spinors" with approximately equal amplitude
and hence the nucleon is constructed from

$$u^+(\rho)\,\gamma_5\left(1-\frac{\not{p}}{m_N}\right)C^{-1} + \alpha\,u^-(\rho)\,\gamma_5\left(1+\frac{\not{p}}{m_N}\right)C^{-1}$$

and the Δ (5.12)

$$u^+(\rho)\,\not{\epsilon}\left(1-\frac{\not{p}}{m_\Delta}\right)C^{-1} + \alpha\,u^-(\rho)\,\not{\epsilon}\left(1+\frac{\not{p}}{m_\Delta}\right)C^{-1}$$

where $u^+(u^-)$ is a positive (negative) energy free
spinor, and α some phase. (Recall as in the non-
relativistic model the quark velocity is small). The
phase α is difficult to estimate although the value

$\alpha = \pm 1$ would be consistent with meson solutions
given in equation 5.9.

5.4 The Feynman Kislinger Ravndal quark model

The F.K.R. quark model [61] generalizes the
harmonic oscillator non-relativistic quark model [56]
to include relativity in the simplest possible manner,
in particular the spin is taken to be independent of the
binding potential and orbital motion.

Consider the non-relativistic harmonic
oscillator quark model for mesons. If p_1, p_2 and
x_1, x_2 are the momentum and positions of the quark
and antiquark respectively then the Hamiltonian is

$$H = \frac{1}{2m_q}p_1^2 + \frac{1}{2m_q}p_2^2 + m_q\,\omega_0^2\,(x_1-x_2)^2 \qquad (5.13)$$

Defining $q = (p_1-p_2)/2$ and $x = x_1-x_2$ as the relative
momentum and position, then in the rest frame equation
13 becomes

$$H = \frac{1}{m_q}q^2 + m_q\,\omega_0^2\,x^2 \qquad (5.14)$$

Defining $\omega = m_q \omega_0$ this may be rewritten in the form

$$4 m_q H = 4 (q^2 + \omega^2 x^2) \qquad\qquad (5.15)$$

Now the relativistic energy squared is $m^2_{meson} = (2 m_q + H)^2$

$\approx 4 m_q^2 + 4 m_q H$ and hence if $4 m_q^2$ is added to

equation 5.15 we obtain

$$m^2_{meson} = 4 (q^2 + \omega^2 x^2) + constant \qquad\qquad (5.16)$$

This equation has the advantage that the quark mass

does not occur explicitly.

The natural relativistic analogue of equation

5.15 is

$$K = -2 (p_1^2 + p_2^2 + 2 \omega^2 (x_1 - x_2)^2) \qquad\qquad (5.17)$$

where $p_{1\mu}$, $p_{2\mu}$, $x_{1\mu}$ and $x_{2\mu}$ are the 4-vector momentum

and positions of the quark and antiquark. (Note

$K \sim 4 m_q H$ then equation 17 follows from equation 13).

Of course K has the dimensions of mass squared and the

oscillator has been chosen to be 4-dimensional to maintain

covariance in a simple way. Defining $p_1 = \frac{P}{2} + q$, $p_2 = \frac{P}{2} - q$

and $x = x_1 - x_2$ equation 5.17 may be rewritten,

separating out the centre of mass motion in the form

$$K = P^2 - 4 (q^2 + \omega^2 x^2)$$

or $$K - P^2 = -4 (q^2 + \omega^2 x^2) \qquad\qquad (5.18)$$

Comparing with equation 15 , $K - P^2$ is identified with the

mass squared operator (In chapter 6 we will present

an alternative argument for this result). Defining the

creation and annihilation operators

$$a^{\dagger}_{\mu} = (q_{\mu} + i \omega x_{\mu})/\sqrt{2\omega} \qquad a_{\mu} = (q_{\mu} - i \omega x_{\mu})/\sqrt{2\omega}$$

and setting $\Omega = 8 \omega$ we obtain

$$m^2 = -\Omega \, a^{\dagger}_{\mu} a^{\mu} + constant \qquad\qquad (5.19)$$

Clearly the states lie on straight Regge trajectories
with slope Ω^{-1}. The ground state meson then
corresponds (apart from the spin) to the oscillator
vacuum state $|0\rangle$ defined by $a_\mu |0\rangle = 0$ and all
the higher excited states are generated by the action
of the creation operators, for instance the first
excited state is $a^+_\mu |0\rangle$. From the commutation
relations $[a_\mu, a_\nu^+] = -g_{\mu\nu}$ it can be seen that the time-
like excitation $a_0^+ |0\rangle$ has negative normalization,
explicitly

$$\| a_0^+ |0\rangle \| = \langle 0 | a_0 a_0^+ |0\rangle = \langle 0 | a_0 a_0^+ - a_0^+ a_0 |0\rangle = - \langle 0 | 0 \rangle = -1 \quad (5.2c)$$

A similar problem occurs in electrodynamics quantized in
a covariant manner, (also dual models c.f. chapter 1)
however in this theory there exist subsiduary (gauge)
conditions which decouple the unwanted states.
(Actually the time like states are cancelled by the
longitudonal states and the gauge conditions effectively
decouple two states making the photon transverse).
F.K.R. eliminate the unwanted time like states by decree.
In the rest frame a state $|s\rangle$ will contain no time like
excitation modes if $a_0 |s\rangle = 0$ or $m a_0 |s\rangle = P.a |s\rangle = 0$
and this is the gauge condition adopted. However now
(unlike Q.E.D.) the set of physical states is no longer
complete and unitarity will be violated. As a
consequence the calculated matrix elements will be too
big and so F.K R. introduce an ad hoc correction factor F
to compensate for this.

Quarks have spin $\frac{1}{2}$ and yet the operator
contains no reference to spin. Of course the spin has
been excluded so as to retain the close relation to the

non-relativistic model, however the spin is important
in the presence of interactions. For the purpose of
deriving the electromagnetic interaction from the mini-
mal substitution $p_{i\mu} \to p_{i\mu} - e_i A_i$ the terms p_i^2 in equations
5.18 is interpreted as $\phi_i \phi_i$ where $\phi_i = p_{i\mu} \gamma_i^\mu$
To first order in the electric charge the electromagnetic
interaction is

$$H_{e.m.} = -2 \sum_i e_i \left(\phi_i A_i + A_i \phi_i \right) \equiv V_\mu \in^\mu \qquad (5.21)$$

where $\in^\mu$ is the polarization vector of the electro-
magnetic field $A_\mu^i = \epsilon_\mu e^{ikx_i}$ and V_μ is the current.
The axial current is given by $A_\mu = \gamma_5 V_\mu$.

We must now find some restriction among the 4
components of the quark spinors. If the quarks move
very slowly inside the hadron as is required for the
non-relativistic model, then we may determine the
spinors by assuming the quarks to be at rest. In the
weak binding limit we may use parity invariance for each
of the quarks separately to relate the large and small
components, hence

$$\gamma_{0i} u_i = u_i \qquad \text{for the quark}$$
$$\gamma_{0i} v_i = -v_i \qquad \text{for the antiquark}$$

Multiplying by the hadron mass m and boosting into a
frame where the hadron is moving with 4-momentum
we obtain

$$(\not p - m) u_i = 0 \qquad \text{for the quark}$$
$$(\not p + m) v_i = 0 \qquad \text{for the antiquark}$$

This is essentially the prescription of F.K.R. although
they use spinors (rather than antispinors) for the anti-

quarks as well as the quarks, presumably on the grounds that this maintains a closer relation to the non-relativistic model. This is exactly the same procedure as in the boosted $U(6,6)$ wave-functions discussed in section 3 except that the mesons have the wrong parity. Thus the spin part of the pseudoscalar meson is

$$u(\uparrow)\,u^T(\downarrow) - u(\downarrow)\,u^T(\uparrow) \propto \gamma_5\,(m-\not{p})\,C^{-1} \qquad (5.24)$$

Similarly the spin one wave-function is

$$\left\{ \begin{array}{c} u(\uparrow)\,u^T(\uparrow) \\ (u(\uparrow)\,u^T(\downarrow) + u(\downarrow)\,u^T(\uparrow))/\sqrt{2} \\ u(\downarrow)\,u^T(\downarrow) \end{array} \right\} \propto \not{\epsilon}\,(m-\not{p})\,C^{-1} \qquad (5.25)$$

which are the same as equation 5.8 apart from the charge conjugation matrix. We emphasise however that this weak binding prescription is completely independent of the other components of the model and strong binding prescriptions as in equations 5.9 or 5.10 are equally good. This is important because it is this aspect of the F.K.R. model together with the anzatz for the currents which essentially determine the results of the model. The harmonic oscillator form for the spacial part of the wave-function matters much less as data exists only for the low lying states.

The F.K.R. model for baryons is a simple extension of the meson model. The quark spinors are constructed in exactly the same way as for mesons. The mass squared operator is slightly more complicated because there are two degrees of freedom. From similar arguments to those for mesons we obtain

$$K = -3\left(\left[p_1^2 + p_2^2 + p_3^2 \right] + 4\omega^2 \left[(x_1 - x_2)^2 + (x_1 - x_3)^2 + (x_2 - x_3)^2 \right] \right) \qquad (5.26)$$

Removing the term due to the centre of mass motion $(P = p_1 + p_2 + p_3)$ we obtain the mass squared operator

$$m^2 = K + P^2 = -\Omega(a^\dagger a + b^\dagger b) = -6[p_\lambda^2 + p_\rho^2 + \omega^2(\rho^2 + \lambda^2)] \qquad (5.27)$$

where $\Omega = 12\omega$ and we have chosen the creation operator $a^\dagger$ to correspond to motion of quarks 1 and 2 about their centre and $b^\dagger$ to correspond to the motion of quark 3 relative to the centre of mass. The corresponding Jacobi co-ordinates are

$$a \longrightarrow \rho = x_1 - x_2 .$$

$$b \longrightarrow \lambda = \tfrac{1}{\sqrt{3}}(x_1 + x_2 - 2x_3) = \sqrt{3}\left[\tfrac{1}{3}(x_1 + x_2 + x_3) - x_3\right] \qquad (5.28)$$

The currents for baryons are defined in a similar manner to those for mesons by the minimal prescription.

Experimental quantities are calculated in the theory by taking matrix elements of the currents in direct analogy with non-relativistic quantum mechanics. Thus if $H_I = H_I^1 + H_I^2$ is a perturbation for a meson state then the amplitude to make a transition from a state i to a state f is

$$\langle f | H_I | i \rangle = \langle h_f | \bar{u}_{2f} (\bar{u}_{1f} H_I^{(1)} u_{1i}) u_{2i} | h_i \rangle + 1 \leftrightarrow 2 \qquad (5.29)$$

where $|h_i\rangle$ and $|h_f\rangle$ are harmonic oscillator states and we have neglected unitary spin factors. Besides the contribution due to $\bar{u}_{1f} H_I^1 u_{1i}$ there will be a projection due to $\bar{u}_{2f} u_{2i}$ because quark 2 will change momentum with the meson. (See fig. 36; also note spinor normalization $\bar{u}u = 1$). F.K.R. consider projections of this sort to be spurious and neglect them.

Electromagnetic processes are calculated by taking matrix elements of the vector current, which is conserved provided predicted masses are used. F.K.R.

choose to include symmetry breaking by using physical
masses, however this causes some unpleasant results.
(See next chapter). Decays by emission of a pseudo-
scalar meson are calculated by replacing the pseudo-
scalar by the divergence of the axial current as in
P.C.A.C. theory but the constant of proportionality is
slightly different from the P.C.A.C. value. The results
emerging from these calculations for mesons are
considered in the next chapter.

5.5 The Bethe Salpeter quark model of

Bohm Joos and Krammer

Consider the Bethe Salpeter equation for a
quark antiquark bound by a covariant potential V, from
section 2 we have in the ladder approximation

$$\left(\frac{\not{P}}{2}+\not{q}-m_q\right)\chi_p(q)\left(\frac{\not{P}}{2}-\not{q}+m_q\right) = \lambda \int V(q-k)\chi_p(k)\frac{d^4k}{(2\pi)^4} \quad (5.30)$$

For finite values of the bound state energy the equation
is extremely complicated. However, for massless bound
states (i.e. $P = 0$) the equation becomes more tractable
and is exactly soluble for the coulomb potential. The
reason for this simplification is that the equation
(see below) now exhibits $O(3,1)$ symmetry.

$$\left(\not{q}-m_q\right)\chi_p(q)\left(\not{q}-m_q\right) = -\lambda \int V(q-k)\chi_p(k)\frac{d^4k}{(2\pi)^4} \quad (5.31)$$

It is possible to define an analytic continuation in the
q_o variable to pure imaginary values [67] and then
equation 31 displays $O(4)$ symmetry. Making an $O(4)$
expansion equation 5.31 reduces to a "hyperradial" eign-
value equation for λ.

B.J.K. [62] approach the equark model in the same spirit. The point is that the quark mass M_q is large compared with the meson masses for the low lying states which suggests taking a first approximation $M_{hadron} = 0$ and then proceeding with a perturbation expansion in M_{hadron}/M_q .

The most general expansion for a local potential is in terms of the Fermi invariants $\Gamma^i = (1, \gamma_5, \gamma_\rho, \gamma_5 \gamma_\rho, \sigma_{\rho\nu})$

$$V(q-k) \chi(k) = \sum_{i=1}^{5} \lambda_i K_i(q-k) \Gamma^i \chi(k) \Gamma^i \qquad (5.32)$$

So as to obtain approximately linear trajectories the potentials are chosen to be covariant oscillators

$$K_i(x) = \alpha_i + \beta_i x^2 \qquad \text{sign}\,\alpha_i = -\,\text{sign}\,\beta_i \qquad (5.33)$$

α_i is the depth of the well (below $V = 0$)

The details of the calculation are both complicated and tedious and we will simply quote some of the results.

The first point of interest is to note that a relativistic quark model does not produce as a matter of course the non relativistic charge conjugation parity spectrum. This result depends upon the potential and there are two simple choices which give the non-relativistic spectrum and these are

$$V(x^2) = (\gamma_5^{(1)} \gamma_5^{(2)} + \gamma_\rho^{(1)} \gamma_\rho^{(2)} + 1^{(1)} 1^{(2)})(\alpha + \beta x^2) \quad \text{ie } T = A = 0 \quad (5.34)$$

$$V(x^2) = (\gamma_5^{(1)} \gamma_5^{(1)} + \sigma_{\rho\nu}^{(1)} \sigma_{\rho\nu}^{(2)} - \gamma_\rho^{(1)} \gamma_5^{(1)} \gamma_5^{(1)} \gamma_\rho^{(2)})(\alpha + \beta x^2) \quad \text{ie } V = S = 0 \quad (5.35)$$

Both interactions include some negative normalization
time like states. In the original paper [62]
interaction 5.34 was chosen although in a more recent
paper [68] the interaction $\gamma_5^{(i)} \gamma_5^{(i)}$ is favoured,
(because this leads to saturation of the quark forces).
In both cases the solutions correspond to one or other
of the forms for strong binding suggested in section 3.
The advantage of the B.J.K. model over the
phenomenological anzatz discussed previously is that
the parameters of the model are related to the meson
mass spectrum.

One important application is to meson decay
amplitudes [68]. Guided by the duality diagram approach
the model shown in fig. 37 is used and produces results
which are in reasonable agreement with experiments.
(The predicted decay widths are a little worse than
those predicted on the F.K.R. model).

5. A relativistic quark model for mesons

5.1 Introduction

The ability of the symmetric non-relativistic harmonic oscillator quark model to classify mesons and baryons and to describe some features of their interactions is well established [15, 66]. In the previous chapter some attempts to derive relativistic generalizations of the model were described [61, 62, 64, 65]. However, the basic puzzle of the quark model remains; namely what is the origin of the success of the model given that physical quarks do not seem to exist (see chapter 1). Of course it is legitimate to explain the apparent absence of quark production by assuming very heavy quarks. However if quarks can exist as free particles then their properties are difficult to understand: for instance quarks appear to obey symmetric statistics which is inappropriate for fermions and also the quark force is not of a simple exchange type. We prefer to take a more abstract view of quarks as being in some way inseparable from the hadron. Specifically a hadron is conceived as an excitation of some basic extended object, and the quarks are expected to arise naturally as internal degrees of freedom in the free field theory of the system. In a model of this sort the harmonic interactions of the quarks can be easily understood. An example of a model of this type is the dual model where the extended object is a rotating string, executing transverse vibrations [69], but this form of the model does not include SU(3) degrees of freedom.

The inseparability of quarks from hadrons may
be expressed by letting the quark mass M_q become infinite.
That this limit relates the bound state quark dynamics to
·the dual model has been demonstrated by Susskind [70] .
Susskind considers the Bethe Salpeter equation for two
scalar quarks in the infinite mass limit, when the
equation becomes linear.   Solving this equation for
harmonic oscillator interactions it is possible to
obtain an expression for the four point function in the
narrow resonance approximation which is closely related
to the Veneziano formula.   Indeed this model was the
precursor to the string models where an infinite set of
frequency modes are included.   The Susskind model is
essentially identical to the F.K.R. model which we may
therefore regard as the lowest order approximation to
the Fubini Veneziano model.

It is our aim in this chapter to build a model
similar to F.K.R. but incorporating spin in a dynamical
manner [76] .   Because quarks have spin $1/2$ the result
should be analogous to the lowest order equation in the
Ramond model [12] for fermions namely (chapter 1
equation 1.31)

$$[\not{p} + i \gamma_s (a^+_\mu b^\mu + b^+_\mu a^\mu) - m_0] | \psi \rangle = 0 \qquad (6.1)$$

where the $b's$ are spin excitation operators and the $a's$
orbital excitation operators.   We interpret the neglect
of the higher excitation modes as being equivalent to
neglecting the sea of quark antiquark pairs.

We are able to construct a model of this type
for mesons by demanding that the squared equation retain
harmonic oscillator form.   The main way that our equation
differs from the dual model result 6.1 is by the
natural inclusion of substantial spin orbit terms and
this is suggestive of the Melosh transformation.   Of
course our quarks are constituent quarks (but not $SU(6)_W$
quarks) whereas the current quarks are regarded as
including the sea of virtual quark antiquark pairs.
In practice this is not the case as the "free current"
quarks of the Melosh transformation are constituent
quarks in exactly the same sense as our model.
However, if constituent quarks are confined to mean
$SU(6)_W$ quarks then the "small components" in both the
Melosh model and our model contained "constituent quark
antiquark" pairs and in this sense our model incorporates
current quarks.

We are able to calculate the quark mass that
enters our model from pion decay and unfortunately it
turns out to be of the same order as the pseudoscalar
meson mass just as in the non-relativistic model and so
the whole scheme seems to be self contradictory.   This
is not the case.   If quarks are inseparable from the
hadron then the quark mass has no meaning and cannot enter
the matrix elements as a physical parameter although this
would be the case if we interpreted the $M_q \rightarrow \infty$ limit
simply as an approximation to heavy quarks.   The
prescription $M_q \rightarrow \infty$ is regarded as a device for
obtaining consistent relativistic results while excluding

quark propagation effects. The form of the matrix elements obtained in this manner is entirely analogous to the dual model and also the F.K.R. model. Quark propagation effects are omitted not because the quarks have large mass but rather because quarks are intrinsic to hadrons and have no separate existence.

When dealing with the 0^{-+} nonet we will assume no $\eta \eta'$ mixing and for the 1^{--} nonet we take $\omega \phi$ to be ideally mixed.

6.2 The Model

Consider two quarks of momenta p_1 and p_2 bound by a covariant potential V. The BS equation is*

$$(\not{p}_1 - m_q) \phi (\not{p}_2 - m_q) = V \phi \qquad (6.2)$$

and if the quark mass, M_q, is large the equation can be approximated by

$$(\not{p}_1 + \not{p}_2) \phi = (m_q - \frac{V}{m_q}) \phi = (m_0 - u) \phi \qquad (6.3)$$

where m_0 is the effective quark mass.

Substituting for the centre of mass and relative momentum variables P, q given by $p_1 = \frac{P}{2} + q$, $p_2 = \frac{P}{2} - q$ the equation becomes

$$\left[\frac{P_\mu}{2} (\gamma_1^\mu + \gamma_2^\mu) + q_\mu (\gamma_1^\mu - \gamma_2^\mu) - m_0 + u \right] \phi = 0 \qquad (6.4)$$

*We consider the quark quark equation. The quark antiquark result is derived using the charge conjugation matrix.

We choose the form of the interaction in the same way as F.K.R. As one can derive their model from a BS equation for scalar quarks

$$(p_1^2 - m_q^2) \phi (p_2^2 - m_q^2) = V\phi \qquad (6.5)$$

giving as $m_q \to \infty$

$$\left[p_1^2 + p_2^2 - m_q^2 + \frac{V}{m_q^2} \right] \phi = 0 \qquad (6.6)$$

the method is strictly analagous. For harmonic oscillator interaction this becomes

$$\left[p_1^2 + p_2^2 + 2\omega^2 x^2 + c \right] \phi = 0$$

$$\left[\frac{P^2}{2} + 2(q^2 + \omega^2 x^2) + c \right] \phi = 0 \qquad (6.7)$$

where $x^\mu = -i \frac{\partial}{\partial q_\mu} = x_1^\mu - x_2^\mu$ is the relative separation of the quarks and 'c' is a constant. Introducing creation and annihilation operators

$$a_\mu = \frac{1}{\sqrt{2\omega}} (q_\mu - i\omega x_\mu)$$

$$a_\mu^+ = \frac{1}{\sqrt{2\omega}} (q_\mu + i\omega x_\mu) \qquad (6.8)$$

We obtain the F.K.R. model

$$\left[P^2 + \Omega\, a_\mu^+ a^\mu + 2c \right] \phi = 0 \qquad (6.9)$$

where $\Omega = 8\omega$ and $P^2 = m^2$ the meson mass squared.

To obtain the interaction for spinor quarks we linearize in the spin space $\frac{1}{2} \otimes \frac{1}{2}$ to get

$$\frac{P_\mu}{2} (\gamma_1^\mu + \gamma_2^\mu) \sim m \sim \frac{\sqrt{\Omega}}{2} (\alpha_+ a + \alpha_- a^+) \qquad (6.10)$$

To ensure that the squared equation has oscillator form
we must eliminate terms quadratic in a^μ and $a^{\mu\dagger}$ by
the conditions

$$\alpha_+^\mu \alpha_+^\nu = \alpha_-^\mu \alpha_-^\nu \equiv 0 \qquad (6.11)$$

eq 6.4 determines the way in which the internal
momenta enter eq 6.10 . These constraints suggest
the form

$$\alpha_\pm^\mu = \frac{1}{2}(I + P_\pm)(\gamma_1^\mu + \gamma_2^\mu). \qquad (6.12)$$

where Lorentz and parity invariance indicate how $P_\pm$ can
be expanded in terms of Fermi bilinear covariants.
Using eq 6.12 one can deduce that

$$\alpha_\pm^\mu = \frac{1}{2}(I \pm \gamma_5^{(1)}\gamma_5^{(2)})(\gamma_1^\mu + \gamma_2^\mu) \qquad (6.13)$$

and the square root equation becomes

$$\left[\frac{P_\mu}{2}(\gamma_1^\mu + \gamma_2^\mu) - m_0 + \frac{\sqrt{\Omega}}{2}(\alpha_+ a + \alpha_- a^\dagger) \right]\phi = 0 \qquad (6.14)$$

Explicitly

$$\frac{\sqrt{\Omega}}{2}(\alpha_+ a + \alpha_- a^\dagger) = (\gamma_1^\mu - \gamma_2^\mu)q_\mu - i\omega\gamma_5^{(1)}\gamma_5^{(2)}(\gamma_1^\mu - \gamma_2^\mu)x_\mu \qquad (6.15)$$

we deduce that

$$U(x_1, x_2) = -i\omega\gamma_5^{(1)}\gamma_5^{(2)}(\gamma_1^\mu - \gamma_2^\mu)(x_1 - x_2)_\mu \qquad (6.16)$$

This form of the interaction, linear in position variables,
which, like the momenta, are contracted with Dirac
matrices can be seen to arise from the position momentum
symmetry characteristic of the harmonic oscillator.
eq (6.15) is clearly invariant under the interchange

$$q_\mu \longleftrightarrow -i\omega\gamma_5^{(1)}\gamma_5^{(2)}x_\mu$$

We note that because the interaction $U(x_1, x_2)$ does not contain a scalar potential we are unable to cancel the large quark mass, m_Q, on which we have based our derivation, to get a small effective quark mass m_0. The apparent inconsistency which arises from m_0 being in fact m_q we shall ignore in order to take advantage of the $m_q \rightarrow \infty$ anzatz. The obvious advantage is the elimination of quark propagator effects which establishes a close relation between our relativistic results and non-relativistic results. This philosophy is entirely consistent with that of F.K.R. (scalar quarks versus our spinor quarks) and our desire to establish a calculational prescription from which we can abstract systematics.

A further advantage of the infinite quark mass picture is that we can regard the internal motion of the constituent quarks as non-relativistic (although we are then obliged to neglect the relative energy in the centre of mass). This allows us to replace the four dimensional operators, a_μ by

$$\eta_\mu = a_\mu - P_\mu \frac{P \cdot a}{m^2}$$

As $\eta_\mu = (0, \underline{a})$ in the rest frame, the close relationship with the non-relativistic model is clear. As well, the negative norm time like states are eliminated. These states in the F.K.R. model are decoupled from physical states by a gauge condition and this has the effect of violating unitarity. As a consequence, the F.K.R. matrix elements are too large and they are obliged to reduce them by using 'an adjustment factor'.

6.3 Properties of the wave functions

The solutions to eq 6.14 can be built up in a Fock space with a vacuum $|0_P\rangle$ defined by

$$\eta_P |0_P\rangle = 0 \tag{6.17}$$

This is just the ordinary non-relativistic oscillator ground state in the rest frame. A general solution of 6.14 can then be written as

$$|\psi_P\rangle = \psi_P(\eta, \eta^\dagger) |0_P\rangle$$

where ψ_P is a 4 x 4 matrix. In calculations, quark operators act on ψ_P from the right, while antiquark operators act from the left. The invariance properties of the solutions under charge conjugation, Lorentz and parity transformations are defined in the same way as for the BS wave functions. In particular, charge conjugation is defined by

$$C \psi_P^T(-\eta, -\eta^\dagger) C^{-1} |0_P\rangle = \eta_P \psi_P(\eta, \eta^\dagger) |0_P\rangle \tag{6.19}$$

Because the wave function does not depend on the relative energy (a consequence of the infinite quark mass approach) we can not use the invariant measure d^4q. This requires redefinition of the scalar product which we do in a way motivated by F.K.R. That is, we replace $|0_P\rangle$ by $|0\rangle$ the 4 dimensional vacuum state, which also satisfies 6.18*. The spin part of the scalar product is defined in the usual way, so we have

$$\langle \phi_{P_2} | \psi_{P_1} \rangle = \langle 0| T_r \, \bar{\phi}_{P_2}(\eta_2^\dagger, \eta_2) \, \psi_{P_1}(\eta_1, \eta_1^\dagger) |0\rangle$$

where $\tag{6.20}$

$$\bar{\phi}_P(\eta_2^\dagger, \eta) = \gamma_0 \, \phi_P^\dagger(\eta_1, \eta_1^\dagger) \gamma_0$$

*Notice that prescription brings the model to the same form as expected from a gauge theory.

We normalize the wave functions by using the matrix elements of the quark current at zero momentum transfer. These define the quark charge, e_q, and give

$$\langle \psi_P | \frac{j_P^q(0)}{e_q} | \psi_P \rangle = -\langle 0 | T_r \, \bar{\psi}_P(\eta^+, \eta) \, \gamma_P \, \psi_P(\eta, \eta^+) | 0 \rangle = 2 P_P \quad (6.21)$$

We compare this with the corresponding BS normalization (Fig. 38).

$$\langle \psi_P | \frac{j_P^q(0)}{e_q} | \psi_P \rangle = -T_r \langle \bar{\psi}_P \gamma_P \psi \, (\frac{\not{P}}{2} + \not{k} + m_q) \rangle = 2 P_P \quad (6.22)$$

which for large m_q becomes

$$\sim -m_q T_r \langle \bar{\psi}_P \gamma_P \psi_P \rangle$$ and we note that our normalization in (6.21) is consistent with the general approach.

As is obvious from the above, the minimal vector current for the quarks is

$$V_P^q = -e_q \, \gamma_P \, e^{iq \cdot x} = -e_q \, \gamma_P \, F \, e^{q \cdot a^+/\sqrt{s\tau}} \, e^{-q \cdot a/\sqrt{s\tau}} \quad (6.23)$$

with $F = \exp \left(-q^2/2s\tau \right)$ and the centre of mass phase factor neglected. The axial current is

$$A_P^q = -\lambda_q \, \gamma_5 \, \gamma_P \, F \, e^{q \cdot a^+/\sqrt{s\tau}} \, e^{-q \cdot a/\sqrt{s\tau}} \quad (6.24)$$

Neglecting the unitary spin factor the antiquark operators are given by

$$O_P^{\bar{q}} = F \, C \, \Gamma_P^T \, C^{-1} e^{-q \cdot a^+/\sqrt{s\tau}} \, e^{q \cdot a/\sqrt{s\tau}} \quad (6.25)$$

where Γ is either γ_P or $\gamma_5 \gamma_P$. The corresponding anti-quark matrix elements are given by

$$\langle \phi_{P_2} | O_P^{\bar{q}} | \psi_{P_1} \rangle = F \, \langle 0 | T_r \, \bar{\phi}(\eta_2^+, \eta_2)$$
$$e^{-q \cdot a/\sqrt{s\tau}} \, e^{q \cdot a/\sqrt{s\tau}} \, \psi_{P_1}(\eta_1, \eta_1^+) \, C \, \Gamma^T C^{-1} | 0 \rangle \quad (6.26)$$

6.4 The Solutions

The solutions for the model were found by the direct method of writing eq (6.14) as a set of coupled equations at the Pauli spinor level in the rest frame, and algebraically reducing them to a single equation; the details are given in appendix 4. The restrictions of charge conjugation and parity were applied from the outset to divide the solutions into two classes character- ised by the value of PC. The classes are PC = - 1 which corresponds in the non relativistic quark model to spin zero, and PC = + 1 which corresponds to spin one. This relation between PC and quark spin is maintained in the relativistic wave functions, but only in general by the large components. With some manipulation one finds that the large components are eigenstates of the number operator and this is used to construct the full solution. This solution, re-written in covariant form, can then be verified by substituting it back into eq (6.14) (see appendix 4).

6.4.1 PC = - 1

We reproduce the non relativistic result that the C = $(-)^{J+1}$, P = $(-)^{J}$ mesons are forbidden and this follows directly from the requirement that the interaction be 3 dimensional. In general however, the interaction can be 4 dimensional, in which case this result becomes strongly dependent on the spin-space structure of the interaction [62].

The solution for a PC = - 1 state of mass m and spin quantum numbers (J, J_z) is

$$\frac{1}{2\sqrt{m_0}} \gamma_5 \left\{ \left(m - m_0 \frac{\not{\phi}}{m}\right) + \sqrt{2} \frac{\not{\phi}}{m} \eta \right\} |N, J, J_z\rangle \qquad (6.27)$$

for $C = (-)^J$, $P = (-)^{J+1}$. $|N, J, J_z\rangle$ is an eigenstate of the harmonic oscillator number operator, $-\eta_\mu^\dagger \eta^\mu$ with eigenvalue N, and J, J_z are orbital angular momentum quantum numbers. We note that in the limit $\Omega \to 0$ the solution reduces to that for a free (mass m_0) quark and antiquark with relative momentum zero and consequently there is no admixture of undesirable negative energy states. We also note that the ground state pseudoscalar solution

$$\frac{1}{2\sqrt{m_0}} \gamma_5 \left(m - m_0 \frac{\not{p}}{m} \right) |0\rangle \tag{6.28}$$

is simply a boosted non-relativistic solution.

The particles lie on straight Regge trajectories

$$m^2 = m_0^2 + \Omega N \quad , \quad N = 0, 1, 2 \cdots \tag{6.29}$$

If we choose the slope of the trajectory to be $\Omega^{-1} = 1$ and take for m_0^2 the average of the square of the pseudoscalar meson masses, $m_0^2 = 0.25$ GeV^2 we reproduce reasonably this section of the mass spectrum (Fig. 39).

The presence of terms containing the inverse of the pseudoscalar mass give rise to large symmetry breaking and the Van Royen-Weisskopf paradox [71]. As this results in unreasonable predictions and not only for pseudoscalar meson decay matrix elements, we avoid it by using predicted rather than physical masses in eq (4.1). Then the 0^- solution (6.28) has the same spin structure as that postulated by Gudeus [55].

In the BS model of BJK the 0^- solutions have a similar form but $\not{p}/m$ is replaced by $\not{p}/m_{quark}$. This has the advantage of resolving the Van Royen-Weisskopf paradox in a natural way [64].

Finally, it is interesting to observe that in fixing the slope parameter, Ω, we have fixed the size of the hadron [72]. The space part of the ground state wave function is

$$\langle \underline{r} = \underline{x}_1 - \underline{x}_2 \mid O_{P=m}\rangle \sim exp\left(-\frac{\omega^2 r^2}{2}\right) \sim exp\left(-\frac{r^2}{2R^2}\right) \qquad (6.30)$$

where $R^2 = 1/\omega = 8/\Omega \sim 8$ natural units. R is essentially the average separation of the quarks and determines the size of the meson. The meson cross section is $\pi R^2 \sim 24$ natural units ~ 10 mb, which is not unreasonable.

6.4.2 PC = + 1

In solving for the PC = + 1 we have the added difficulty that the solutions are not, in general, unique. However for special cases, including the leading trajectory, the states are unambiguous. These cases occur when the spin is equal to the orbital angular momentum in the large components.

The problem of ambiguity arises because the eigenvalue equation at the Pauli spinor level demands an eigenstate of the number operator. As a direct consequence the quark spin and the orbital angular momentum are decoupled and for a given meson spin, two possible values of orbital angular momentum are allowed. This degeneracy has the compensation that there is no spin orbit splitting. Also, as the first such case occurs for a spin 1 meson with N = 2 the effect is irrelevant for practical calculations. The criterion we impose to get a general solution is to require the rest frame wave function to have no spin zero components, in accord with the unambiguous solutions.

The unnormalized $PC = + 1$ states are then given by

$$\frac{1}{2\sqrt{m_0}}\left\{\left(m + m_0\frac{\not{P}}{m}\right)\left(\not{\epsilon} + \Omega\frac{\eta^{\dagger}\epsilon\cdot\eta}{m^2 - m_0^2}\right) - i\sqrt{\Omega}\,\frac{\gamma_5}{m}\,\mathcal{E}(P\eta^{\dagger}\epsilon\gamma)\right\}|N,M\rangle \quad (6.31)$$

where $C = P = (-)^{\ell}$, $\mathcal{E}_{\mu}$ is a spin one wave function and $\mathcal{E}(P\eta^{\dagger}\epsilon\gamma)$ is the Levi-Civita tensor dotted into four 4 vectors. The solution has not been separated into its possible spin states of $\ell+1$, $\ell-1$ and ℓ. As in the $PC = - 1$ solution we note that in the limit $\Omega \to 0$ the solution reduces to that for a free quark and antiquark (mass m_0) with relative momentum zero and we are able to conclude that there is no negative energy admixture.

The term $\frac{\eta^{\dagger}\epsilon\cdot\eta}{m^2 - m_0^2}$, which vanishes in the case $J = \ell$, is responsible for adding the extra orbital angular momentum in the large components for the cases, $J = \ell \pm 1$, where the solution is not unique.

In order to understand the significance of the other terms in eq. (6.31) it is easiest to consider the ground state vector meson solution

$$\frac{1}{2\sqrt{m_0}}\left\{\left(m + m_0\frac{\not{P}}{m}\right)\not{\epsilon} - i\sqrt{\Omega}\,\frac{\gamma_5}{m}\,\mathcal{E}(P\eta^{\dagger}\epsilon\gamma)\right\}|0\rangle \quad (6.32)$$

The term involving $(m + m_0\frac{\not{P}}{m})$ is closely related to a boosted nonrelativistic wave-function. In fact if $m_0 = m$ it is just that and the term reduces to the solution of Gudeus [65]. The vector meson solution of BJK

$$\left(1 + \frac{\not{P}}{m_q}\right)\not{\epsilon}|0\rangle \quad , \quad \langle q|0\rangle = \exp(-q^2/2\Omega) \quad (6.33)$$

is also similar to this term.

In the last term of eq. (5.32), the quark spin is coupled to a P-wave orbital state (in the small components) and hence corresponds to a spin orbit interaction. This feature is absent from the solutions of BJK and Gudeus. Experiments, on the other hand, indicate the necessity of some spin orbit coupling, even if it is not the amount predicted and consequently we regard this property of the solution as most desirable. The presence of this spin orbit interaction does not contradict our previous assertion that there is no spin orbit splitting.

The mass spectrum is again linear and independent of any arbitrariness of the solutions. It is

$$m^2 = m_0^2 + \Omega(N+2).$$
(6.34)

With the parameters given previously the mass of the vector meson is predicted to be 1.58 GeV, or about twice the correct answer. Despite the fact that this result, which comes from a strong spin-spin interaction, is much too big, it is clear that spin-spin coupling is needed to make the vector mesons more massive than the pseudo-scalar nonet. In calculations we will take the PC=1 trajectory to be

$$m_+^2 = m_0^2 + \Omega(N + .5).$$
(6.35)

We have chosen the numbers so that the average value of the vector meson mass squared is approximately correct. Also, as might be anticipated in view of the non-relativistic approximation of the internal motion, the quantum number spectrum displayed in Fig. 40 is identical to that given by the non-relativistic quark model.

6.5 Applications

Following F.K.R. we calculate experimental observables from current matrix elements, neglecting quark propagation effects $(m_q \to \infty)$. Unlike F.K.R. we have a problem with our vector currents as they are not, in general, conserved. For particular cases however, they are and these cover most of the important applications. The specific cases where the electromagnetic current is conserved are the equal mass transition and the PC = + 1 to pseudoscalar meson transition. For the rest we add a momentum term to the coupling to ensure conservation.

6.5.1 Lepton decays of pseudoscalar and vector mesons

From the correspondence in section 3 between the BS and current normalization we have $\psi_{BS} = a \psi$ where $a = 1/\sqrt{m_q}$. The pseudoscalar meson decay matrix element is then given by

$$\langle \text{Vac} \mid A_\mu(0) \mid 0^{-+} \text{meson} \rangle = a \, \text{Tr} \, \gamma_5 \gamma_\mu \psi_P(x_\mu = 0) \equiv f_P \, P_\mu \quad (6.36)$$

$\psi_P(x_\mu = 0)$ is the pseudoscalar wave-function at the origin. The result is $f_P = a \, \dfrac{\sqrt{m_0}}{m_P} \left(\dfrac{\Omega}{4\pi} \right)$ (6.37)

As already mentioned we cannot use the physical masses because of the $1/m_P$ term which will give rise to the large symmetry breaking in the Van Royen-Weisskopf paradox. We avoid this difficulty by using unbroken masses, $m_P = m_0$ which give

$$f_\pi = f_K = 0.112 \, a \text{ GeV} \quad (6.38)$$

Comparing with experimental values [73] $f_K^{exp} = 0.105$ GeV, $f_\pi^{exp} = 0.095$ GeV we see that 'a' is compatable with

unity and a small quark mass. This is consistent with
the earlier identification of m_q and m_o but incompatable
with the heavy quark approximation. However, we are not
using a heavy quark approximation in our calculation of
matrix elements, rather we are using it to generate
relativistic expressions similar in form to those of the
non-relativistic quark model. The quarks themselves
are regarded as being inseparable from the hadron where
the quark mass can have little meaning.

  Similarly the vector meson decay to a pair of
leptons is predicted. Neglecting the unitary spin
factor we have

$$\langle Vac | V_\rho(0) | 1^{-+} meson \rangle = a\, Tr\, \gamma_\rho \psi_V(x=0) = g_V m_V G_{V\rho} \quad (5.39)$$

which gives the result

$$\frac{3}{\sqrt{2}} g_\phi = 3 g_\omega = g_\rho = \frac{a}{\sqrt{2 m_0}} \left(\frac{\Omega}{4\pi}\right) = 0.08a \; GeV \quad (5.40)$$

The experimental result is

$$\frac{3}{\sqrt{2}} g_\phi = 0.168 \, GeV, \quad 3 g_\omega = .156 \, GeV \quad g_\rho = .160 \, GeV \quad (5.41)$$

  Taking a=1 we get about half the experimental
result which is comparable with other quark models. For
example BJK predict g_V to be about twice the
experimental value with the quark mass determined from
pion decay, while F.K.R. predict $g_\pi = g_K = g_\rho$ etc.

6.5.2 Matrix elements of the vector current

  The form factor for $K\pi$ coupling in K_{ℓ_3} decay
is calculated from the matrix element of the vector
current

$$\langle \pi | V_\rho(0) | K \rangle = \frac{F}{2\sqrt{2}} \left[\left(\frac{m_\pi}{m_K} - \frac{m_K}{m_\pi}\right)(p_K + p_\pi)_\rho - \left(\frac{m_K}{m_\pi} - \frac{m_\pi}{m_K}\right)(p_K - p_\pi)_\rho \right] \quad (5.42)$$

$$\equiv f_+(q^2)(p_K + p_\pi)_\rho + f_-(q^2)(p_K - p_\pi)_\rho$$

To be consistent we evaluate (6.42) using unbroken masses, $m_\pi = m_K = m_0$ and predict $f_-(q^2) = 0$. This does not agree with the experimental result of $f_-(0) \approx f_+(0) \approx 1.0$ [73]. As this disagreement is attributable to current conservation and the use of unbroken masses it is clear that a symmetry breaking scheme must be added to our model if these results are to be well described. Had we used physical masses in (6.42) we would have achieved good predictions but violated our prescription for calculation.

We have more success in predicting the electromagnetic decays of the vector mesons. Neglecting the unitary spin factor we obtain for the matrix element of the quark current

$$T^q = -i \langle \pi | \varepsilon^{\mu *} J_\mu^q(o) | 1^{+-} meson \rangle$$

$$= -\frac{e\, m_2}{m_1 m_0} F \left(1 + \left(\frac{m_0}{m_2}\right)^2 \right) \varepsilon(q\, \epsilon_2^*\, p_1\, \epsilon_1) \qquad (6.43)$$

where the kinematics are indicated in Fig. 41.

The first term in eq. (6.42) corresponds to an orbital magnetic moment, while the second is analogous to an intrinsic moment. The antiquark amplitude differs only in sign, so combining with the unitary spin factor we get the results in Table 13.

The coupling constant, g, is defined by

$$T = e\, g_\gamma\, \varepsilon(q\, \epsilon_2^*\, p_1\, \epsilon_1) \qquad (6.44)$$

and we have used unbroken masses in its evaluation. The quantities dotted into the Levi-Civita tensor are taken at their physical values, primarily for convenience, as any other procedure has a minor effect on the results.

6.5.3 Meson decays by emission of a pseudoscalar meson

Following F.K.R. we calculate the amplitude for pseudoscalar meson emission by replacing the pseudoscalar meson interaction by the divergence of the axial vector current which is given by

$$\partial_\mu A^\mu_q = -i\, \lambda_q\, F\, \gamma_5\, \sigma\, e^{q \cdot q^+/\sqrt{3\tau}}\, e^{-q \cdot q/\sqrt{3\tau'}} \qquad (6.45)$$

In the decays $1^+ \to 1^- 0^-$, $2^{\pm} 1^- 0^-$ the corresponding vector current is not conserved and consequently we should adjust the axial vector current to be

$$\partial_\mu A^\mu_q = -i\, \lambda_q\, F\, \gamma_5\, [g_1 \sigma + g_2\, q \cdot (p_i + p_i)]\, e^{q \cdot q^+/\sqrt{3\tau}}\, e^{q \cdot q/\sqrt{3\tau}} \qquad (6.46)$$

where g_1, g_2 are constrained to ensure electromagnetic current conservation and $g_1^2 + g_2^2 = 1$. For the actual predictions presented in Table 15, we use eq. (6.45).

The overall strength of the interaction is determined by one adjustable parameter f, and the decay amplitude from an initial state, i, to a final state, f, by emission of a pseudoscalar is

$$T = -i\, f \sum_\alpha \langle f | \partial_\mu A^\mu_\alpha | i \rangle \qquad (6.47)$$

where the summation is over quarks and anti-quarks. Expressions for the matrix elements with the unitary factor λ_q removed are given in Table 2.

Decay widths are calculated using the formula

$$\Gamma = \left(\frac{R}{2J_i + 1}\right) \frac{\sum |T|^2}{2 m_i^2} |q|. \qquad (6.48)$$

where q is the 3 momentum of the decay products (in the rest frame of the initial particle i) and the summation is over the initial and final spins. The factor R is to account for the different charge modes allowed in the decay (see F.K.R.).

In calculating the decay widths the dynamical
quantities, the decay constants, are input using unbroken
masses, while for the kinematic phase space, we use
physical masses. For example, the decay width

$$\Gamma(1^- \to 0^{-+} 0^{-+}) = R \frac{2}{3} \frac{g^2}{m_1^2} |q|^3 \tag{6.49}$$

is calculated by putting physical masses into q and
unbroken masses into (g/m_1).

As can be seen from Table 15, this prescription
yields good agreement with data. However, this is not
surprising as it is simply reflecting the SU(3) symmetry
of the coupling constants. In the F.K.R. model the
relative values of decay width for a given decay type are
in less good agreement with data but this is due to the
symmetry breaking introduced by using physical masses
throughout. This problem is particularly acute in the
case of decays into two pseudoscalar mesons where
different results are obtained depending on which meson is
replaced by the axial current. The use of unbroken
masses avoids this asymmetry.

The value of the coupling constant, f, is
expected to be close to that given by PCAC theory, that is

$$f_\pi = f_{\pi NN}^{1/2} / m_\pi g_A = 1.65. \quad \text{Using this value for the}$$

coupling constant the decay widths are found to be too
large and reduction to a value of $f = 1.46$ GeV^{-1} is
indicated in order to give a good fit to the data. We
display the decay width data, our best fit, and that of
F.K.R. (Γ_F) in Table 15.

The results for the vector and tensor decay
widths are all within 20% of the experimental values,
which is reasonably good considering that we have not
introduced symmetry breaking, and it is an improvement
on F.K.R.   For the $2^+ \to 0^- 1^-$ decays our results are
less good than F.K.R's, however we could still modify
our results by generating the axial vector current from
a conserved current as in eq. (6.46).

In the other two types of decay considered,
$1^{+-} \to 1^- 0^-$ and $1^{++} \to 1^- 0^-$ we again have the problem that
the underlying current is not conserved and consequently
that these results could be improved.   The results as
calculated however are at least the correct order of
magnitude and are no worse than those of F.K.R.   On the
other hand the helicity properties, which depend
critically on the type of coupling are worse in our model
as can be seen from Table 16.

The unfavourable comparison with experiment
for the $K^{**}(1240) \to K^* \pi$ and $A_1 \to \rho \pi$ decays is perhaps
mitigated by possible contamination of the resonances by
Deck effect [73].

6.6 Conclusions

We do not test the harmonic oscillator
character of our wave functions because only the lowest
two states are used, it is the spin structure we test.
However, our basic assumption of harmonic oscillator
forces gave rise to the spin structure so that any success
of the model is attributable to this assumption.

The large components of the wave-functions are analogous to boosted non-relativistic wave-functions and occur in all relativistic models. The main difference arises from whether m_{quark} or m_{hadron} is regarded as the fundamental mass. The novel feature of our model is the inclusion of a spin orbit term in the small components which, nonetheless, did not cause splitting of the trajectories. This extra orbital term is needed to produce some of our good results, the least ambiguous case being the electromagnetic decays where the orbital term contributes half of the result. We regard this success in the electromagnetic case as our most important result, as it does not depend on arbitrary parameters.

The significance of the results for the decay widths is harder to evaluate because the prescription which replaces the pseudoscalar interaction by the divergence of the axial vector current is not quite as well established as the corresponding formalism for electromagnetic decays. Further, we do not adhere strictly to PCAC theory as we use a coupling constant different (but not by much) from the theory.

Given that the relative success for any one decay type just depends on the SU(3) symmetry and the prescription to use unbroken masses, the fact that the coupling constant is an independent parameter means that Table 15 contains only four independent results. Also, because the data for the $1^{++} \to 1^{-}0^{-}$ decay is ambiguous, there are really only three numbers to compare with

experiment.   Of these, two compare well while the
third, B→ωπ is a factor of two out.   This lack of
success may be due to our decision not to modify the
axial vector current so that it corresponds to a
conserved electromagnetic current.

To summarise, we have proposed an equation
in which the internal quark motion is closely related
to that in a non-relativistic model but is treated in
a covariant way.   Our model is most closely related
to that of P.K.R. but has the advantage of incorporating
spin in a more dynamical way.   In compensation for
their simple treatment of spin, P.K.R. are able to
include baryons in their scheme.   The extension of our
model to include baryons is clearly the next step.

7. Relativistic quark models and diffraction dissociation

7.1 Introduction

We now return to the problem of treating diffraction scattering in terms of elastic scattering of the hadronic constituents, assuming the constituents to be quarks. As mentioned in chapter 4 the dynamical version of the non-relativistic quark model predicts cross-section dips in the forward direction for all except elastic scattering and this is contrary to data. Nevertheless the non-relativistic SU(6) quark model of C.F.Z. and its $SU(6)_W$ generalization is able to unify most of the experimental results for diffraction and hence one is encouraged to believe that the difficulties of the non-relativistic quark model are due to the neglect of relativistic effects rather than any intrinsic defect. In this chapter we consider the application of relativistic quark models to diffraction. It is shown that the t = 0 zero in the single scattering amplitude for the non-relativistic model is not present in the relativistic models. However, apart from this problem the SU(6) C.F.Z. model does not predict the meson dissociations correctly as the $\pi \to A_1$ and $K \to Q$ transitions are forbidden whereas experiment gives large cross-sections. The reason for this prediction is that in the C.F.Z. model the basic quark quark amplitude is assumed to be spin independent and hence singlet triplet transitions are forbidden. The $\pi \to A_1$ transition is allowed in a model with quark spin flip but then the $\pi \to A_2$ transition is

also allowed and both cross-sections are predicted
to have forward dips. Furthermore T.C.H.C. is not
predicted. To obtain the correct results substantial
spin-orbit interaction is needed. Indeed the evidence
favours large spin orbit interactions for mesons quite
apart from diffraction. However, for baryons the spin
orbit effects are much less prominent and this explains
the relative success of the SU(6) quark model in this
sector.

The B.J.K. and F.K.R. models contain no spin orbit
interaction and so like the C.F.Z. model fail to
reproduce the meson dissociation data. However, the
linearized oscillator model considered in chapter six
includes large spin orbit terms. Furthermore, with a
general coupling the quark and antiquark scattering is
not the same and this has the consequence that the
$\pi \rightarrow B$ and $\pi \rightarrow \rho$ transitions are allowed diffractively
contrary to the data. If we wish the model to include
the G-parity selection rule then this uniquely specifies
the quark quark interaction to be spin independent as in
the C.F.Z. model. With this coupling the $\pi \rightarrow A_1$
transition is allowed while the $\pi \rightarrow A_2$ transition is
forbidden. Furthermore the $\pi \rightarrow A_1$ vertex is predicted
to conserve T.C.H. while all the other successful
predictions of the C.F.Z. model are retained. However,
in common with other quark models (c.f. B.J.K.) the
inelastic transitions for instance $\pi \rightarrow A_3$ are predicted
to be of the same order as the elastic transitions
Furthermore the diffractive slopes are not predicted
correctly and the two problems are probably related. A

factor inhibiting the production of high mass states
as in the F.K.R. model is needed to predict cross-sections
in accord with the data.

We also consider how the relativistic approach
might be extended to include fermion dissociation and
also multiple scattering.

7.2 Diffraction dissociation in the F.K.R. model [77]

Because the pomeron trajectory has a small
slope and intercept at spin one it is reasonable to
believe that the pomeron coupling is similar to that
for a spin one object (c.f. chapters 3 and 4). This
suggests replacing the diffractive vertex for the trans-
ition $A \rightarrow A^*$ by

$$G(A \rightarrow A^*) \propto \sum_i \langle A^* | V_\mu^i | A \rangle \qquad (7.1)$$

where i labels the quarks and antiquarks and V_μ is a
vector object. The simplest picture is to assume the
coupling to be spin independent as in the C.F.Z. model
but then the $\pi \rightarrow A_1$ transition is forbidden. Motivated
by the connection between the electromagnetic form factors
and the diffractive cross-section Ravndal [77] makes the
hypothesis that the pomeron coupling is associated with
the SU(3) singlet component of the conserved vector
current. So as to reproduce the observed G parity
selection rule the quark-quark and antiquark-antiquark
couplings are assumed to be equal. As $t = 0$, $J = 1$
does not correspond to a pole on the pomeron trajectory
and the slope is small we may replace the pomeron propogator
by a pure imaginary constant. Hence the amplitude for

the process $AB \to A^*B^*$ is

$$T(AB \to A^*B^*) = \sum_{ij} i e_\rho^2 \langle A^*| V_\mu^i |A \rangle \langle B^*| V^{rj} |B \rangle \qquad (7.2)$$

where e_ρ is a universal constant. Clearly the model allows all transitions conserving SU(3) quantum numbers and generalized charge conjugation C.

Unfortunately the F.K.R. model predictions for the electromagnetic form factors are bad [61], and consequently the present model will give wrong predictions for the elastic vertices. As elastic vertices are needed to construct the amplitude for the dissociation processes $AB \to A^*B$ we must arrange the elastic vertex to conform more closely to the data. Ravndal chooses to arrange the NN vertex to conserve S.C.H. and have the experimental form factor. Similarly the $\pi\pi$ vertex is taken to be the experimental pion form factor.

All the nucleon dissociation processes $N \to N^*$ are allowed and although this violates Morrisons rule it is not necessarily wrong [29,33, also see chapter 2]. Ravndal compares the $D_{13}(1520)$ and $F_{15}(1688)$ diffractive production with the data. The model is successful in the sense that the cross-section is of the correct order of magnitude, however the shape of the differential cross-section is not correct. The problem is the same as the Kislinger model [48] namely that current conservation implies that the cross-section is zero at $t = 0$.

The predictions for bosons are not good and are roughly similar to the $SU(6)_W$ model with quark spin flip. Both $\pi \to A_1$ and $\pi \to A_2$ transitions are allowed but do not

conserve F.C.T.C. and like the SU(6)$_w$ model predict transverse helicities in the rest frame of the produced particle. Furthermore the cross-sections for A_1 and A_2 production are predicted to be equal and about a factor 2 - 3 too big.

7.3 The Bethe Salpeter quark model applied to meson dissociation [43, 78]

In this section the C.F.Z. model of spin independent quark quark forces is formulated in a relativistic context [73].

The scattering of two composite objects is considered to be made up of the scattering of the individual constituents and this is expressed by the Glauber multiple scattering expansion for the transition matrix T.

$$1 - S = T = \sum_{ij} t_{ij} - \frac{1}{2!} \sum' t_{ij} t_{k\ell} + \frac{1}{3!} \sum' t_{ij} t_{k\ell} t_{mn} - \cdots \quad (7.3)$$

t_{ij} is the elastic scattering amplitude for scattering of quark i on quark j, the quarks of course being in different hadrons. The $'$ on the summation signs indicate omitting terms in which the same pairs of quarks scatter off each other more than once, for instance the factor $t_{ij} t_{ij}$ which is clearly included in the amplitude t_{ij} (see fig. 42). The scattering amplitude for the process $AB \to A^*B^*$ is given by $\langle A^*B^*/1-S/AB \rangle$ and how this is calculated in a relativistic model will be indicated presently.

We first of all consider the model for the quark quark scattering amplitude t_{ij}. The most general amplitude is like that for NN elastic scattering and is given by

$$t_{ij} = \sum_{m=1}^{5} \Gamma_m \Gamma_m f_m^{ij}(s_{ij}, t) \quad (7.4)$$

where $\Gamma_m = 1, \gamma_5, \gamma_\mu, \gamma_5 \gamma_\mu, \sigma_{\mu\nu} \qquad m = 1, 2, 3, 4, 5$.

For spin independence as in the C.F.Z. model we would simply choose:

$$t_{ij} = S_{ij} \, f^{ij}(t) \qquad\qquad S_{ij} = (p_i + p_j)^2 \qquad (7.5)$$

the factor S_{ij} being included so that the cross-section is energy independent, and this is the choice of N. Byers [78]. However, it is interesting to consider the problem a little further. Diffraction proceeds primarily by natural parity exchange for which the reduced coupling is

$$G_\beta^+\left(\tfrac{1}{2}, \tfrac{1}{2}\right) = g_1(t)\, p_\beta^2 + g_2(t)\, \gamma_\beta^i \qquad p^i = \tfrac{1}{2}(p_i + p_i') \quad (7.6)$$

As the exchange has approximately constant angular momentum $J = 1$ and there is no pole in the region near $J = 1$, the full quark quark amplitude is approximately

$$\left(g_1\, p_\beta^i + g_2\, \gamma_\beta^i\right)\left(g_1\, p^{j\beta} + g_2\, \gamma^{j\beta}\right) = g_1^2\, v_{ij} + g_1 g_2 \left(p^i \gamma^j + p^j \gamma^i\right)$$
$$+ \; g_2^2\, \gamma^i \gamma^j$$

where $v_{ij} = p^i \cdot p^j$. Hence it can be seen that the effect of choosing the scalar interaction is to set the coupling $g_2 = 0$ and this result corresponds to postulating T.C.H.C. for the individual quark quark scatterings. The other simple choice is $g_1 = 0$ and this corresponds to S.C.H.C. It is clear that on niave grounds the model is expected to trivially reproduce T.C.H.C. for bosons but fail to produce S.C.H.C. for NN scattering.

Now consider the scattering process $AB \rightarrow A^* B^*$ by scattering of quark i in A and j in B as shown in fig. 43, clearly the contribution to the scattering amplitude is given by

$$\sum_{m=1}^{5} f_m^{ij}(s_{ij}, t)\left[\int \frac{d^4 q}{(2\pi)^4}\, \mathrm{Tr}\left[-\bar{\chi}_{A^*}(p_A + k, q + \tfrac{k}{2})\, \Gamma_m\, \chi_A(p_A, q)\left(\tfrac{\not{p}_A}{2} - \not{q} + m_q\right)\right]\right.$$
$$\times \left[\int \frac{d^4 q'}{(2\pi)^4}\, \mathrm{Tr}\left[-\bar{\chi}_{B^*}(p_B - k, q' - \tfrac{k}{2})\, \Gamma_m\, \chi_B(p_B, q')\left(\tfrac{\not{p}_B}{2} - \not{q}' + m_q\right)\right]\right] \qquad (7.7)$$

For scalar interaction $m = 1$ $\Gamma_1 = 1$, $f_m = 0$ $m \neq 0$

and $f_1^{ij}(s_{ij}, t) = s_{ij} f(t) \xrightarrow[s \to \infty]{} \frac{s}{4} f(t)$

It is assumed that the same function $f(t)$ describes quark-quark; quark antiquark and antiquark-antiquark scattering so that the G parity selection rule is reproduced. The results have been calculated by Byers [78] for the Bethe Salpeter wave-functions of the B.J.K. [62] for mesons.

We first of all consider the transitions

$\pi \to \pi (0^+)$, $B(1^{+-})$, $A_2 (2^{-+}) \cdots$ (i.e. singlet mesons).

The $\pi \to B$ amplitude vanishes in accord with the G parity selection rule, but the transitions conserving G parity $\pi \to \pi$, A_3 etc. are all allowed and conserve T.C.H. as anticipated. Unfortunately all the allowed singlet $\to$ singlet transitions have about comparable magnitude and increase with increasing J. This is opposite to the data where the $\pi \to \pi$ amplitude is much bigger than the $\pi \to A_3$ amplitude.

For the singlet triplet transitions the model fails completely as might be anticipated from the non-relativistic result. The cross-section for $\pi \to A_1$ $K \to Q$ etc. is no longer strictly zero but is nevertheless negligible $\left(\sigma_{\pi A_1} \sim \frac{\sqrt{\beta_V}}{m_q} \sigma_{\pi\pi} \right.$ with $\sqrt{\beta_V} \sim \frac{3}{8}$ and $m_q \sim 4 \text{ GeV} \right)$. Clearly it is inadequate simply to introduce spin dependent interactions as this would correspond to the $SU(6)_W$ model with quark spin flip and of course this is wrong. The reason for the inadequacy of the B.J.K. model is the absense of spin orbit terms in the wave-functions.

Clearly because of the lack of success of the single scattering approximation it is not worth considering multiple scattering corrections or applying the model with anzatzed wave-functions to baryons. However, both these refinements and easily incorporated and are shown diagramatically in figs. 44 and 45.

7.4 Application of the linearized oscillator quark model to diffraction scattering

In applying the linearized oscillator model to diffraction we follow the approach of Ravndal [77] and replace the pomeron by a vector object J_α but do not demand current conservation.

$$J_\alpha = e_\rho F \left(g_1(t) Q_\alpha + g_2(t) X_\alpha \right) e^{q \cdot a^\dagger/\sqrt{x}} e^{-q \cdot q/\sqrt{x}} \quad (7.8)$$

With this coupling the quark and antiquark amplitudes are not in general the same and this has the consequence that the G parity can change at a diffractive vertex. We choose $g_2 = 0$ to retain the G parity selection rule.

The calculations of diffractive vertices are performed in exactly the same way as for electromagnetic transitions and the results are presented in table 17. The results for the singlet $\rightarrow$ singlet transitions are rather similar to those of the B.J.K. type model [78]. The model predicts F.C.A.C. (any quark model does!) but the predicted cross-sections for the high mass production processes is too big, specifically

$$\frac{d\sigma}{dt} \left(\pi\pi \rightarrow \pi\pi \right) \Big|_{t=0} \sim \frac{d\sigma}{dt} \left(\pi\pi \rightarrow \pi A_3 \right) \Big|_{t=0} .$$ Physically this bad result arises because the diffractive size increases

with mass.   To see this we consider the elastic vertex at zero momentum transfer $\langle \psi^J | J_\alpha | \psi^J \rangle \propto \mathcal{G}_\alpha m_J$.

In principal the diffractive coupling can depend on the hadron mass, however in a model where the quarks are considered to be real this is unintelligible because the pomeron interacts with the individual quarks and hence any mass dependence must come from the wave-functions. If we assume that the diffractive size is about the same for all hadrons then this suggests that we divide our previous results by a factor $\sqrt{m_1 m_2}$.   The basic coupling $\mathcal{G}_\alpha$ now becomes $\mathcal{G}_\alpha / \sqrt{m_1 m_2}$ which is dimensionless.   We now predict that $\frac{d\sigma}{dt}(\pi\pi \to \pi\pi)\Big|_{t=0} \sim 5 \frac{d\sigma}{dt}(\pi\pi \to \pi A_3)\Big|_{t=}$ which is more reasonable although the A_3 production cross-section is still too big.   To fit the differential cross-section is still too big.   To fit the differential cross-section we must assume that the coupling e_ρ is a function of t as the t dependence arising from the elementary quark scattering is too weak (c.f. the B.J.K. model [73]).

The results for the singlet-triplet transitions are an improvement on the B.J.K. type model.   The $\pi \to A_1$ transition is allowed, essentially because of the presence of spin orbit interaction, however the $\pi \to A_2$ transition is forbidden and this is consistent with Morrison's rule. Most other models either predict both the $\pi \to A_1$ and A_2 transitions to be forbidden or allowed (e.g. C.F.Z. both forbidden, F.J.K. both allowed).   The evidence as to whether the A_2 is produced diffractively is in dispute, but it has been argued that the energy dependence is

inappropriate to diffraction. Furthermore we predict

T.C.H.C. for the $\pi \to A_1$ transition and also

$$\frac{d\sigma}{dt}\left(\pi\pi \to \pi\pi\right)\Big|_{t=0} \sim 10 \frac{d\sigma}{dt}\left(\pi\pi \to \pi A_1\right)\Big|_{t=0}$$

which is roughly consistent with the predicted $\pi\pi \to \pi A_3$

cross-section.

We also consider the $\rho \to \rho$ process which by

vector dominance is related to vector meson photo-

production $\gamma \to \rho$. Although the prediction does

not correspond to pure S.C.H.C. as in experiment [3], a

substantial amount of s-channel non-flip amplitude is

present. (See tables 4 and 5) and so the predicted

density matrices may not be too far astray.

Because of the relative lack of success in

the meson sector it is not reasonable to give a detailed

discussion of baryon dissociation using anzatzed

wave-functions. Furthermore as spin orbit forces are

less evident for baryons than mesons the predictions

for the helicity vertices for N $\longrightarrow$ N* follow on general

grounds for any quark model. (See chapter 4).

8.   Conclusions

One of our main concerns in this thesis has been an investigation of diffraction scattering paying particular attention to the helicity properties of diffractive amplitudes.   In chapter one we considered the consequences of the analogy between diffraction scattering and optical diffraction and gave a very simple argument for S.C.H.C. for diffractive vertices when the quantum numbers of the produced state are the same as the parent state ($N \rightarrow N$, $\gamma \rightarrow \rho$, $N \rightarrow P_{11}$ ...)   However, the spin and parity of a diffractive vertex may change and then there is considerable controversy as to the production mechanism.   In chapter two we supported the view that much of the boson production $\left(\pi \rightarrow A_1 , K \rightarrow Q \cdots \right)$ corresponds to mass-enhancement effects, probably produced by a (modified) Deck mechanism.   Both S.C.H.C. and Morrisons rule were predicted in accord with the data. However for fermion data the most prominant cross-section peaks ($N*(\frac{1}{2}^+,1470)$, $N*(\frac{3}{2}^-,1520)$, $N*(\frac{5}{2}^+,1688)$) seem to correspond to genuine resonances.

In chapter three we considered the fermion data from a phenomenological point of view and assumed diffraction to proceed by pomeron exchange.   We adopted a covariant Regge formalism and calculate the asymptotic s-channel helicity vertices in terms of covariant couplings for both boson and fermion transitions.   These results can be applied for any Regge exchange processes.

We propose that the pomeron coupling to the $N \rightarrow N^*$ vertex is characterized by γ_β coupling and show that this hypothesis is consistent with the available data. Without detailed fitting it is seen that the elastic and $N \rightarrow N^*(\frac{1}{2}^+, 1470)$ transitions are in accord with the hypothesis. We fit the data for $\pi N \rightarrow \pi N^*(\frac{3}{2}^-, 1520, \frac{5}{2}^+, 1688)$ testing the γ_β hypothesis and other proposed helicity rules as well as considering various nonsense mechanisms. It is demonstrated that both S.C.H.C. and γ_β coupling give satisfactory fits to the data, but S.C.H.C. cannot be a universal rule as it fails for the elastic vertex. (when γ_β coupling reduces to S.C.H.C.).

In the next chapter we considered some constituent models for diffraction dissociation. We showed that an $SU(6)_W$ model with quark spin flip was consistent with the fermion data. However, the model failed to reproduce the $\pi \rightarrow A_1$, $K \rightarrow Q$ data where spin orbit terms were needed. Furthermore the single scattering amplitude in the non-relativistic quark model is predicted to be zero in the forward direction for inelastic transitions. In view of the success of the $SU(6)_W$ model it was suggested that this embarrassing result would not appear in a relativistic model.

In chapter five we considered some relativistic quark models and chapter six we proposed a new model. The model is closely related to the non-relativistic harmonic oscillator model and as in the F.K.R. approach is designed for calculational simplicity rather than theoretical adequacy. It is an improvement over the

F.K.R. model in that spin is treated dynamically, however this refinement makes the treatment of baryons more difficult, the present model being confined to mesons. But it is hoped that the treatment of baryons as a three quark problem (rather than di-quark-quark) will be possible. Our philosophy for justifying and improving the model is based on the Dual models where the "quarks" are regarded as representing the internal degrees of freedom of the hadron but nevertheless being inseparable from it. Consequently the quark mass has no meaning in our approach. Working in analogy with the dual model it is anticipated that multi-quark effects $(q\bar{q}q\bar{q}$ states, quark sea, etc.) may be included in the model. Already in the present version of the model spin orbit terms are naturally included and this is the most novel feature of our model. Furthermore this is suggestive of "current" quarks, but we have not yet checked that our model satisfies current algebra.

We test the model by considering the predictions for decays by emission of pseudoscalar mesons and photons and find reasonable agreement with experiment. We also consider $\pi \to \mu e \nu$, $\rho \to e^+ e^-$ and K_{ℓ_3} decay.

In chapter seven we apply the model to diffraction dissociation. Because of the presence of spin orbit terms in our wave-functions the $\pi \to A_1$ transition is allowed, but the $\pi \to A_2$ transition forbidden. This is interesting not only because there is some experimental support for this result but also because all previous models either allow both or forbid both. Furthermore F.C.H.C. is predicted again in agreement with experiment.

Unfortunately the predicted cross-section sizes are wildly incorrect as we predict $\sigma(\pi\pi \to \pi\pi) \sim \sigma(\pi\pi \to \pi A_3)$ This result, however, is a disease our model has in common with other relativistic quark models (J.K.R. and B.J.K.).

References

1.   J. D. Jackson   Classical Electrodynanics. Ch. 9.

2.   M. L. Good and W. D. Walker. PR 120 (1960) 1857

3.   J. Ballan et al. PRL 24   (1970) 960

4.   V.D. Barger and D.B.Cline. Phenomenological
     Theories of High Energy scattering.

5.   L. Van Hove. Proceedings of Erice Summer
     School 1972.

6.   D. Amati, S. Fubini and A. Staghellini.
     PL 1 (1962) 29

7.   S. Mandelstam NC 30   (1963) 1128 and 1148

8.   H. Cheng and T. T. Wu. PRL 24 (1970) 1456

9.   B. W. Lee   PR D1   (1970) 2361

10. H. B. Nielson and P. Olesen. PL 32B (1970) 203

11. P. Olesen NP B29 (1971) 77

12. P. Ramond PR D3   (1971) 2415

13. M. A. Virasoro   PR 1D (1970) 2933

14. R. C. Brower PR D6 (1972) 1655 and
     P. Goddard and C. Thorn PL 40B 235 1972

15. M. Gell Mann PL 8   (1964) 214 and
     G. Zweig CERN Preprint TH 401, 412 (1964) (unpublished)

16. H. J. Lipkin and S. Meshkov PRL 14 (1965) 670

17. S. D. Drell and K. Johnson SLAC preprint 1091 (1972)

18. A. N. Mitra and R. Majumdar. PR 150 (1966) 1194

19. M. Gell Mann and Y. Ne'eman. The Eightfoldway and
     S. Adler and R. Dashen. Current Algebras

20. H. J. Melosh   Caltech Thesis (1973) (unpublished) and
     M. Gell Mann proceedings of Erice Summer School 1972.

21. J. Benecke, T. T. Chou, C. N. Yang and Q. Yen
    P.R. 188 (1969) 2159

22. P. L. Frampton and P. V. Ruuskanen PL 39B (1972) 78
    and J. C. Van der Velde proceedings of the VII
    Recontre de Moriand Meribel-der-Allures, France
    (results quoted from reference 30)

23. D. R. O. Morrison, Review of quasi-two body
    reactions, Proc. 15th Int. Conf. on high energy
    physics, Kiev 1970.

24. R. T. Deck, PRL 13 (1964) 169.

25. D. R. O. Morrison, PR 165 (1968) 1699

26. G. Ascoli et al, PRL 26 (1971) 929

27. J. V. Beaupre et al, PL 34B (1971) 160

28. J. W. Lansa et al, NP B37 (1972) 364

29. Y. T. Oh et al, PL 42B (1972) 497

30. G. L. Kane Proceedings of the XII Cracow
    school of theoretical physics (1972)

31. G. F. Chew, Com. on Nuc and Particle Physics II
    (1968) 74

32. R. G. Roberts PL 35B (1970) 525,
    J. Bartsche et al NP B24 (1970) and
    S. Pokovski and H. Satz NP B19 (1970) 113

33. E. W. Anderson et al PRL 25 (1970) 699

34. L. Van Hove PL 24B (1967) 183

35. A. D. Scadron PR 165 (1968) 1640

36. F. D. Gault and H. F. Jones NP B30 (1971) 68

37. F. D. Gault and P. J. Walters NCL 4 (1972) 461

38. F. D. Gault and P. J. Walters NP B49 (1972) 273

39. Edelstein et al PR D5 (1972) 1073

40. F. D. Gault J. Phys. A: Gen. Phys 4 (1971) 38

41.   H. F. Jones and M. D. Scadron PR <u>171</u> (1968) 1809

42.   T. T. Chou and C. N. Yang PR <u>175</u> (1968) 1832

43.   R. H. Dalitz Proceedings of the XII Cracow
       school of theoretical physics (1972)

44.   J. S. Bell CERN preprint TH 1717 CERN (1973)

45.   R. Carlitz, S. Frautschi and G. Zweig PRL <u>23</u> (1969)
       1134.

46.   P. G. O. Freund, H. F. Jones and R. J. Rivers
       PL <u>36B</u> (1971) 89

47.   R. Carlitz, M. B. Green and A. Zee. Institute
       for advanced study pre-print (unpublished) 1971

48.   M. Kislinger CAL TEC. pre-print CALT-68-341 (1971)

49.   T. T. Wu and C. N. Yang PR <u>137</u> (1965) B708

50.   D. E. Parry N.C.L. <u>4</u> (1972) 267

51.   N. Byers and S. Frautschi "Quanta" Ed. P.G.O.Freund
       C. J. Goebel and Y. Nambu, Chicago (1970)

52.   A. Le Yaouanc, L. Oliver, O. Pene and
       J. C. Raynal NP <u>B29</u> (1971) 204

53.   J. S. Bell CERN pre-print TH 1717 CERN (1973)

54.   A. Le Yaouanc, L. Oliver, O. Pene and J.C. Raynal
       NP B37 (1972) 541

55.   P. G. O. Freund PRL <u>20</u> (1968) 235 and
       H. Harari PRL <u>20</u> (1968) 1385

56.   J. Rasner PRL <u>22</u> (1969) 689 and
       H. Harari PRL <u>22</u> (1969) 562

57.   M. Gell-Mann. Proceedings of the 1972 Erice
       summer school and references therein

58.   A. Pagnamenta N.C. <u>53A</u> (1968) 30 and
       P. Narayanaswamy and A. Pagnamenta N.C. <u>53A</u> (1968) 635

59.   R. H. Dalitz.   Proceedings of the 13th International Conference on high energy physics (1966). Reprinted in J.J.J. Kokkedee "The Quark Model"

60.   S. Mandelstam   Comments on Nuc. and Particle Physics III   65 and 147

61.   R. P. Feynman, M. Kislinger and F. Ravndal PR D3 (1971) 2706

62.   M. Bohm, H. Joos and M. Kramer   NP B51 (1973) 397

63.   E. E. Salpeter and H. A. Bethe   PR 82 (1951) 1232

64.   C. H. Llewellyn-Smith, AP 53 (1969) 521

65.   T. Gudeus   PR 134 (1969) 1788

66.   O. W. Greenberg   PRL 13 (1964) 598;
       R. H. Dalitz Lectures at the 2nd Hawaii Tropical Conference on particle physics (1967);
       D. Faiman and A. W. Hendry   PR 173 (1968) 1720 and PR 180 (1969) 1572;   L. A. Copley, G. Karl and E. Obryke, PL 29 B (1969) 117

67.   G. C. Wick   PR 96 (1954) 1124

68.   M. Bohm, H. Joos and M. Kramer   CERN preprint TH 1715 CERN (1973)

69.   P. Goddard, J. Goldstone, C. Reobi, C. B. Thorn NP B56 (1973) 109

70.   L. Susskind   PRL 24 (1968) 944

71.   R. Van Royen and V. Weisskopf NC 50 (1967) 617 and R. Van Royen and V. Weisskopf NC 51 (1967) 583

72.   A. Le Yaouanc, L. Oliver, P. Pene, J. C. Raynal, Orsay preprint (1972) LPHE 72/6

73.   Particle Data Group R.M.P. 45 (1973)

74.   G. Ebel et al. NP B33 (1971) 317

75.   E. W. Colglazier and J. L. Rosner, N.P. B27
      (1972) 349

76.   P. . . Walters, A.M. Thomson and F. D. Gault.
      Durham preprint (1973)

77.   '. Ravndal P.L. 37B   300 (1971)

78.   M. Byers.   Proceedings of the XII Cracow school
      of theoretical physics (1972).

Appendix 1   Basic Conventions

a) Units

Natural units are used throughout with

$$\hbar = c = 1 \quad \text{and} \quad 1 \text{ GeV} = 1 \text{ nat. unit}$$

Hence one natural unit of length $= \dfrac{\hbar c}{1 \text{ GeV}} = 1.973 \times 10^{-14} \text{cm}$

and $1 \text{ mb} = 10^{-27} \text{ cm}^2 = .3893$ nat. units.

b) 4-vectors

Contravariant 4 vector $A^\mu = (A^0, A^1, A^2, A^3) = (A^0, \underset{\sim}{A})$

Metric $g_{\mu\nu} = (1; -1, -1, -1)$ with $A_\mu = g_{\mu\nu} A^\nu$

where all repeated indices are summed, Greek indices from 0 to 3 and Latin indices over the values 1, 2 and 3.

4 position $x^\mu = (x^0, \underset{\sim}{x})$ where x^0 is the time and $\underset{\sim}{x}$ the spacial position.

4-momentum operator $p^{op\,\mu} = i \partial^\mu = i \dfrac{\partial}{\partial x_\mu} = \left(i \dfrac{\partial}{\partial x^0}, -i \underset{\sim}{\nabla} \right)$

c) Dirac matrices γ^μ

Anti commutation relations $\{\gamma^\mu, \gamma^\nu\} = 2 g_{\mu\nu}$

$$\gamma_0 = \beta \quad \text{and} \quad \underset{\sim}{\gamma} = \beta \underset{\sim}{\alpha}$$

In the Dirac Pauli representation

$$\gamma^0 = \begin{pmatrix} 1 & 0 \\ 0 & -1 \end{pmatrix} \qquad \{\gamma^i\} = \underset{\sim}{\gamma} = \begin{pmatrix} 0 & \underset{\sim}{\sigma} \\ -\underset{\sim}{\sigma} & 0 \end{pmatrix}$$

Pauli matrices $\underset{\sim}{\sigma}$

$$\sigma_1 = \begin{pmatrix} 0 & 1 \\ 1 & 0 \end{pmatrix} \qquad \sigma_2 = \begin{pmatrix} 0 & -i \\ i & 0 \end{pmatrix} \qquad \sigma_3 = \begin{pmatrix} 1 & 0 \\ 0 & -1 \end{pmatrix}$$

where $\sigma^{\mu\nu} = \dfrac{i}{2}[\gamma^\mu, \gamma^\nu]$, $\sigma^{ij} = \begin{pmatrix} \sigma_k & 0 \\ 0 & \sigma_k \end{pmatrix} \varepsilon_{ijk}$, $\sigma^{0i} = i\alpha^i$

and $\gamma_5 = \gamma^5 = i\gamma^0 \gamma^1 \gamma^2 \gamma^3 = \begin{pmatrix} 0 & 1 \\ 1 & 0 \end{pmatrix}$

Feynman slash $\not{A} = A_\mu \gamma^\mu$

Free particle Dirac spinor $u_\lambda(p)$ is defined by the

equation $\qquad (\not{p} - m)\, u_\lambda(p) = 0$

The antispinor $V_\lambda(p)$ satisfies the equation

$$(\not{p} + m)\, V_\lambda(p) = 0$$

In both cases $\qquad p_0 > 0$

Adjoint spinor $\qquad \bar{u}_\lambda(p) = u_\lambda^\dagger(p)\,\gamma_0$

and if u transforms under a lorentz transformation Λ

to $u' = S(\Lambda)\,u$ then $\bar{u} \xrightarrow{\Lambda} \bar{u}\, S^{-1}(\Lambda)$

Normalization conditions

$$\bar{u}_\lambda(p)\, u_\lambda(p) = 2m \quad \text{and} \quad \bar{V}_\lambda(p)\, V_\lambda(p) = -2m$$

the index λ defines the spin direction.

c) Kinematic invariants for basic scattering process $AB \to CD$.

Referring to fig. 46, we define the invariant S

$S = (p_A + p_B)^2 = (p_C + p_D)^2$ and this is just the square of

the centre of mass energy in the direct channel $AB \to CD$

which is also called the s-channel. $t = (p_C - p_A)$

$= (p_D - p_B)^2$ and this is the effective

mass squared of an exchange as shown in fig 47. In the

channel $A\bar{C} \to \bar{B}D$ $\sqrt{t}$ becomes the centre of mass

energy and hence this channel is called the t channel.

Referring to fig. 48 for scattering in the direct channel

centre of mass we have

$$t = m_A^2 + m_B^2 - 2\, p_{0_A} p_{0_C} + 2\, p p' \cos\theta \underset{s \to \infty}{\sim} -\frac{s}{2}(1 - \cos\theta).$$

Also $u = (p_A - p_D)^2 = (p_B - p_C)^2$. In the channel $A\bar{D} \to C\bar{B}$

$\sqrt{u}$ is the centre of mass energy and hence this channel

is referred to as the u channel.

d) Cross-section formula

All states are normalized such that the probability density $= 2 p_0$ and hence the probability current is a 4-vector.

Suppose $\mathcal{M}$ is the amplitude for some process $AB \to C_1 C_2 \cdots C_n$

Then the probability/sec

$$= 2\pi \frac{\sum |\mathcal{M}|^2}{2 p_{0_A} 2 p_{0_B} \prod_{i=1}^{\wedge} 2 p_{0_i}} \prod_{j=1}^{n-1} \frac{d p_j}{(2\pi)^3} \, \delta\left(p_{0_A} + p_{0_B} - \sum p_{0_C} \right)$$

$$= (2\pi)^4 \frac{\sum |\mathcal{M}|^2}{2 p_{0_A} 2 p_{0_B}} \, \delta^4\left(p_A + p_B - \sum p_C \right) \prod_{i=1}^{\wedge} (2\pi) \delta\left(p_{C_i}^2 - m_{C_i}^2 \right) \frac{d^4 p_i}{(2\pi)^4}$$

$\mathcal{M}$ is a relativistic invariant.

The differential cross-section for $AB \to CD$ in the centre of mass is

$$\frac{d\sigma}{d\Omega} = \frac{1}{64 \pi^2} \frac{q}{p s} \sum |\mathcal{M}|^2$$

where q is the outgoing momentum and p is the incident momentum. The invariant cross-section

$$\frac{d\sigma}{dt} = \frac{d\sigma}{d\Omega} \frac{d\Omega}{dt} = \frac{1}{64 \pi} \frac{1}{p^2 s} \sum |\mathcal{M}|^2$$

with $4 p^2 s = \left(s^2 - 2s(m_A^2 + m_B^2) + (m_A^2 - m_B^2)^2 \right) \underset{s \to \infty}{\rightsquigarrow} s^2$

Asymptotically $\quad \dfrac{d\sigma}{dt} \underset{s \to \infty}{\rightsquigarrow} \dfrac{1}{16 \pi s^2} \sum |\mathcal{M}|^2$

Appendix 2

Covariant couplings for NN' vertices and some theorems for fermion vertices.

a) The NN' couplings

Consider the NN' vertex shown in fig. 49 in the rest frame of the exchange particle (i.e. the t-channel). The spin, S of the NN' system is either 0 or 1 and as the total angular momentum must be J then the orbital angular momentum L is as given below

for S = 0, L = J and when S = 1, L = J - 1, J or J + 1

If parity is conserved then for natural parity vertices L = J and for the unnatural parity vertex L = J $\pm$ 1, and hence in general there are two independent couplings. As only one label β_1 is needed to account for the NN' system having spin 1 the natural parity coupling is

$\left(g_1 \, P_{\beta_1} + g_2 \, \gamma_{\beta_1} \right) P_{\beta_2} \cdots P_{\beta_J}$. The momentum couplings just correspond to orbital angular momentum. The unnatural parity coupling is simply obtained by multiplying the natural parity coupling by γ_5.

b) Theorem: For fermion vertices $V^+ \left(g, m_+, m_- \right) = (-)^{S-\lambda'} V^- \left(f, m_-, m_+ \right)$ where $m_\pm = \frac{1}{2} \left(m' \pm m \right)$ and g, f are the natural and unnatural parity coupling functions respectively.

Proof:

Suppose $G^+(g)$ is the coupling corresponding to the natural parity vertex $V^+(g)$, then $G^+(f)\gamma_5$ is the coupling corresponding to the unnatural parity vertex $V^-(f)$. The factor γ_5 can be absorbed into the initial spinor

$$u_\lambda(p) = \frac{1}{\sqrt{p_0 + m}} \left(p_0 + m + \gamma_5 \, \underline{\sigma} \cdot \underline{p} \right) \varphi_\lambda = \left(\sqrt{p_0 + m} + \gamma_5 \lambda \sqrt{p_0 - m} \right) \varphi_\lambda$$

where φ_λ is a two component spinor with helicity λ. The vertex $V^+(g)$ involves the factor $G^+(g)\,u(\rho)$ while for the vertex $V^-(g)$ the corresponding quantity is

$$G^+(f)\,\gamma_5\,u(\rho) = \left(\gamma_5 \sqrt{\rho_0 + m} + \lambda \sqrt{\rho_0 - m}\right)\varphi_\lambda.$$

Clearly the results will be identical on the replacement

$$m \to -m \quad \text{or} \quad m_\pm \to m_\mp \qquad \text{while changing the sign}$$

of the vertex for negative helicity. Hence we have the

rule $\quad V^+(g, m_+, m_-) = (-)^{\lambda - s}\, V^-(f, m_-, m_+)$

c) <u>Theorem</u>: For $\tfrac{1}{2} \to J$ vertices, to obtain the flip vertex

$V^{\pm}_{\frac{1}{2}, \lambda'}$ from the non flip $V^{\pm}_{\frac{1}{2}, \lambda'}$ requires the

substitutions $\left(m_\pm g_{2n-1} + g_{2n}\right) \to \tfrac{1}{2}\, g_{2n-1}$ and $t'\,g_{2n-1} \to 2\left(m_\pm g_{2n-1} + g_{2n}\right)$

Proof: Referring to table 6 it can be seen that the only relevant part of the coupling for the spinor part of the wave-functions is $G = \left(g_{2n-1}\, \rho_\beta + g_{2n}\, \gamma_\beta\right)$. We need only prove the theorem for natural parity vertices because of the theorem proved in part (b). The final state wave-function is $\overline{\psi} = \left(c_+ T^{*\,m - \frac{1}{2}}\, \overline{u}_+ + c_- T^{*\,m + \frac{1}{2}}\, \overline{u}_-\right)$

Now

$$\overline{u}_+ \left(g_{2n-1}\, \rho_\beta + g_{2n}\, \gamma_\beta\right) u_+ \;\leadsto\; 2\left(m_+ g_{2n-1} + g_{2n}\right)\rho_\beta$$

$$\overline{u}_+ \left(g_{2n-1}\, \rho_\beta + g_{2n}\, \gamma_\beta\right) u_- \;\leadsto\; g_{2n-1}\sqrt{-t}\; \rho_\beta$$

From parity $\quad \overline{u}_-\, G\, u_+ = -\, g_{2n-1}\sqrt{-t}\; \rho_\beta$

and $\quad\quad \overline{u}_-\, G\, u_- = 2\left(m_+ g_{2n-1} + g_{2n}\right)\rho_\beta$

Hence $\overline{\psi}\, G\, u_+ \to \overline{\psi}\, G\, u_-$ upon the substitutions

$$2\left(m_+ g_{2n-1} + g_{2n}\right) \to g_{2n-1}\sqrt{-t} \quad \text{and} \quad g_{2n-1}\sqrt{-t} \to -2\left(m_+ g_{2n-1} + g_{2n}\right)$$

Recalling that for flip vertices the angular momentum factor $\sqrt{-t}$ is divided out we obtain the result that for

$$V^+_{\frac{1}{2}, \lambda} \to V^-_{-\frac{1}{2}, \lambda} \quad \text{we make the substitutions}$$

$$2\left(m_+ g_{2n-1} + g_{2n}\right) \to g_{2n-1} \quad \text{and} \quad g_{2n-1}\, t' \to 2\left(m_+ g_{2n-1} + g_{2n}\right).$$

Appendix 3

Covariant couplings for $\rho\rho'$ and s-channel helicity vertices for bosons

a) The $\rho\rho'$ coupling

Consider the $\rho\rho'$ vertex in the rest frame of the spin J exchange. The spin S of the $\rho\rho'$ system can be 0, 1 or 2 and as the total angular momentum must be J the orbital angular momentum L can take on the values listed below

for $S = 2$ $L = J \pm 2$, $J \pm 1$ and J

     $S = 1$ $L = J \pm 1$ and J

and for

     $S = 0$ $L = J$

If the exchange is of natural parity and hence the whole vertex has natural parity, parity conservation implies

$(-)^{L} = (-)^{J}$ and hence the allowed values of L are

for $S = 2$ $L = J \pm 2$, and J, $S = 1$ $L = J$ and for $S = 0$ then $L = J$. There are as a consequence 5 independent couplings. Labeling the incoming ρ by an index μ and the final ρ' by ν the couplings are

     $S = 0$ $L = J$ $g_{\mu\nu} Q_{\alpha_1} Q_{\alpha_2} \cdots Q_{\alpha_J}$

     $S = 1, 2$ $L = J$ $\begin{cases} g_{\mu\alpha_1} Q_\nu Q_{\alpha_2} \cdots Q_{\alpha_J} \\ g_{\nu\alpha_1} Q_\mu Q_{\alpha_2} \cdots Q_{\alpha_J} \end{cases}$

     $S = 2$ $L = J - 2$ $g_{\mu\alpha_1} g_{\nu\alpha_2} Q_{\alpha_3} \cdots Q_{\alpha_J}$

     $S = 2$ $L = J + 2$ $Q_\mu Q_\nu Q_{\alpha_1} Q_{\alpha_2} \cdots Q_{\alpha_J}$

Clearly only the internal labels α_1 and α_2 are relevant and the reduced covariant coupling is

$$G^{+}_{\mu\nu}(1, 1, J) = \left[\, g_1 Q_\mu Q_\nu Q_{\alpha_1} Q_{\alpha_2} + g_2\, g_{\mu\nu} Q_{\alpha_1} Q_{\alpha_2} + \right.$$

$$\left. g_3\, g_{\mu\alpha_1} Q_\nu Q_{\alpha_2} + g_4\, g_{\nu\alpha_1} Q_\mu Q_{\alpha_2} + g_5\, g_{\mu\alpha_1} g_{\nu\alpha_2} \right]$$

b) <u>Asymptotic s-channel vertices for bosons -</u>
   <u>some useful results</u>

The part of the vertex which survives asymptotically must be proportional to $Q_{\alpha_1} Q_{\alpha_2} \cdots Q_{\alpha_J}$ as other terms will correspond to lower s-dependence in the amplitude. Using this result and the formula listed below the asymptotic s-channel helicity vertices given in table 5 are easily reproduced.

Referring to fig. 50

Initial spin 1 vectors from which the Rita Schwinger wave-functions are built are

$$\epsilon^{\pm} = \frac{1}{\sqrt{2}} \begin{pmatrix} \mp 1 \\ -i \\ 0 \\ 0 \end{pmatrix} \qquad \epsilon^{0} = \frac{1}{m} \begin{pmatrix} 0 \\ 0 \\ q_c \\ q \end{pmatrix} \longrightarrow \frac{Q_\mu}{2}$$

The final spin vectors are

$$\epsilon^{\pm \, \prime *} = \frac{1}{\sqrt{2}} \begin{pmatrix} \mp \cos\theta \\ i \\ \pm \sin\theta \\ 0 \end{pmatrix} \qquad \epsilon_2^{0 \, \prime *} = \frac{1}{m'} \begin{pmatrix} q_0' \cos\theta \\ 0 \\ q_c' \cos\theta \\ q \end{pmatrix} \longrightarrow \frac{Q_\mu}{2}$$

$$q' = (q\sin\theta, \, 0, \, q\cos\theta \, ; \, q_c')$$

$$t = \Delta^2 = (q - q')^2 = -q^2 \theta^2$$

Then for large s and small t

$$\epsilon^{\pm \, \prime *} \cdot \epsilon^{\pm} \longrightarrow -1 \qquad \epsilon^{* \, 0} \cdot \epsilon^0 \longrightarrow -2R/mm'$$
$$\epsilon^{\pm \, \prime *} \cdot Q \longrightarrow \mp \sqrt{-t}/2\sqrt{2} \qquad \epsilon^{\prime * 0} \cdot Q \longrightarrow -T/m'$$
$$\epsilon^{\pm} \cdot Q \longrightarrow \mp \sqrt{-t}/2\sqrt{2} \qquad \epsilon^{0} \cdot Q \longrightarrow -T'/m'$$

with $\quad R = \left(-\frac{t}{4} + \frac{m'^2 + m^2}{4} \right)$

$\quad T = \left(\frac{t}{4} + m_+ m_- \right)$ and $T' = \left(\frac{t}{4} - m_+ m_- \right)$.

Appendix 4

The solutions to the linearized oscillator model for mesons

Defining $\mu = m_0/\sqrt{2\omega}$ and $\epsilon = E/\sqrt{2\omega}$ the quark-quark equation in the rest frame is

$$[\mu - \frac{\epsilon}{2}(\gamma_0^{(1)} + \gamma_0^{(2)})]|\psi\rangle = (\underset{\sim}{a}_+ \cdot \underset{\sim}{a} + \underset{\sim}{a}_- \cdot \underset{\sim}{a}^\intercal)|\psi\rangle \qquad (1.)$$

Rotational symmetry implies that the angular momentum and its z component m are good quantum numbers and hence we may write the wave-function in the form

$$|\psi(qq)\rangle = \begin{pmatrix} |1;\overset{jm}{\ell_1,s_1}\rangle & |2;\overset{jm}{\ell_2,s_2}\rangle \\ |3;\overset{jm}{\ell_2,s_2}\rangle & |4;\overset{jm}{\ell_4,s_4}\rangle \end{pmatrix} \qquad (2)$$

A.4.2 The discrete symmetries

i) Parity

If η_p is the parity of the meson then because the antiparticle has negative intrinsic parity $(-\eta_p)$ is the parity for the corresponding quark quark wave-function. Then parity invariance is

$$\gamma_0 |\psi(qq,-\underset{\sim}{a},-\underset{\sim}{a}^\intercal)\rangle \gamma_0 = -\eta_p |\psi(qq,\underset{\sim}{a},\underset{\sim}{a}^\intercal)\rangle$$

$$\begin{pmatrix} 1 & 0 \\ 0 & -1 \end{pmatrix}\begin{pmatrix} (-)^{\ell_1}|1\rangle & (-)^{\ell_2}|2\rangle \\ (-)^{\ell_3}|3\rangle & (-)^{\ell_4}|4\rangle \end{pmatrix}\begin{pmatrix} 1 & 0 \\ 0 & -1 \end{pmatrix} = \begin{pmatrix} (-)^{\ell_1}|1\rangle & (-)^{\ell_2+1}|2\rangle \\ (-)^{\ell_3+1}|3\rangle & (-)^{\ell_4}|4\rangle \end{pmatrix} = -\eta_p \begin{pmatrix} |1\rangle & |2\rangle \\ |3\rangle & |4\rangle \end{pmatrix}$$

Hence $\eta_p = (-)^{\ell_1+1}$ which agrees with the non-relativistic result as $|1\rangle$ and $|4\rangle$ are the large components. $\ell \equiv \ell_1 = \ell_4 = \ell_2 \pm 1 = \ell_3 \pm 1$ and hence

$$J = \ell, \quad \ell \pm 1.$$

ii) Charge conjugation

The quark antiquark wave-function

$|\psi(q\bar{q})\rangle = |\psi(q\bar{q})\rangle C$ where C is the charge conjugation matrix

$$C = \begin{pmatrix} 0 & \sigma_y \\ \sigma_y & 0 \end{pmatrix} \qquad C^{-1} = C^T \qquad \text{and} \qquad C^2 = -1$$

Charge conjugation invariance is

$$C \, |\psi(q\bar{q}; -\underline{a}, -\underline{a}^\dagger)\rangle^T \, C^{-1} = \eta_c \, |\psi(q\bar{q}; \underline{a}, \underline{a}^\dagger)\rangle$$

where η_c is the charge conjugation parity. For the particle particle equation this becomes

$$|\psi(qq; -\underline{a}, -\underline{a}^\dagger)\rangle^T \, C^{-1} = \eta_c \, |\psi(qq; \underline{a}, \underline{a}^\dagger)\rangle C$$

or $\quad |\psi(qq; -\underline{a}, -\underline{a}^\dagger)\rangle^T = -\eta_c \, |\psi(qq; \underline{a}, \underline{a}^\dagger)\rangle \qquad (3)$

Explicitly this becomes

$$\begin{pmatrix} (-)^{\ell_1}|1\rangle^T & (-)^{\ell_3}|3\rangle^T \\ (-)^{\ell_2}|2\rangle^T & (-)^{\ell_4}|4\rangle^T \end{pmatrix} = -\eta_c \begin{pmatrix} |1\rangle & |2\rangle \\ |3\rangle & |4\rangle \end{pmatrix}$$

Hence

$$\begin{pmatrix} |1\rangle^T & -|3\rangle^T \\ -|2\rangle^T & |4\rangle^T \end{pmatrix} = \eta_{PC} \begin{pmatrix} |1\rangle & |2\rangle \\ |3\rangle & |4\rangle \end{pmatrix} \qquad \eta_{PC} = \eta_P \eta_C \qquad (4)$$

For $\eta_{PC} = +1 \implies |1\rangle, |4\rangle \propto \underline{\sigma} \cdot \underline{\xi} \, i\sigma_y$ i.e. pure spin 1 object

and $\eta_{PC} = -1 \implies |1\rangle, |4\rangle \propto i\sigma_y$ which is a pure spin zero object

Note that this result is exactly analogous to the non-relativistic result and this follows from the decision to make the interaction 3-dimensional rather than 4-dimensional (i.e. neglecting q_0). Then for parity $\eta_P \to -\eta_P$ and for charge conjugation $\eta_P \to -\eta_P$ but for a 4-dimensional interaction, under parity $a_P \to (a_c; -\underline{a})$

whereas charge conjugation $a_\mu \to (-a_0, -\underline{a})$ and we do not automatically obtain the simple relation given by equation 4.

Also $\qquad |3\rangle^T = -\eta_{PC} |2\rangle$

Hence if $\qquad |3\rangle = \alpha |s=1\rangle + \beta |s=0\rangle$

Then $\qquad |2\rangle = \eta_{PC} (-\alpha |s=1\rangle + \beta |s=0\rangle)$.

A.4.3 Reduction of the equation to a set of Pauli spinor equations

The wave-function is written as a 4 x 4 matrix $\psi_{\alpha\beta}$ where α is the index corresponding to quark 1 and β quark 2.

Hence

$$\left[\mu - \frac{\epsilon}{2} (\gamma_c^{(1)} + \gamma_c^{(2)}) \right] |\psi\rangle = \begin{pmatrix} \overline{\mu - \epsilon} \, |1\rangle & \mu |2\rangle \\ \mu |3\rangle & \overline{\mu + \epsilon} \, |4\rangle \end{pmatrix} \qquad (5)$$

$$(\gamma^{(1)} - \gamma^{(2)}) |\psi\rangle = \begin{pmatrix} \underline{\sigma} |3\rangle - |2\rangle \underline{\sigma}^T & \underline{\sigma} |4\rangle + |1\rangle \underline{\sigma}^T \\ -\underline{\sigma} |1\rangle - |4\rangle \underline{\sigma}^T & -\underline{\sigma} |2\rangle + |3\rangle \underline{\sigma}^T \end{pmatrix} \qquad (6)$$

$$\gamma_5^{(1)} \gamma_5^{(2)} (\gamma^{(1)} - \gamma^{(2)}) |\psi\rangle = \begin{pmatrix} -\underline{\sigma} |2\rangle + |3\rangle \underline{\sigma}^T & -\underline{\sigma} |1\rangle - |4\rangle \underline{\sigma}^T \\ \underline{\sigma} |4\rangle + |1\rangle \underline{\sigma}^T & \underline{\sigma} |3\rangle - |2\rangle \underline{\sigma}^T \end{pmatrix} \qquad (7)$$

From 6 and 7 we obtain

$$\underline{\alpha}_+ |\psi\rangle = \frac{1}{2} \begin{pmatrix} \underline{\sigma} |3-2\rangle + |3-2\rangle \underline{\sigma}^T & \underline{\sigma} |4-1\rangle - |4-1\rangle \underline{\sigma}^T \\ \underline{\sigma} |4-1\rangle - |4-1\rangle \underline{\sigma}^T & \underline{\sigma} |3-2\rangle + |3-2\rangle \underline{\sigma}^T \end{pmatrix} \qquad (8)$$

$$\underline{\alpha}_- |\psi\rangle = \frac{1}{2} \begin{pmatrix} \underline{\sigma} |3+2\rangle - |3+2\rangle \underline{\sigma}^T & \underline{\sigma} |4+1\rangle + |4+1\rangle \underline{\sigma}^T \\ -\underline{\sigma} |4+1\rangle - |4+1\rangle \underline{\sigma}^T & -\underline{\sigma} |3+2\rangle + |3+2\rangle \underline{\sigma}^T \end{pmatrix} \qquad (9)$$

where $\qquad |3-2\rangle = |3\rangle - |2\rangle \qquad$ etc.

Hence from equations 1, 5, 8 and 9 we obtain the set
of coupled equations

$$(\mu - \epsilon)|1\rangle = \tfrac{1}{2}\,\underline{a}\{\underline{\sigma}|3-2\rangle + |3-2\rangle\underline{\sigma}^T\} + \tfrac{1}{2}\underline{a}^\dagger\{\underline{\sigma}|3+2\rangle - |3+2\rangle\underline{\sigma}^T\} \qquad (10a.)$$

$$(\mu + \epsilon)|4\rangle = \tfrac{1}{2}\,\underline{a}\{\underline{\sigma}|3-2\rangle + |3-2\rangle\underline{\sigma}^T\} - \tfrac{1}{2}\underline{a}^\dagger\{\underline{\sigma}|3+2\rangle - |3+2\rangle\underline{\sigma}^T\} \qquad (10b.)$$

$$\mu|2\rangle = \tfrac{1}{2}\,\underline{a}\{\underline{\sigma}|4-1\rangle - |4-1\rangle\underline{\sigma}^T\} + \tfrac{1}{2}\underline{a}^\dagger\{\underline{\sigma}|4+1\rangle + |4+1\rangle\underline{\sigma}^T\} \qquad (10c.)$$

$$\mu|3\rangle = \tfrac{1}{2}\,\underline{a}\{\underline{\sigma}|4-1\rangle - |4-1\rangle\underline{\sigma}^T\} - \tfrac{1}{2}\underline{a}^T\{\underline{\sigma}|4+1\rangle + |4+1\rangle\underline{\sigma}^T\} \qquad (10d.)$$

A.4.4   Case I :   The PC = -1 solutions

Charge conjugation implies $|1\rangle$ and $|4\rangle$ are
pure S = 0 states and hence

$$|1\rangle, |4\rangle \propto \begin{pmatrix} 0 & 1 \\ -1 & 0 \end{pmatrix} |\varphi\rangle \qquad As \quad (\uparrow\downarrow - \downarrow\uparrow) \propto \begin{pmatrix} 0 & 1 \\ -1 & 0 \end{pmatrix}$$

Now $\sigma_x^T = \sigma_x$, $\sigma_y^T = -\sigma_y$, $\sigma_z^T = \sigma_z$ and as $\{\sigma_x, \sigma_y\} = 0$, $\{\sigma_z, \sigma_y\} = 0$
and $[\sigma_y, \sigma_y] = 0$ then

$$\underline{\sigma}|1\pm4\rangle + |1\pm4\rangle\underline{\sigma}^T \equiv 0$$

Hence equations 10c and 10d reduce to

$$\mu|2\rangle = \mu|3\rangle = \tfrac{1}{2}\underline{a}\{\underline{\sigma}|4-1\rangle - |4-1\rangle\underline{\sigma}^T\} \implies |3-2\rangle = 0 \qquad (11)$$

or $|3\rangle = |2\rangle$

Using this result equations 10a and 10b become

$$(\mu - \epsilon)|1\rangle = -(\mu + \epsilon)|4\rangle = \tfrac{1}{2}\underline{a}^\dagger\{\underline{\sigma}|3+2\rangle - |3+2\rangle\underline{\sigma}^T\} \qquad (12)$$

$$\implies |4\rangle = \left(\frac{\epsilon - \mu}{\epsilon + \mu}\right)|1\rangle \implies |4-1\rangle = -\frac{2\mu}{\epsilon + \mu}|1\rangle$$

From 11 and 12 we obtain

$$|3\rangle = |2\rangle = \frac{\underline{a}}{\epsilon + \mu}\{|1\rangle\underline{\sigma}^T - \underline{\sigma}|1\rangle\} \qquad (13).$$

$$\underset{\sim}{\sigma} \cdot \underset{\sim}{a} = \begin{pmatrix} a_3 & a_- \\ a_+ & -a_3 \end{pmatrix} \quad \text{and} \quad \underset{\sim}{\sigma}^T \underset{\sim}{a} = \begin{pmatrix} a_3 & a_+ \\ a_- & -a_3 \end{pmatrix} \tag{13}$$

Defining
$$|i\rangle = \begin{pmatrix} 0 & 1 \\ -1 & 0 \end{pmatrix} |\varphi\rangle \tag{14}$$

Then

$$\underset{\sim}{a} \left\{ |i\rangle \underset{\sim}{\sigma}^T - \underset{\sim}{\sigma} |i\rangle \right\} = -2 \begin{pmatrix} -a_- & a_3 \\ a_3 & a_+ \end{pmatrix} |\varphi\rangle \equiv -2|x\rangle \tag{15}$$

Note $|x\rangle$ is a spin 1 object and so the affect of $(\underset{\sim}{\sigma_i} - \underset{\sim}{\sigma})\cdot \underset{\sim}{a}$ on a spin 0 object is to step up the spin by one unit. From equations 12, 13 and 15 we obtain the eigen value equation

$$(\epsilon^2 - \mu^2)|i\rangle = 2 \underset{\sim}{a}^+ \left\{ \underset{\sim}{\sigma} |x\rangle - |x\rangle \underset{\sim}{\sigma}^T \right\} \tag{16}$$

It is easily shown that

$$\underset{\sim}{a}^+ \left\{ \underset{\sim}{\sigma} |x\rangle - |x\rangle \underset{\sim}{\sigma}^T \right\} = 2N \begin{pmatrix} 0 & 1 \\ -1 & 0 \end{pmatrix} |\varphi\rangle \quad \text{where } N = \underset{\sim}{a}^+ \underset{\sim}{a} \tag{17}$$

where N is the number operator.

Thus substituting in 16 we see that $|\varphi\rangle$ is an eignstate of the number operator and

$$\epsilon^2 = \mu^2 + 4N$$

or

$$m^2 = E_N^2 = m_0^2 + 8\omega N = m_0^2 + \Omega N \tag{18}$$

Hence we have straight Regge trajectories and as $\ell = j$ for $\eta_{PC} = -1$, $\eta_P = (-)^{j+1}$, $\eta_C = (-)^j$ The ground state solution is the pseudoscalar 0^{-+}.

From equations 12 and 13 we obtain

$$|4\rangle = \left(\frac{\epsilon_N - \mu}{\epsilon_N + \mu}\right) |\varphi_{\ell=j}^N\rangle$$

and

$$|2\rangle = |3\rangle = -\frac{2}{(\epsilon_N + \mu)} |\chi^N\rangle \quad \text{where} \quad |\chi^N\rangle = \begin{pmatrix} -a_- & a_3 \\ a_3 & a_+ \end{pmatrix} |\varphi_{\ell=j}^N\rangle$$

We must also check that the solution is non spurious (i.e. that it corresponds to positive energy).

Let $\Omega \longrightarrow 0$ then $\epsilon_N \rightarrow \mu \Rightarrow |4\rangle = 0$

$|2\rangle \sim \frac{1}{\mu}$ (harmonicoscillator state)

$\frac{\sqrt{\Omega}}{m_0}$ (H.O. state) $\underset{\Omega \to 0}{\longrightarrow} 0$ Hence $|2\rangle$, $|3\rangle \longrightarrow 0$ and so the solution reduces to the product of two positive energy spinors at rest in the absence of interaction. (Note odd parity H.O. states $\overset{\Omega \to 0}{\longrightarrow} 0$ while even parity H.O. states $\overset{\Omega \to 0}{\longrightarrow}$ constant). Hence we deduce that the solution is non spurious.

A.4.5 Case II : The PC = +1 solutions

Adding equations 10(a) and 10(b) we obtain

$$\mu |1+4\rangle + \epsilon |4-1\rangle = (\mathcal{G}_1 + \mathcal{G}_2) \cdot \underline{a} |3-2\rangle \qquad 19(a)$$

Subtracting equations 10(a) and 10(b) gives

$$\mu |4-1\rangle + \epsilon |4+1\rangle = -(\mathcal{G}_1 - \mathcal{G}_2) \cdot \underline{a}^\dagger |3+2\rangle \qquad 19(b)$$

Adding 10(c) and 10(d)

$$\mu |3+2\rangle = (\mathcal{G}_1 - \mathcal{G}_2) \cdot \underline{a} |4-1\rangle \qquad 19(c)$$

Subtracting 10(c) and 10(d)

$$\mu |3-2\rangle = -(\mathcal{G}_1 + \mathcal{G}_2) \underline{a}^\dagger |4+1\rangle \qquad 19(d)$$

Defining $|4+1\rangle = |+\rangle$ and $|4-1\rangle = |-\rangle$, then from 19(a) and 19(d) we obtain

$$\mu|+\rangle + \epsilon|-\rangle = -\frac{1}{\mu}(\underline{\sigma}_1 + \underline{\sigma}_2)\,\underline{a}\,(\underline{\sigma}_1 + \underline{\sigma}_2)\cdot\underline{a}^\dagger|+\rangle \qquad 20(a)$$

Similarly substituting equation 19(c) into 19(b) gives the result

$$\mu|-\rangle + \epsilon|+\rangle = -\frac{1}{\mu}(\underline{\sigma}_1 - \underline{\sigma}_2)\cdot\underline{a}\,(\underline{\sigma}_1 - \underline{\sigma}_2)\cdot\underline{a}^\dagger|+\rangle \qquad 20(b)$$

Substituting the expression for $|-\rangle$ from 20(a) into 20(b) we obtain the basic eign value equation.

$$(\epsilon^2 - \mu^2)|+\rangle = (\underline{\sigma}_1 - \underline{\sigma}_2)\underline{a}^\dagger(\underline{\sigma}_1 - \underline{\sigma}_2)\underline{a}|+\rangle + (\underline{\sigma}_1 + \underline{\sigma}_2)\underline{a}(\underline{\sigma}_1 + \underline{\sigma}_2)\underline{a}^\dagger|+\rangle \qquad 20(c)$$

As $(\underline{\sigma}_1 + \underline{\sigma}_2)\underline{a}^\dagger(\underline{\sigma}_1 - \underline{\sigma}_2)\underline{a}^\dagger \equiv 0$

Note that eign value equation 20(c) is identical to equation 16 for spin zero states because $(\underline{\sigma}_1 + \underline{\sigma}_2)\underline{a}^\dagger|s=0\rangle \equiv 0$

Now from charge conjugation we know that $|1\rangle$ and $|4\rangle$ are spin one states and hence we may write

$$|+\rangle = \begin{pmatrix} |u\rangle & |s\rangle \\ |s\rangle & |d\rangle \end{pmatrix} \quad \left(\sim \underline{\sigma}\cdot\underline{\epsilon}\, i\sigma_y |\varphi\rangle\right) \qquad 21$$

Now

$$\frac{1}{2}(\underline{\sigma}_1 + \underline{\sigma}_2)\cdot\underline{a}^\dagger|+\rangle = \begin{pmatrix} a_3^\dagger|u\rangle + a_-^\dagger|s\rangle & \frac{1}{2}(a_+^\dagger|u\rangle + a_-^\dagger|d\rangle) \\ \frac{1}{2}(a_+^\dagger|u\rangle + a_-^\dagger|d\rangle) & a_+^\dagger|s\rangle - a_3^\dagger|d\rangle \end{pmatrix}$$

which is a spin one object.

and

$$\frac{1}{2}(\underline{\sigma}_1 - \underline{\sigma}_2)\cdot\underline{a}|+\rangle = \begin{pmatrix} 0 & a_3|s\rangle + \frac{1}{2}(a_-|d\rangle - a_+|u\rangle) \\ -(a_3|s\rangle + \frac{1}{2}(a_-|d\rangle - a_+|u\rangle)) & 0 \end{pmatrix}$$

which is a spin zero state. Define

$$|\chi\rangle = a_3|s\rangle + \frac{1}{2}(a_-|d\rangle - a_+|u\rangle)$$

Then we obtain

$$\frac{i}{4}(\mathcal{S}_1+\mathcal{S}_2)\underline{a}\,(\mathcal{S}_1+\mathcal{S}_2)a^\dagger|+\rangle =$$

$$\begin{pmatrix} a_3\left(a_3^\dagger|u\rangle+a_-^\dagger|s\rangle\right)+\frac{1}{2}a_-\left(a_+^\dagger|u\rangle+a_3^\dagger|d\rangle\right) & \frac{1}{2}\left(a_+(a_3^\dagger|u\rangle+a_-^\dagger|s\rangle)+a(a_+^\dagger|s\rangle-a_3^\dagger|d\rangle)\right) \\ \frac{1}{2}\left(a_+(a_3^\dagger|u\rangle+a_-^\dagger|s\rangle)+a_-(a_+^\dagger|s\rangle-a_3^\dagger|d\rangle)\right) & \frac{1}{2}a_+(a_+^\dagger|u\rangle+a_-^\dagger|d\rangle)-a_3(a_+^\dagger|s\rangle-a_3^\dagger|d\rangle) \end{pmatrix}$$

(22)

Also

$$\frac{i}{4}(\mathcal{S}_1-\mathcal{S}_2)a^\dagger(\mathcal{S}_1-\mathcal{S}_2)\underline{a}|+\rangle = \begin{pmatrix} -a_-^\dagger|\chi\rangle & a_3^\dagger|\chi\rangle \\ a_3^\dagger|\chi\rangle & a_+^\dagger|\chi\rangle \end{pmatrix}.$$

(23)

which is a spin one state.   Note that from 22 and 23

$$\frac{1}{4}\left[(\mathcal{S}_1+\mathcal{S}_2)\underline{a}\,(\mathcal{S}_1+\mathcal{S}_2)a^\dagger+(\mathcal{S}_1-\mathcal{S}_2)a^\dagger(\mathcal{S}_1-\mathcal{S}_2)\underline{a}\right]|s=1\rangle=(N+2)|s=1\rangle$$

and hence the eign value equation 20(c) becomes

$$(\epsilon_N^2-\mu^2)=4(N+2).$$

i.e. the Regge trajectory is

$$m_N^2=\epsilon_N^2=m_0^2+\mathcal{S}2(N+2). \qquad \mathcal{S}2=8\omega$$

Note that there are 3 degenerate equations (for $|u\rangle,|d\rangle$ and $|s\rangle$) and hence there is no effective spin orbit interaction at the two component level.

In the case $j=\ell$ then the solution is unique and we have

$$(\mathcal{S}_1-\mathcal{S}_2)\underline{a}\,|N;j=\ell,m\rangle=0 \qquad (24)$$

For the cases $j=\ell\pm1$ both angular momenta ℓ and $\ell\pm2$ are allowed in general and the relative proportion is not determined.

Then we obtain

$$\frac{1}{4}(\sigma_1+\sigma_2)\underset{\sim}{a}(\sigma_1+\sigma_2)a^\tau |+\rangle =$$

$$\begin{pmatrix} a_3\left(a_3^\tau|u\rangle+a_-^\tau|s\rangle\right)+\frac{1}{2}a_+\left(a_+^\tau|u\rangle+a_3^\tau|d\rangle\right) & \frac{1}{2}\left(a_+\left(a_3^\tau|u\rangle+a_-^\tau|s\rangle\right)+a_-\left(a_+^\tau|s\rangle-a_3^\tau|d\rangle\right)\right) \\ \frac{1}{2}\left(a_+\left(a_3^\tau|u\rangle+a_-^\tau|s\rangle\right)+a_-\left(a_+^\tau|s\rangle-a_3^\tau|d\rangle\right)\right) & \frac{1}{2}a_+\left(a_+^\tau|u\rangle+a_3^\tau|d\rangle\right)-a_3\left(a_+^\tau|s\rangle-a_3^\tau|d\rangle\right) \end{pmatrix}$$

$$(22)$$

Also

$$\frac{1}{4}(\sigma_1-\sigma_2)a^\dagger(\sigma_1-\sigma_2)\underset{\sim}{a}|+\rangle = \begin{pmatrix} -a_-^\tau|\chi\rangle & a_3^\dagger|\chi\rangle \\ a_3^\dagger|\chi\rangle & a_+^\tau|\chi\rangle \end{pmatrix} \qquad (23)$$

which is a spin one state.   Note that from 22 and 23

$$\frac{1}{4}\left[(\sigma_1+\sigma_2)\underset{\sim}{a}\,(\sigma_1+\sigma_2)a^\dagger+(\sigma_1-\sigma_2)a^\dagger(\sigma_1-\sigma_2)\underset{\sim}{a}\right]|s=1\rangle = (N+2)|s=1\rangle$$

and hence the eign value equation 20(c) becomes

$$\left(\epsilon_N^2-\mu^2\right) = 4(N+2).$$

i.e. the Regge trajectory is

$$m_N^2 = \epsilon_N^2 = M_0^2 + \Omega(N+2). \qquad \Omega = 8\omega$$

Note that there are 3 degenerate equations (for $|u\rangle,|d\rangle$

and $|s\rangle$) and hence there is no effective spin orbit

interaction at the two component level.

In the case $j=\ell$ then the

solution is unique and we have

$$(\sigma_1-\sigma_2)\underset{\sim}{a}\,|N; j=\ell,m\rangle = 0 \qquad (24)$$

For the cases $j=\ell\pm1$ both angular momenta ℓ and $\ell\pm2$

are allowed in general and the relative proportion is

not determined.

i) The case $j = \ell$ $C = P = (-)^{j+1}$

It is easily seen that we may write the $j = \ell$ state in the form

$$|N; j=\ell, m\rangle = \begin{pmatrix} -L_- & L_z \\ L_z & L_+ \end{pmatrix} |N; \ell, m\rangle = \underline{L} \cdot \underline{\sigma}(i\sigma_y) |N; \ell, m\rangle$$

Now writing

$$|+\rangle = A_+ |N; j=\ell, m\rangle \quad \text{and} \quad |-\rangle = A_- |N; j=\ell, m\rangle$$

From equation 20(b) and equation 24 we have

$$A_- = -\frac{E}{m_0} A_+$$

$$2A_+ = A_+ + A_- = -\frac{(E-m_0)}{m_0} A_+$$

and $\quad 2A_1 = A_+ - A_- = \frac{(E+m_0)}{m_0} A_+$

Letting $\quad A_+ = 2m_0$

we have $\quad A_+ = -(E-m_0) \quad$ and $\quad A_1 = (E+m_0)$.

From equation 24 $\quad (\underline{\sigma}_1 - \underline{\sigma}_2) \underline{q} |4-1\rangle = 0 \quad$ and hence from equation 19(c) we deduce that $|3\rangle = |2\rangle$.

Equation 19(d) then reads $\quad -2\rho |2\rangle = \rho |3-2\rangle = -(\underline{\sigma}_1 + \underline{\sigma}_2) \underline{q}^\dagger |4+1\rangle$

or $\quad |2\rangle = \frac{m_0}{\rho}(\underline{\sigma}_1 + \underline{\sigma}_2) \underline{q}^\dagger |N; j=\ell, m\rangle = \frac{\sqrt{\Omega}}{2}(\underline{\sigma}_1 + \underline{\sigma}_2) \underline{q}^\dagger |N; j=\ell, m\rangle$

$$= i\sqrt{\Omega} (\underline{q}^\dagger \wedge \underline{L}) \cdot \underline{\sigma}(i\sigma_y) |N; \ell, m\rangle$$

Hence the full solution may be written in the form

$$\left|\psi_{j=\ell\,^m/_0}^{N_s=1}\right\rangle_{\substack{\text{rest} \\ \text{frame}}} = \begin{pmatrix} (E+m_0)\underline{L}\cdot\underline{\sigma}(i\sigma_y) & i\sqrt{\Omega}(\underline{q}^\dagger\wedge\underline{L})\cdot\underline{\sigma}(i\sigma_y) \\ -i\sqrt{\Omega}(\underline{q}^\dagger\wedge\underline{L})\cdot\underline{\sigma}(i\sigma_y) & -(E-m_0)\underline{L}\cdot\underline{\sigma}(i\sigma_y) \end{pmatrix} |N; \ell, m\rangle$$

Note as $\Omega \to 0 \quad E \to m_0 \quad$ solution $\to \begin{pmatrix} \sim & 0 \\ 0 & 0 \end{pmatrix}$

which corresponds to the product of two positive energy spinors at rest and hence the state is non-spurious.

ii) Case $j = \ell \pm 1$.

As the eigen value equation determines only the number of excitations for a given angular momentum two values of the orbital momentum are possible. As stated in the previous section when $j = \ell$ the solution is unique. Also for the leading trajectory $N = \ell$ $j = \ell + 1$ and also $N = \ell - 1$ $j = N$ the solutions are easily seen to be unique. In all these cases $|3\rangle = -|2\rangle$ or the small components have spin one. This motivates us to adopt the criterion (no spin zero components) $|3\rangle = -|2\rangle$. to fix the solutions uniquely. This is arbitrary but as the first ambiguous case occurs for $N = 2$, $j = 1$ it is unimportant for practical calculations. (We can, of course, determine a second solution orthogonal to the original for cases with ambiguities).

$$ |N; j, \ell, m\rangle = \sum_{-1}^{+1} \langle \ell, m; 1 m' | j m \rangle | N; \ell, m - m'\rangle \, \underset{\sim}{\varepsilon}_{m'} \cdot \underset{\sim}{\varepsilon} (1\sigma_3). $$

where $\underset{\sim}{\varepsilon}$ is a spin one wave-function and represents the spin of the quarks.

For pure spin 1 wave-functions $\left(|3\rangle = -|2\rangle \right)$. and hence

$$ |3 + 2\rangle \propto (\underset{\sim}{\varsigma}_1 - \underset{\sim}{\varsigma}_2) \, \underline{q} \, |-\rangle. = 0 \tag{25} $$

From equation 20(b)

$$ |+\rangle = -\frac{\mu}{\varepsilon} |-\rangle $$

and $2|1\rangle = -\left(\frac{\varepsilon + \mu}{\varepsilon}\right) |-\rangle$ also $2|4\rangle = \left(\frac{\varepsilon - \mu}{\varepsilon}\right) |-\rangle$. $\tag{26}$

Equation 25 also determines the orbital mixture as it implies

$$ |-\rangle \propto \frac{1}{4} (\underset{\sim}{\varsigma}_1 + \underset{\sim}{\varsigma}_2) \, \underline{q} \, (\underset{\sim}{\varsigma}_1 + \underset{\sim}{\varsigma}_2) \, q^\dagger | N; j, m\rangle $$

$$ = (N + 2) | N; j, m\rangle - \frac{1}{4} (\underset{\sim}{\varsigma}_1 - \underset{\sim}{\varsigma}_2) \, q^\dagger (\underset{\sim}{\varsigma}_1 - \underset{\sim}{\varsigma}_2) \, \underline{q} \, | N; j, m\rangle. $$

Choose the normalization such that

$$|-\rangle = -2E\left((N+2)|N;j,m\rangle - \tfrac{1}{4}(\underline{\mathscr{S}}_1-\underline{\mathscr{S}}_2)\underline{a}^\dagger(\underline{\mathscr{S}}_1-\underline{\mathscr{S}}_2)\underline{a}\,|N;j,m\rangle\right)$$

we obtain from 25

$$|1\rangle = (E+m_0)\left((N+2)|N;j,m\rangle - \tfrac{1}{4}(\underline{\mathscr{S}}_1-\underline{\mathscr{S}}_2)\underline{a}^\dagger(\underline{\mathscr{S}}_1-\underline{\mathscr{S}}_2)\underline{a}\,|N;j,m\rangle\right)$$

$$|4\rangle = -(E-m_0)\left((N+2)|N;j,m\rangle - \tfrac{1}{4}(\underline{\mathscr{S}}_1-\underline{\mathscr{S}}_2)\underline{a}^\dagger(\underline{\mathscr{S}}_1-\underline{\mathscr{S}}_2)\underline{a}\,|N,j,m\rangle\right)$$

$$\tfrac{1}{2}(\underline{\mathscr{S}}_1-\underline{\mathscr{S}}_2)\underline{a}\cdot\underline{\mathscr{S}}\cdot\underline{\mathscr{S}}(i\sigma_y) = \underline{\mathscr{S}}\cdot\underline{a}\,(i\sigma_y)$$

and

$$\tfrac{1}{2}(\underline{\mathscr{S}}_1-\underline{\mathscr{S}}_2)\underline{a}^\dagger\,\underline{\mathscr{S}}\cdot\underline{a}\,(i\sigma_y) = \underline{\mathscr{S}}\cdot\underline{a}^\dagger\,\underline{\mathscr{S}}\cdot\underline{a}\,(i\sigma_y)$$

Hence (renormalizing $\times \Omega$) and projecting to definite angular momentum states; we have

$$|1\rangle = \sum_{m'} \underbrace{\langle \ell, m-m',1,m'|j,m\rangle}_{C^j_{m m'}}(E+m_0)\left((E^2-m_0^2)\,\underline{\mathscr{S}}\cdot\underline{\mathscr{S}} - \Omega\,\underline{\mathscr{S}}\cdot\underline{a}^\dagger\,\underline{\mathscr{S}}\cdot\underline{a}\right)$$

$$(i\sigma_y)|N,\ell,m-m'\rangle \qquad (27)$$

From equation 19(d)

$$|2\rangle = -|3\rangle = \tfrac{1}{2\mu}(\underline{\mathscr{S}}_1+\underline{\mathscr{S}}_2)\underline{a}^\dagger|+\rangle$$

and as

$$|+\rangle = 2m_0\left((E^2-m_0^2)|N,j,\ell,m\rangle - \tfrac{\Omega}{4}(\underline{\mathscr{S}}_1-\underline{\mathscr{S}}_2)\underline{a}^\dagger(\underline{\mathscr{S}}_1-\underline{\mathscr{S}}_2)\underline{a}\,|N,j,\ell,m\rangle\right)$$

we have

$$|2\rangle = \tfrac{m_0}{\mu}\left(E^2-m_0^2\right)(\underline{\mathscr{S}}_1+\underline{\mathscr{S}}_2)\cdot\underline{a}^\dagger\,|N;j,\ell,m\rangle$$

Now $\tfrac{1}{2}(\underline{\mathscr{S}}_1+\underline{\mathscr{S}}_2)\underline{a}^\dagger(\underline{\mathscr{S}}\cdot\underline{\mathscr{S}})\,i\sigma_y = i(\underline{a}^\dagger\wedge\underline{\mathscr{S}})\cdot\underline{\mathscr{S}}\,(i\sigma_y)$.

Hence

$$|2\rangle = \sum_{m'} i\sqrt{\Omega}\,(E^2-m_0^2)(\underline{a}^\dagger\wedge\underline{\mathscr{S}}_{m'})\cdot\underline{\mathscr{S}}\,(i\sigma_y)|N;\ell,m-m'\rangle\,C^j_{m m'}$$

and the full solution is given by

$$|\psi^{Nj}_{\ell m\,s=1}\rangle = \sum_{m'}\begin{pmatrix} (E+m_0)\left(\underline{\mathscr{S}}\cdot\underline{\mathscr{S}} - \Omega\,\dfrac{\underline{\mathscr{S}}\cdot\underline{a}^\dagger\,\underline{\mathscr{S}}\cdot\underline{a}}{m^2-m_0^2}\right)i\sigma_y & i\sqrt{\Omega}(\underline{a}^\dagger\wedge\underline{\mathscr{S}}_{m'})\underline{\mathscr{S}}\,i\sigma_y \\[2mm] -i\sqrt{\Omega}(\underline{a}^\dagger\wedge\underline{\mathscr{S}}_{m'})\underline{\mathscr{S}}\,i\sigma_y & (E-m_0)\left(\underline{\mathscr{S}}\cdot\underline{\mathscr{S}} - \Omega\,\dfrac{\underline{\mathscr{S}}\cdot\underline{a}^\dagger\,\underline{\mathscr{S}}\cdot\underline{a}}{m^2-m_0^2}\right)\sigma_y \end{pmatrix}$$

$$\times\, C^j_{m m'}\,|N;\ell,m-m'\rangle \qquad (28)$$

Note as $\Omega \to 0$, $E^2-m_0^2 \to 2\Omega$ and the solution is again seen to be non-singular.

A.4.6 Lorentz covariant form of the solutions

In the rest frame $E = M$ = mass of the state. In boosting to a general frame we make the replacements

$$\underline{\underline{\epsilon}} \rightarrow - \epsilon_\mu \qquad \text{etc.}$$

The PC = -1 solution is

$$\begin{pmatrix} (m+m_0) i\sigma_y & -\sqrt{\Omega} \underline{\epsilon} \underline{\sigma} i\sigma_y \\ -\sqrt{\Omega} \underline{\epsilon} \underline{\sigma} i\sigma_y & (m-m_0) i\sigma_y \end{pmatrix} |N; j=\ell, m\rangle.$$

The matrix part of the wave-function will be expanded in terms of the Dirac matrices and $|N; j=\ell, m\rangle$. is taken to be a lorentz scalar made up of N, $\eta_\mu^\dagger$ variables contracted with a wave-function $T_{\mu_1 \cdots \mu_N}^{jm}$

$$\begin{pmatrix} (m+m_0) i\sigma_y & 0 \\ 0 & (m-m_0) i\sigma_y \end{pmatrix} = (m+m_0\gamma_0)\gamma_5 C = \gamma_5 (m-m_0\gamma_0)C$$

$$\xrightarrow[\text{frame}]{\text{In arbitrary}} \gamma_5 (m - m_0 \frac{\not{p}}{m}).$$

Also

$$\begin{pmatrix} 0 & -\underline{\epsilon}\underline{\sigma} i\sigma_y \\ -\underline{\epsilon}\underline{\sigma} i\sigma_y & 0 \end{pmatrix} = -\gamma_0\underline{\gamma}\cdot\underline{\epsilon}\,\gamma_5 C \longrightarrow \gamma_5 \frac{\not{p}}{m} \eta C.$$

in an arbitrary frame

To obtain the particle antiparticle equation multiply.

C^{-1} and hence the Lorentz covariant solution for PC = -1 is

$$|N; j m; PC=-\rangle = \gamma_5 \left[\left(m - m_0 \frac{\not{p}}{m}\right) + \sqrt{\Omega} \frac{\not{p}}{m} \eta \right] |N, j, m\rangle \quad (29)$$

where $|N, j, m\rangle = T_{\mu_1 \cdots \mu_N}^{jm} \eta^{\dagger \mu_1} \cdots \eta^{\dagger \mu_N} |0\rangle.$

with T^{jm} is a spin j wave-function formed from N spin one wave-functions.

In an exactly similar manner the PC = +1

$j = \ell$ solution may be written in the form

$$|N; j = \ell, m; PC = +\rangle = \left[\left(m + m_0 \frac{\not{\phi}}{m}\right) \not{\psi} - i \sqrt{52} \frac{\gamma_5}{m} \mathcal{E}(P \eta^\dagger L \gamma) \right] |N, \ell, m\rangle \quad (30)$$

where $\mathcal{E}(ABCD) = \mathcal{E}_{\mu\nu\lambda\sigma} A^\mu B^\nu C^\lambda D^\sigma$, $\mathcal{E}_{\mu\nu\lambda\sigma}$

is the antisymmetric permutation symbol $\mathcal{E}_{\mu\nu\lambda\sigma} = +1$

for even permutations of the variables 0, 1, 2, 3 and

$\mathcal{E}_{\mu\nu\lambda\sigma} = -1$ for odd permutations.

The general solution for PC = +1 is

$$|N; j, \lambda; PG+\rangle = \sum_{m'} C^j_{\lambda m'} \left\{ \left(m + m_0 \frac{\not{\phi}}{m}\right)\left(\not{\phi} + \frac{52 \, \eta^\dagger \in_m \eta}{P^2 - m_0^2}\right) - i \sqrt{52} \times \right.$$

$$\left. \frac{\gamma_5}{m} \mathcal{E}(P \eta^\dagger \in_m \gamma) \right\} |N; \ell, \lambda - m'\rangle$$

$$(31)$$

A.4.7   <u>Normalization of wave-functions</u>

Normalization condition is

$$Tr \langle \overline{\psi} \gamma_\mu \psi \rangle = - 8 m_0 P_\mu \qquad (32)$$

For the PC = -1 states

$$\langle \overline{\psi}_- \gamma_\mu \psi_- \rangle = \langle N, j, m | \left[\eta^\dagger \frac{\not{\phi}}{m}\sqrt{52} + \left(m - m_0\frac{\not{\phi}}{m}\right) \right] \gamma_5 \gamma_\mu \gamma_5 \times$$

$$\left[\left(m - m_0 \frac{\not{\phi}}{m}\right) + \frac{\not{\phi}}{m} \eta \right] |N; j, m\rangle$$

Anything linear in η or $\eta^\dagger$ vanishes as $\langle N | N \pm 1 \rangle = 0$

and also Tr (odd No. of γ matrices) = 0 and thus

$$Tr \langle \overline{\psi} \gamma_\mu \psi \rangle = -2 m_0 \langle N; j, m | Tr \not{P} \gamma_\mu | N; j, m \rangle = -8 m_0 P_\mu$$

and hence state given by equation 29 satisfies

normalization condition 32.

For PC = + $j = \ell$ states

$$\langle \overline{\psi} | = \langle N; \ell, m | \left[\not{\psi} \left(m + m_0 \frac{\not{\phi}}{m}\right) + i \sqrt{52} \mathcal{E}\left(\frac{P}{m} \eta L \gamma\right) \gamma_5 \right]$$

and hence

$$Tr \langle \bar{\psi} \gamma_\rho \psi \rangle = \langle N; \ell, m | m_0 Tr [\not{4} \gamma_\rho \not{\phi} \not{4}] + m_0 Tr [\not{4} \not{\phi} \gamma_\rho \not{4}] | N; \ell, m \rangle.$$

As $L \cdot P = 0$ we obtain

$$Tr \langle \bar{\psi} \gamma_\rho \psi \rangle = -8 m_0 \langle N; \ell, m | P_\rho \cdot L_\rho L^r | N; \ell, m \rangle$$

$$L_\rho L^\nu = L_0 L^0 - \underline{L} \cdot \underline{L}$$ in the rest frame this has the

eign value $-\ell(\ell+1)$ and as $L_\rho L^\nu$ is an invariant

and $j = \ell$ the correctly normalized state is

$$| N; j = \ell \ PC = -1 \rangle = \frac{1}{\sqrt{j(j+1)}} \left[(m + m_0 \frac{\not{\phi}}{m}) \not{4} - i\sqrt{52} \frac{\gamma_5}{m} \mathcal{E}(P \eta^\dagger L \gamma) \right] | N; j, m \rangle.$$

The normalization for $j = \ell \pm 1$ is difficult in
general although the ground state vector meson solution
is already correctly normalized

$$| N = 0 \ 1^{-+} \rangle = \left[(m + m_0 \frac{\not{\phi}}{m}) \not{\epsilon} - i\sqrt{52} \frac{\gamma_5}{m} \mathcal{E}(P \eta^\dagger \in \gamma) \right] | 0 \rangle.$$

A.4.8 Verification of covariant solutions

It will now verify that equations 29, 30 and 31
do indeed satisfy the equation.

$$\left[m_0 - \frac{1}{2}(\not{\phi}_1 + \not{\phi}_2) \right] | \psi \rangle = -\frac{\sqrt{52}}{2} \left[\alpha_{+\rho} \eta^\nu + \alpha_{-\rho} \eta^{\dagger \nu} \right] | \psi \rangle \qquad (33)$$

by substituting back into the equation

i)   The PC = -1 solution

$$| \psi \rangle = \gamma_5 \left[(m - m_0 \frac{\not{\phi}}{m}) + \sqrt{52} \frac{\not{\phi}}{m} \eta \right] | \varphi \rangle C$$

$$\not{\phi}_1 | \psi \rangle = -\gamma_5 \left[(m \not{\phi} - m m_0) + \sqrt{52} m \eta \right] | \varphi \rangle C$$

$$\not{\phi}_2 | \psi \rangle = -\gamma_5 \left[(m \not{\phi} - m m_0) - \sqrt{52} m \eta \right] | \varphi \rangle C$$

where we have used $\{\phi \eta\} = 0$ because $P \cdot \eta = 0$

Hence we obtain

$$\left[m_0 - \tfrac{1}{2}(\not{p}_1 + \not{p}_2) \right]|\psi\rangle = \gamma_5 \left[\frac{(m^2 - m_0^2)}{m}\phi + \sqrt{\Omega}\,\frac{\phi \eta}{m} \right]|\phi\rangle C \quad (34)$$

$$\eta_1|\psi\rangle = -\gamma_5 \left[(m + m_0\frac{\phi}{m})\eta - \sqrt{\Omega}\,\frac{\phi}{m}\eta\eta \right]|\phi\rangle C$$

$$\eta_2|\psi\rangle = -\gamma_5 \left[(m - m_0\frac{\phi}{m})\eta + \sqrt{\Omega}\,\frac{\phi}{m}\eta\eta \right]|\phi\rangle C$$

$$\tfrac{1}{2}(\eta_1 - \eta_2)|\psi\rangle = -\gamma_5 \left[m_0\frac{\phi \eta}{m} - \sqrt{\Omega}\,\frac{\phi}{m}\eta\eta \right]|\phi\rangle C$$

and

$$\tfrac{1}{2}\gamma_5^{(1)}\gamma_5^{(2)}(\eta_1 - \eta_2)|\psi\rangle = -\gamma_5 \left[m_0\frac{\phi \eta}{m} + \sqrt{\Omega}\,\frac{\phi}{m}\eta\eta \right]|\phi\rangle C$$

Hence $\qquad \alpha_+\eta|\psi\rangle = -2\gamma_5 m_0\frac{\phi \eta}{m}|\phi\rangle C$

Similarly

$$\alpha_-\eta^\dagger|\psi\rangle = 2\gamma_5\sqrt{\Omega}\,\frac{\phi}{m}\eta_\mu^\dagger\eta^\mu|\phi\rangle C$$

and therefore

$$(\alpha_+\eta + \alpha_-\eta^\dagger)|\psi\rangle = 2\gamma_5\frac{\phi}{m}\left[-m_0\eta + \sqrt{\Omega}\,\eta_\mu^\dagger\eta^\mu \right]|\phi\rangle C \quad (35)$$

Substituting 34 and 35 into equation 33 we obtain

$$\gamma_5\frac{\phi}{m}\left[m^2 - m_0^2 + \Omega\,\eta_\mu^\dagger\eta^\mu \right]|\phi\rangle C = 0$$

Hence we obtain the eign value equation

$$(m^2 - m_0^2 + \Omega\,\eta_\mu^\dagger\eta^\mu)|\phi\rangle = 0$$

and the PC = -1 solution given by equation 29 satisfies 33.

ii) The PC = +1 solution

We have

$$|\psi\rangle = \left[\left(m+m_0\frac{\not{p}}{m}\right)\not{A} - i\sqrt{2}\frac{\gamma_5}{m}\mathcal{E}(P\eta^\dagger\in\gamma)\right]|\varphi\rangle C.$$

where $A_\mu = \in_\mu + \Omega\frac{\eta^\dagger\in\eta}{m^2-m_0^2}$ and $P\cdot A = P\cdot\eta = 0$

$$\not{p}_1|\psi\rangle = \left[m(\not{p}+m_0)\not{A} + i\sqrt{2}\frac{\gamma_5}{m}\not{p}\mathcal{E}(P\eta^\dagger\in\gamma)\right]|\varphi\rangle C$$

$$\not{p}_2|\psi\rangle = -\left[-m(\not{p}+m_0)\not{A} + i\sqrt{2}\frac{\gamma_5}{m}\not{p}\mathcal{E}(P\eta^\dagger\in\gamma)\right]|\varphi\rangle C$$

Hence

$$\left[m_0-\tfrac{1}{2}(\not{p}_1+\not{p}_2)\right]|\psi\rangle = \left[\tfrac{1}{m}(m_0^2-m^2)\not{p}\not{A} - i\sqrt{2}\frac{\gamma_5}{m}m_0\mathcal{E}(P\eta^\dagger\in\gamma)\right]|\varphi\rangle C \quad (35)$$

Also

$$\gamma_1|\psi\rangle = \left[\left(m-m_0\frac{\not{p}}{m}\right)\eta\not{A} + i\sqrt{2}\frac{\gamma_5}{m}\eta\mathcal{E}(P\eta^\dagger\in\gamma)\right]|\varphi\rangle C.$$

$$\gamma_2|\psi\rangle = -\left[\left(m+m_0\frac{\not{p}}{m}\right)\eta_\mu\not{A}\gamma^\mu + i\sqrt{2}\frac{\gamma_5}{m}\eta\mathcal{E}(P\eta^\dagger\in\gamma) - 2i\sqrt{2}\frac{\gamma_5}{m}\mathcal{E}(P\eta^\dagger\in\eta)\right]|\varphi\rangle C.$$

Hence we obtain the equation

$$(\gamma_1-\gamma_2)|\psi\rangle = \left[\underline{m2\eta\cdot A} - m_0\frac{\not{p}}{m}\eta_\mu[\gamma_\mu,\not{A}] + \right.$$

$$\left. 2i\sqrt{2}\frac{\gamma_5}{m}\eta\mathcal{E}(P\eta^\dagger\in\gamma) - 2i\sqrt{2}\frac{\gamma_5}{m}\mathcal{E}(P\eta^\dagger\in\eta)\right]|\varphi\rangle C.$$

Now

$$\eta\cdot A|\varphi\rangle = \left(1+\Omega\frac{\eta\eta^\dagger}{m^2-m_0^2}\right)\in\cdot\eta|\varphi\rangle \equiv 0$$

$$\gamma_5^{(1)}\gamma_5^{(2)}(\gamma_1-\gamma_2)|\psi\rangle = \left[m_0\frac{\not{p}}{m}\eta_\mu[\gamma_\mu,\not{A}] + 2i\frac{\gamma_5}{m}\eta\mathcal{E}(P\eta^\dagger\in\gamma)\right.$$

$$\left. -2i\sqrt{2}\frac{\gamma_5}{m}\mathcal{E}(P\eta^\dagger\in\eta)\right]|\varphi\rangle C.$$

from which we deduce

$$\alpha_+\eta|\psi\rangle = \left[2i\sqrt{2}\frac{\gamma_5}{m}\eta\mathcal{E}(P\eta^\dagger\in\gamma) - 2i\sqrt{2}\frac{\gamma_5}{m}\mathcal{E}(P\eta^\dagger\in\eta)\right]|\varphi\rangle C \quad (37)$$

and

$$\alpha_- \eta^\dagger |\psi\rangle = - m_o \frac{\not{p}}{m} \eta_p^\dagger [\gamma_p, \not{A}] |\varphi\rangle C$$

Also

$$\eta_p^\dagger [\gamma_p, \not{A}] = \eta_p^\dagger [\gamma_p, \not{\epsilon}]$$

and as

$$P \cdot \eta^\dagger = P \cdot \epsilon = 0$$

we obtain

$$\not{p} \eta_p [\gamma_p, \not{A}] = 2i \gamma_5 \epsilon (P \eta^\dagger \epsilon \gamma).$$

and hence

$$\alpha_- \eta^\dagger |\psi\rangle = -2 \frac{m_o}{m} i \gamma_5 \epsilon (P \eta^\dagger \epsilon \gamma) |\varphi\rangle C \qquad (38)$$

Substituting equations 36, 37 and 38 into equation 33
we obtain

$$\left[\frac{1}{m} (m_o^2 - m^2) \not{p} \not{A} - i \sqrt{\Omega} \frac{\gamma_5}{m} m_o \epsilon (P \eta^\dagger \epsilon \gamma) \right] |\varphi\rangle C$$

$$= - \sqrt{\Omega} \left[i \sqrt{\Omega} \frac{\gamma_5}{m} \eta \epsilon (P \eta^\dagger \epsilon \gamma) - i \sqrt{\Omega} \frac{\gamma_5}{m} \epsilon (P \eta \epsilon \eta) \right.$$

$$\left. + \frac{m_o}{m} i \gamma_5 \epsilon (P \eta^\dagger \epsilon \gamma) \right] |\varphi\rangle C$$

which may be re-written

$$D|\psi\rangle \overset{!}{=} 0 = \left[\frac{1}{m}(m_o^2 - m^2) \not{p} \not{A} + i \frac{\Omega}{m} \gamma_5 [\eta \epsilon (P \eta^\dagger \epsilon \gamma) - \right. \qquad (39)$$

$$\left. \epsilon (P \eta^\dagger \epsilon \eta)] \right] |\varphi\rangle C$$

As

$$\gamma_p \gamma_\nu = g_{p\nu} + \frac{1}{2} [\gamma_p \gamma_\nu]$$

$$[\eta \epsilon (P \eta^\dagger \epsilon \gamma) - \epsilon (P \eta^\dagger \epsilon \eta)] = \frac{1}{2} \eta_p [\gamma^p, \epsilon (P \eta^\dagger \epsilon \gamma)]$$

$$= \frac{1}{2} \eta_p \epsilon_\nu (P \eta^\dagger \epsilon) [\gamma^p \gamma^\nu]$$

Now

$$i \gamma_5 [\gamma^p \gamma^\nu] = - \epsilon_{p\nu} (\gamma \gamma).$$

Hence we have

$$B = i \gamma_5 [\eta \epsilon (P \eta^\dagger \epsilon \gamma) - \epsilon (P \eta^\dagger \epsilon \eta)]$$

$$= \epsilon_\nu (\eta \gamma \gamma) \epsilon^\nu (P \eta^\dagger \epsilon)$$

$$B = \begin{vmatrix} 0 & \eta \cdot \eta^\dagger & \eta \cdot \in \\ \not{p} & \eta^\dagger & \not{\in} \\ \not{p} & \eta^\dagger & \not{\in} \end{vmatrix}$$

$$= -\eta \eta^\dagger [\not{p}\not{\in}] + \eta \cdot \in [\not{p}\eta^\dagger]$$

As

$$[\eta_\rho, \eta_\nu^\dagger] = \left(-g_{\mu\nu} + \frac{p_\mu p_\nu}{m^2}\right)$$

then

$$\eta \cdot \in [\not{p}\eta^\dagger] = -[\not{p}, \not{\in}] + [\not{p}\eta^\dagger] \eta \cdot \in$$

Thus we may re-write

$$B = -\left(\eta \eta^\dagger + 1\right) [\not{p}\not{\in}] + [\not{p}\eta] \eta \cdot \in$$

B acts directly on the state $|\varphi\rangle$ and hence

$$B = -\frac{(m_0^2 - m^2)}{\Omega}\left([\not{p}, \not{\in}] - \Omega[\not{p}\eta]\frac{\eta \cdot \in}{m_0^2 - m^2}\right)$$

$$= -2\frac{(m_0^2 - m^2)}{\Omega} \not{p} \not{A}$$

Substituting into equation 39 we see that $D|\psi\rangle = 0$ and hence verify that $|\psi\rangle$ is indeed a solution to equation 29.

Appendix 5

The decay $\quad 1^{-+} \to 0^+ 1^{-+}, (B^+ \to \pi^+ \omega^0)\quad$ an example calculation

The correctly normalized B and ω wave-functions are

$$|B\rangle = -\frac{\gamma_5}{2\sqrt{m_0}}\left[\left(m_1 - m_0\frac{\not{p}_1}{m_1}\right) + \sqrt{2}\frac{\not{p}_1}{m_1}\not{\eta}_1\right]\eta_1^\dagger\cdot\epsilon_1\,|0\rangle$$

$$|\omega\rangle = \frac{1}{2\sqrt{m_0}}\left[\left(m_2 + m_0\frac{\not{p}_2}{m_2}\right)\not{\epsilon}_2 - i\sqrt{2}\frac{\gamma_5}{m_2}\epsilon(\not{p}_2\not{\eta}_1\epsilon_2\gamma)\right]|0\rangle$$

where the unitary spin factors have been omitted. The kinematics is given in fig. 41. The pseudoscalar meson is replaced by the divergence of the axial current which is for the quark

$$\partial_\mu A^\mu = -i\gamma_5\not{q}\,F\,e^{q\cdot a^\dagger/\sqrt{2}}\,e^{-q\cdot a/\sqrt{2}}$$

The decay amplitude for emission of a pseudoscalar from a quark line is

$$\langle\omega|\partial_\mu A^\mu|B\rangle = iF\frac{Tr}{4m_0}\langle 0|\left[\left(m_2 - m_0\frac{\not{p}_2}{m_2}\right)\not{\epsilon}_2 + i\sqrt{2}\frac{\gamma_5}{m_2}\epsilon(\not{p}_2\not{\eta}_2\epsilon_2\gamma)\right]e^{q\cdot a^\dagger/\sqrt{2}}$$

$$\gamma_5\not{q}\gamma_5 e^{-q\cdot q/\sqrt{2}}\left[\left(m_1 - m_0\frac{\not{p}_1}{m_1}\right) + \sqrt{2}\frac{\not{p}_1\not{\eta}_1}{m_1}\right]\eta_1^\dagger\cdot\epsilon_1\,|0\rangle$$

Using the results

$$\left[e^{-q\cdot a/\sqrt{2}}, \eta^\dagger\cdot\epsilon\right] = \frac{q\cdot\epsilon}{\sqrt{2}}\,e^{-q\cdot a/\sqrt{2}}$$

$$\left[\eta_\mu, e^{q\cdot a^\dagger/\sqrt{2}}\right] = \left(-\frac{q_\mu}{\sqrt{2}} + p_\mu\frac{p\cdot q}{m^2}\right)e^{q\cdot a^\dagger/\sqrt{2}}$$

we obtain the result

$$\langle\omega|\partial_\mu A^{q\mu}|B\rangle = -i\frac{FTr}{4m_0}\langle 0|\left[\left(m_2 - m_0\frac{\not{p}_2}{m_2}\right)\not{\epsilon}_2 + i\frac{\sqrt{2}\gamma_5}{m_2}\epsilon(\not{p}_2\not{\eta}_2\epsilon_2\gamma) - \right.$$

$$\left. i\frac{\gamma_5}{m_2}\epsilon(\not{p}_2 p_1\epsilon\gamma)\right]\not{q}\left[\left(m_1 - m_0\frac{\not{p}_1}{m_1}\right) + \sqrt{2}\frac{\not{p}_1\not{\eta}_1}{m_1}\right]\left(\eta_1^\dagger\cdot\epsilon + \frac{q\cdot\epsilon_1}{\sqrt{2}}\right)|0\rangle$$

Taking the trace this becomes

$$\langle \omega | \partial_\mu A^{q\mu} | B \rangle = -i \frac{F}{\not{4} m_0} \langle 0 | \left[m_1 m_2 \, q \cdot \epsilon_2 + \frac{m_2}{m_1} \sqrt{\Omega} \left(-P_1 \cdot \epsilon_2 q \cdot \eta_1 + q \cdot P_1 \epsilon_2 \cdot \eta_1 \right) \right.$$

$$+ \frac{m_0^2}{m_1 m_2} \left(-P_2 \cdot q \, \epsilon_2 \cdot P_1 + P_1 \cdot P_2 q \cdot \epsilon_2 \right) + \frac{\sqrt{\Omega}}{m_1 m_2} \varepsilon_\mu (P_2 \eta_2 \epsilon_2) \varepsilon^\mu (q \, P_1 \eta_1)$$

$$- \frac{\sqrt{\Omega}}{m_1 m_2} \varepsilon_\mu (P_2 P_1 \epsilon_1) \varepsilon^\mu (q \, P_1 \eta_1) \right] \left(\eta_1^\dagger \epsilon_1 + \frac{q \cdot \epsilon_1}{\sqrt{\Omega}} \right) | 0 \rangle$$

Simplifying and taking matrix elements we get

$$\langle \omega | \partial_\mu A^{q\mu} | B \rangle = -i \frac{\sqrt{\Omega} \, F}{m_0} \left[\epsilon_1 \cdot \epsilon_2 \left(\frac{m_2}{m_1} - \frac{P_1 \cdot P_2}{m_1 m_2} \right) P_1 \cdot P_2 + \right.$$

$$q \cdot \epsilon_1 \, q \cdot \epsilon_2 \left[\frac{m_1 m_2}{\Omega} \left(1 + \left(\frac{m_0}{m_1} \right)^2 \right) + \frac{1}{m_1 m_2} \left(m_2^2 - P_1 \cdot P_2 \right) \right] \right]$$

In an exactly similar manner the amplitude for pseudo-scalar emission from an antiquark is

$$\langle \omega | \partial_\mu A^{q\mu} | B \rangle = -i \frac{\sqrt{\Omega}}{m_0} F \left[- \epsilon_1 \cdot \epsilon_2 \left(\frac{m_2}{m_1} - \frac{P_1 \cdot P_2}{m_1 m_2} \right) P_1 \cdot P_2 + \right.$$

$$q \cdot \epsilon_1 \, q \cdot \epsilon_2 \left[\frac{m_1 m_2}{\Omega} \left(1 + \left(\frac{m_0}{m_1} \right)^2 \right) - \frac{1}{m_1 m_2} \left(m_2^2 - P_1 \cdot P_2 \right) \right] \right].$$

The unitary spin wave-functions are

$$B^+ = u\bar{d}, \quad \pi^+ = u\bar{d} \quad \text{and} \quad \omega^0 = \frac{1}{\sqrt{2}} (u\bar{u} + d\bar{d})$$

using ideal mixing

$$\langle \omega | \lambda^q_{i \in i2} | B \rangle = - \langle \omega | \bar{\lambda}^{\bar{q}}_{i \in i2} | B \rangle = \frac{1}{\sqrt{2}}.$$

Hence the full decay amplitude is

$$T = \sqrt{2} \, \frac{F \sqrt{\Omega} \left(m_2^2 - P_1 \cdot P_2 \right)}{m_0 \, m_1 \, m_2} \left[(P_1 \cdot P_2) g_{\mu\nu} + q_\mu q_\nu \right] \epsilon_1^\mu \epsilon_2^{*\nu}$$

Table captions

1. Cross section, slope and helicity structure for some quasi two body diffractive reactions

2. Regge classification scheme

3. Tabulation of the components of the D resonances

4. Covariant boson couplings

5. Boson helicity vertices

6. Covariant fermion couplings

7. Fermion helicity vertices

8. Nonsense mechanisms at $\alpha = J_0$

9. $\pi N \to \pi N^*(5/2^+, 1688)$ fit parameters

10. $\pi N \to \pi N^*(3/2^-, 1525)$ fit parameters

11. Predicts of the constituent models of diffraction dissociation

12. The differential structure for fermion dissociations [33]

13. Coupling constants for electromagnetic decays [74]

14. Amplitudes for decoys by emission of a pseudoscalar meson

15. Widths for decay by emission of a pseudoscalar meson

16. Ratio of helicity amplitudes for $1^+ \to 1^- 0^-$ decays [75]

17. Amplitudes for diffractive vertices in the linearized oscillator model

TABLE 1

Basic properties of
diffractive cross-sections

Slope B is defined by $\dfrac{d\sigma}{dt} = A e^{Bt}$ $E_{Lab} \sim 15\,GeV$.

Process	Cross-section (μb)	Slope B (GeV^{-2})	Helicity structure
$\gamma N \to \gamma N$	$.087 \pm .01$	6	S.C.H.C.
$\pi^- N \to \pi^- N$	4030 ± 120	7 - 9	S.C.H.C.
$K N \to K N$	1300 ± 100	5 - 6	S.C.H.C.
$\bar{K} N \to \bar{K} N$	2200 ± 100	7 - 8	S.C.H.C.
$N N \to N N$	8030 ± 300	9 - 10	S.C.H.C.
$\gamma N \to \rho^0 N$	13 ± 3	6 - 8	S.C.H.C. [3]
$\pi^- N \to A_1^- N$	100 ± 30	9 - 11	T.C.H.C. [26]
$\pi^- N \to A_3^- N$	30 ± 10	8	T.C.H.C.
$K^0 N \to Q^0 N$		5 - 7	T.C.H.C. [27]
$\bar{K}^0 N \to \bar{Q}^c N$		8 - 10	T.C.H.C.
$N N \to N P_{11}$	400 ± 50	14 - 17	S.C.H.C.
$\pi N \to \pi P_{11}$	180 ± 20	16 ± 13	
$N N \to N D_{13}$	140 ± 25	51 ± 15	Both t ch. amps [29]
$\pi N \to \pi D_{13}$	60 ± 5	46 ± 4	$T^t_{\frac{1}{2}\frac{1}{2}}$ $T^t_{\frac{1}{2}-\frac{1}{2}}$ possible
$N N \to N F_{15}$	290 ± 20	46 ± 1	Both t ch amps [28]
$\pi N \to \pi F_{15}$	155 ± 5	48 ± 2	$T^t_{\frac{1}{2}\frac{1}{2}}$ $T^t_{\frac{1}{2}-\frac{1}{2}}$ possible

TABLE 2

Regge classification scheme

Cross-section σ

$$\sigma = A(P_{lab})^{-n} \sim S^{-n/2}$$

Type	n	exchange quantum numbers
Diffractive	0 - .2	vacuum quantum numbers
forward scattering	2 - 2.5	non-strange mesons
	2.5 - 3.5	strange mesons
backward scattering	3 - 5	baryon quantum numbers
Exotic	10 - 15	Quantum numbers belonging to no known particle e.g. $\Delta Q = 3$, $\Delta B = 2$ etc.

TABLE 3

<u>Tabulation of the particles R which together with
the pion make the Deck resonance D as in fig. 17</u>

"D resonance"	Component state (R,π)	Comments
A_1	ρ,π	
A_3	f^0,π	
Q	$K^*(890),\pi$ and ρK	
L	$K^*(1420),\pi$	
$N^*(1300)$?	$N\pi$	Not clear that $N^*(1300)$ has either a resonance or a Deck mass enhancement
$N^*(1410)$	$\Delta\pi$	In neither of these states is the system in a relative s-wave
$N^*(1710)$	$N^*(1470),\pi$	

TABLE 4

Covariant boson couplings (*)

$G^+(0,0)$ $\quad g \quad$ $\qquad G^-(0,0) \quad 0$

$G_\mu^+(0,1) \quad g_1 Q_{\alpha_1} Q_{\alpha_2} + g_2 g_{\alpha\mu} \qquad G_\mu^-(0,1) \quad \frac{1}{2} f \varepsilon_{\mu\alpha}(Q\Delta)$

$G_{\mu\nu}^+(0,2) \qquad g_1 Q_{\alpha_1} Q_{\alpha_2} Q_{\alpha_3} Q_{\alpha_4} + \qquad G_{\mu\nu}^-(0,2) \quad \frac{1}{2} \varepsilon_{\mu\alpha_1}(Q\Delta)\left(f_1 Q_{\alpha_1} Q_\nu + f_2 g_{\alpha_2\nu}\right)$

$g_2 g_{\alpha_1\mu} Q_{\alpha_2} Q_\nu \;+\; g_3 g_{\alpha_1\mu} g_{\alpha_2\nu}$

$G_{\mu\nu\sigma}^+(0,3) \qquad g_1 Q_{\alpha_1} Q_{\alpha_2} Q_{\alpha_3} Q_\mu Q_\nu Q_\sigma \qquad G_{\mu\nu\sigma}^-(0,3) \; \frac{1}{2}\varepsilon_{\mu\alpha_1}(Q\Delta)\Big(f_1 Q_{\alpha_2} Q_{\alpha_3} Q_\nu Q_\sigma +$

$+ \; g_2 g_{\alpha_1\mu} Q_{\alpha_2} Q_{\alpha_3} Q_\nu Q_\sigma + g_3 g_{\alpha_1\mu} g_{\alpha_2\nu} Q_{\alpha_3} Q_\sigma \qquad f_2 g_{\alpha_2\nu} Q_{\alpha_3} Q_\sigma + f_3 g_{\alpha_2\nu} g_{\alpha_3\sigma}\Big)$

$+ \; g_4 g_{\alpha_1\mu} g_{\alpha_2\nu} g_{\alpha_3\sigma}$

$G_{\mu\nu}^+(1,1) \qquad g_1 Q_\mu Q_\nu Q_{\alpha_1} Q_{\alpha_2} + g_2 g_{\mu\nu} Q_{\alpha_1} Q_{\alpha_2} + g_3 g_{\mu\alpha_1} Q_\nu Q_{\alpha_2}$

$+ \; g_4 g_{\nu\alpha_1} Q_\mu Q_{\alpha_2} + g_5 g_{\mu\alpha_1} g_{\nu\alpha_2}$

---

* The notation is $G^\pm(S_1, S_2)$ where the $\pm$ refers to a normal/abnormal coupling

TABLE 5

Boson helicity vertices (*)

$V^+(0,0)$	g	$V^-(0,0)$	0
$V^+_{01}(0,1)$	$-g_1/2\sqrt{2}$	$V^-_{01}(0,1)$	$-if/2\sqrt{2}$
$V^+_{00}(0,1)$	$(g_2-Tg_1)/\mu'$	$V^-_{00}(0,1)$	0
$V^+_{02}(0,2)$	$g_1/8$	$V^-_{02}(0,2)$	$if_1/8$
$V_{01}(0,2)$	$-(g_2-2Tg_1)/4\mu'$	$V^-_{02}(0,2)$	$-i(f_2-Tf_1)/4\mu'$
$V^+_{00}(0,2)$	$g_1 t'/4\sqrt{6} + \frac{2}{\sqrt{6}\mu'}(g_1T^2-g_2T+g_3)$	$V^-_{00}(0,2)$	0
$V^+_{03}(0,3)$	$-g_1/16\sqrt{2}$	$V^-_{03}(0,3)$	$-if_1/16\sqrt{2}$
$V^+_{02}(0,3)$	$(g_2-3Tg_1)/8\sqrt{3}\,\mu'$	$V^-_{02}(0,3)$	$i(f_2-2Tf_1)/8\sqrt{3}\,\mu'$
$V^+_{01}(0,3)$	$-3t'g_1/16\sqrt{30} +(-3T^2g_1+2Tg_2-g_3)/\mu'^2\sqrt{30}$	$V^-_{01}(0,3)$	$-it'f_1/16\sqrt{30} + i(-T^2f_1+Tf_2-f_3)/\sqrt{30}\,\mu'^2$
$V^+_{00}(0,3)$	$t'(g_2-3Tg_1)/4\sqrt{10}\,\mu' + (-T^3g_1+T^2g_2-Tg_3+g_4)2/\sqrt{10}\,\mu'^2$	$V^-_{00}(0,3)$	0
$V^+_{1-1}(1,1)$	$g_1 t/8$		
$V^+_{11}(1,1)$	$-g_1 t/8 - g_2$		
$V^+_{01}(1,1)$	$(-g_1T+2g_2+g_4)/2\sqrt{2}\,\mu'$		
$V^+_{10}(1,1)$	$(-g_1T'+2g_2+g_3)/2\sqrt{2}\,\mu$		
$V^+_{00}(1,1)$	$(g_1TT'-2g_2R-T'g_3-Tg_4+g_5)/\mu\mu'$		

Parity $\quad V^\pm_{-\lambda_1,-\lambda_2} = \pm(-)^{\lambda_1-\lambda_2}V^\mp_{\lambda_1\lambda_2}$

For definitions of T,T',R and $\mu_\pm$ see appendix 3

(*) the helicity phase conventions are those of Jacob and Wick NP 7 404 (1959) except we take $\varphi=0$ and do not include a factor $(-)^{s_2-\lambda_2}$ for particle 2.

Table 6

Covariant fermion couplings[a]

$G^+(\frac{1}{2},\frac{1}{2})$	$g_1 P_\beta + g_2 \gamma_\beta$
$G^+_\mu(\frac{1}{2},\frac{3}{2})$	$(g_1 P_{\beta_1} + g_2 \gamma_{\beta_1})P_{\beta_2}P_\mu + (g_3 P_{\beta_1} + g_4\gamma_{\beta_1})g_{\beta_2\mu}$
$G^+_{\mu\nu}(\frac{1}{2},\frac{5}{2})$	$(g_1 P_{\beta_1} + g_2 \gamma_{\beta_1})P_{\beta_2}P_{\beta_3}P_\mu P_\nu + (g_3 P_{\beta_1} + g_4 P_{\beta_1})g_{\beta_2\mu}P_{\beta_3}P_\nu$
	$\quad + (g_5 P_{\beta_1} + g_6\gamma_{\beta_1})g_{\beta_2\mu}g_{\beta_3\nu}$
$G^+_{\mu\nu\sigma}(\frac{1}{2},\frac{7}{2})$	$(g_1 P_{\beta_1} + g_2 \gamma_{\beta_1})P_{\beta_2}P_{\beta_3}P_{\beta_4}P_\mu P_\nu P_\sigma$
	$\quad + (g_3 P_{\beta_1} + g_4\gamma_{\beta_1})g_{\beta_2\mu}P_{\beta_3}P_{\beta_4}P_\nu P_\sigma$
	$\quad + (g_5 P_{\beta_1} + g_6\gamma_{\beta_1})g_{\beta_2\mu}g_{\beta_3\nu}P_{\beta_4}P_\sigma$
	$\quad + (g_7 P_{\beta_1} + g_8\gamma_{\beta_1})g_{\beta_2\mu}g_{\beta_3\nu}g_{\beta_4\sigma}$

Abnormal couplings
$$C^-(f) = C^+(f)\gamma_5$$

[a] The notation is $C^\pm(S_1,S_2)$ where the $\pm$ refers to a normal/abnormal coupling. The normality of a vertex is the product of the three normalities at the vertex.

TABLE 7

Fermion helicity vertices[a]

$V^+_{\frac{1}{2},\frac{1}{2}}(\frac{1}{2},\frac{1}{2})$	$2(m_+ g_1 + g_2)$
$V^+_{\frac{1}{2},\frac{1}{2}}(\frac{1}{2},\frac{3}{2})$	$-g_1 t'/2\sqrt{6} - \frac{2}{m'}\sqrt{\frac{2}{3}}\left(T(m_+ g_1 + g_2) - (m_+ g_3 + g_4)\right)$
$V^+_{\frac{1}{2},\frac{3}{2}}(\frac{1}{2},\frac{3}{2})$	$-(m_+ g_1 + g_2)/\sqrt{2}$
$V^+_{\frac{1}{2},\frac{1}{2}}(\frac{1}{2},\frac{5}{2})$	$t'(m_+ g_1 + g_2)/2\sqrt{10} + t'(2T g_1 - g_3)/2\sqrt{10}\, m' +$
	$4\left(T^2(m_+ g_1 + g_2) - T(m_+ g_3 + g_4) + (m_+ g_5 + g_6)\right)/\sqrt{10}\, m'^2$
$V^+_{\frac{1}{2},\frac{3}{2}}(\frac{1}{2},\frac{5}{2})$	$g_1 t'/8\sqrt{5} + (2T(m_+ g_1 + g_2) - (m_+ g_3 + g_4))$
$V^+_{\frac{1}{2},\frac{5}{2}}(\frac{1}{2},\frac{5}{2})$	$(m_+ g_1 + g_2)/4$
$V^+_{\frac{1}{2},\frac{1}{2}}(\frac{1}{2},\frac{7}{2})$	$-3g_1 t'^2/16\sqrt{70} + t'(3T(m_+ g_1 + g_2) - (m_+ g_3 + g_4))/\sqrt{70}\, m' -$
	$t'(3T^2 g_1 - 2T g_3 + g_5)/\sqrt{70}\, m'^2 -$
	$8\left(T^3(m_+ g_1 + g_2) - T^2(m_+ g_3 + g_4) + T(m_+ g_5 + g_6) - (m_+ g_7 + g_8)\right)/\sqrt{70}$
$V^+_{\frac{1}{2},\frac{3}{2}}(\frac{1}{2},\frac{7}{2})$	$-3t'(m_+ g_1 + g_2)/\sqrt{42}\, 8'^2 - 2t'(-3T g_1 + g_2)/8\sqrt{42}\, m' -$
	$-2\left(3T^2(m_+ g_1 + g_2) - 2T(m_+ g_3 + g_4) + (m_+ g_5 + g_6)\right)/\sqrt{42}\, m'^2$
$V^+_{\frac{1}{2},\frac{5}{2}}(\frac{1}{2},\frac{7}{2})$	$-t' g_1/16\sqrt{14} - (3T(m_+ g_1 + g_2) - (m_+ g_3 + g_4))/2\sqrt{14}\, m'$
$V^+_{\frac{1}{2},\frac{7}{2}}(\frac{1}{2},\frac{7}{2})$	$-(m_+ g_1 + g_2)/8\sqrt{2}.$

Abnormal vertices: $V^+_{\lambda_1 \lambda_2}(g; m_+, m_-) \longrightarrow V^-_{\lambda_1 \lambda_2}(f; m_-, m_+)(-)^{S_i - \lambda_i}$

Parity: $V^\pm_{-\lambda_1, -\lambda_2} = \pm(-)^{\lambda_1 - \lambda_3} V^\pm_{\lambda_1, \lambda_3}$, $T = (m_+ m_- + t'/4)$, $m_\pm = (m' \pm m)/2$

Nucleon flip: $V^\pm_{\pm\lambda_1, \pm\lambda_3} \rightarrow V^\pm_{\mp\lambda_1, \pm\lambda_3}$ requires the substitutions:

$(m_+ g_{2n-1} + g_{2n}) \rightarrow \pm g_{2n-1}/2$, $t' g_{2n-1} \rightarrow \pm 2(m_+ g_{2n-1} + g_{2n})$

[a] The helicity phase conventions used here are those of Jacob and Wick, ref. AP7 404, except that we take $\phi = 0$ and do not include a factor $(-)^{S_i - \lambda_2}$ for particle 2.

TABLE 8

Nonsense mechanisms at $\alpha = J_0$

	Choosing Sense	NC	GM	Chew	SFP
g_s	1	$(\alpha - J_0)$	$(\alpha - J_0)^{1/2}$	$(\alpha - J_0)^{1/2}$	1
g_n	$(\alpha - J_0)$	$(\alpha - J_0)$	$(\alpha - J_0)^{1/2}$	$(\alpha - J_0)^{3/2}$	1

TABLE 9(a)

$$\pi N \rightarrow \pi N^*(5/2^+, 1688) \quad \text{fit parameters}$$

Nonsense mechanism	Coupling model	G_1	G_2	G_3	$G_4^{(b)}$	$G_5^{(b)}$	$G_6^{(b)}$	A	α'_ρ	χ^2/pt
S.F.P	T.C.H.C	58.8						2.70	.212	1.02
	R.G.C		78.3					2.71	.193	1.02
	γ-coupling		77.9		-0.5		-0.5	2.71	.190	1.02
	S.C.H.C						20.9	1.30	.255	2.24
G.M.	T.C.H.C	733						3.92	.60	35
	R.G.C		1003					3.92	.60	34
	γ-coupling		2256				1010	4.72	.326	18
	S.C.H.C						790	4.10	.22	32
Sense.	γ-coupling		77.5		-25.16		-21.9	2.70	.174	1.01

a) $g_{\pi\bar{\pi}\rho}\, g_i = G_i\, e^{At}\, N_i(\alpha_\rho), \quad \alpha_\rho = 1 + \alpha'_\rho t$

b) g_4, g_5 and g_6 are covariant nonesense couplings at $\alpha = 1$

TABLE 10[(a)]

$$\pi N \to \pi N^*(\tfrac{3}{2}^-, 1525) \qquad \text{fit parameters}$$

nonsense mechanism	coupling model	G_1	G_2	G_3	$G_4^{(b)}$	A	α_ρ'	χ^2/pt
S.F.P.	T.C.H.C	-9.1				2.5	0.10	3.2
	RGC		-15.3			2.7	0.10	3.0
	G_1, G_2	58.7	-63.3			3.2	0.07	1.3
	γ coupling		-20.9		-9.9	3.4	0.06	1.2
	S.C.H.C				5.7	1.8	0.10	4.4
G.M.	T.C.H.C	-143.6				3.9	0.59	7.4
	R.G.C		-163.0			3.4	0.70	7.6
	G_1, G_2	3443	-7387			5.9	0.045	6.0
	γ coupling		-1880		573	5.2	0.04	5.7
	S.C.H.C				263	4.5	0.21	5.8
Sense.	γ coupling		10.4		2048	3.56	0.108	1.2

(a) $\quad g_{\pi\pi\rho} \, g_i = G_i \, e^{At} \, N_i(\alpha_\rho) \,, \quad \alpha_\rho = 1 + \alpha_\rho' t$

(b) $\quad g_4$ is a covariant nonsense coupling at $\alpha = 1$

TABLE 11

Predictions of the constituent

models of diffraction dissociation

$N \to N^*$ state in quark model	Morrisons rule allowed?	C.F.Z allowed	C.Y $\frac{d\sigma}{dt}\big|_{t=0}$?	F.J.R allowed	Kislinger $\frac{d\sigma}{dt}\big|_{t=0}=0$?
$^2S_{1/2}+$ N(940)	Y	Y	N	Y	N
$^2S_{1/2}+$ N*(1470)	Y	Y	N	Y	Y
$^2P_{3/2}-$ N*(1520)	Y	SU(6): N	Y	Y	Y
$^2P_{1/2}-$ N*(1550)	N	SU(6): N	Y	Y	N
$^4P_{5/2}-$ N*(1680)	N	SU(6):S:N	Y	Y	N
$^4P_{3/2}-$ N*(1710)	Y	SU(6):S:N	Y	Y	Y
$^4P_{1/2}-$ N*(1730)	N	SU(6);S:N	Y	Y	N
$^2D_{5/2}+$ N*(1688)	Y	Y	N	Y	Y
$^2D_{3/2}+$ N*(1860)?	N	Y	N	Y	N
$^2S_{1/2}+$ N*(1750)	Y	Y	N	Y	Y
$^2F_{7/2}+$ N*(2190)	Y	SU(6): N	Y	Y	Y
$(K) \to \pi^*(K^*)$ quark model states.					
$^1S_0-$ π(140)	Y	Y	N	Y	N
$^3S_1-$ ρ(750)	G:N	G:N	G:N	G:N	G:N
$^1P_1+$ B(1220)	G:Y	G:N	G:Y	G:N	G:Y
$^3P_0+$ S(962)	N	P^a:S:N	P^a:Y	P^a:N	P^a
$^3P_1+$ A$_1$(1070)	Y	S:N	Y	Y	Y
$^3P_2+$ A$_2$(1315)	N	S;P^b;N	P^b;Y	P^b:Y	$P^b \to$ Y
$^1D_2-$ A$_3$; π_A(1640)	Y	Y	N	Y	$P^b \to$ Y
$^3D_1-$	G:N	G:S;P^b:N	G:P^b:N	G;P^b N	$P^b \to$ Y
$^3D_2-$	G:Y	G:S :N	G N	G N	Y
$^3D_3-$	G:N	G:S:P^b:N	G:P^b:N	G:P^b:N	$P^b \to$ Y
$^1S_0-$ K(495)	Y	Y	N	Y	N
$^3S_1-$ K*(890)	N	S:G:P^b:N	$P^b \to$ Y	G:P^b:N	$P^b \to$ Y
$^1P_1+$ K*(1320)	Y	G :N	Y	G :N	Y
$^3P_0-$ K$_\pi$(1100)	N	P^a:S:N	P^a:Y	P^a:N	P^a
$^3P_1+$ Q(1340)	Y	S:N	Y	Y	Y
$^3P_2+$ K**(1420)	N	P^b:S:N	Y	P^b Y	$P^b \to$ Y
$^1D_2-$ L(1780)?	Y	Y	N	Y	Y
$^3D_1-$	N	S:G:P^b:N	$P^b \to$ Y	G;P^b:N	$P^b \to$ Y
$^3D_2-$	Y	S:G: N	N	G :N	Y
$^3D_3-$	N	S:G:P^b N	$P^b \to$ Y	G:P^b N	$P^b \to$ Y

a = absolutly forbbidden for natural parity exchange (P, f, f') [See Ch 3 and tables]
b = Production of zero helicity states vanishes identically.
N = No   Y = Yes   G = G parity forbbidden   SU(6) = SU(6) forbbidden.
= generalized charge conj. forbbidden   Taken from ref. [a5]

TABLE 12

The differential structure for

fermion dissociations [33]

Reaction	max $\left(\frac{d\sigma}{dt}\right)$	$t \approx 0$ differential structure	C.F.Z.
$\pi N \to \pi N$	~ 40 mb/GeV^2	strong forward peak	allowed
$\pi N \to \pi N^*(1470)$	~ 1 mb/GeV^2	forward peak	allowed
$\pi N \to \pi N^*(1520)$	$\sim 2 \times 10^{-1}$ mb/GeV^2	forward dip ?	SU(6) forbidden
$\pi N \to \pi N^*(1688)$	$\sim .5$ mb/GeV^2	forward plateau ?	allowed
$\pi N \to \pi N^*(2140)$	$\sim 10^{-1}$ mb/GeV^2	forward dip	SU(6) forbidden

TABLE 13

Decay	g_γ (GeV^{-1})	$g_\gamma^{exp.}$ (GeV^{-1})
$\omega^o \rightarrow \pi^o \gamma$	-2.2	-2.89 ± 0.26
$\phi^o \rightarrow \pi^o \gamma$	0	-0.16 ± 0.02
$\phi^o \rightarrow \eta^o \gamma$	-1.2	-0.82 ± 0.12

TABLE 14

Decay type	Quark amplitude $-i\langle f\|\partial_\mu A^{\mu a}\|i\rangle$	Antiquark amplitude $-i\langle f\|\partial_\mu \bar{A}^{\mu a}\|i\rangle$
$\rightarrow 0^+ 0^+$	$-\dfrac{m_1 m_2}{m_0} F \Lambda_2 \, q\cdot\epsilon_1$	$\dfrac{m_1 m_2}{m_0} F \Lambda_2 \, q\cdot\epsilon_2$
$\rightarrow 0^+ 0^+$	$\dfrac{m_1 m_2}{m_0} F \Lambda_2 \, q_\mu q_\nu T^{(2)\mu\nu}$	$\dfrac{m_1 m_2}{m_0} F \Lambda_2 q_\mu q_\nu T^{(2)\mu\nu}$
$\rightarrow 1^- 0^+$	$-\dfrac{iF}{m_1 m_2\sqrt{\Omega}}(\Sigma+\Omega) T_2^{\alpha\beta}\mathcal{E}_{\alpha\mu\nu\lambda}\left(p_1^\mu p_2^\nu \epsilon_2^{\lambda*}\right)q_\beta$	$\dfrac{iF}{m_1 m_2\sqrt{\Omega}}(\Sigma+\Omega) T_2^{\alpha\beta}\mathcal{E}_{\alpha\mu\nu\lambda}\left(p_1^\mu p_2^\nu \epsilon_2^{\lambda*}\right)q_\beta$
$+\rightarrow 1^- 0^+$	$-\dfrac{F\sqrt{\Omega}}{m_0}\Big\{\epsilon_1\cdot\epsilon_2^*\Big(\dfrac{p_1\cdot p_2}{m_1 m_2}\Delta_2\Big)+$ $q\cdot\epsilon_1\, q\cdot\epsilon_2^*\Big(\dfrac{m_1 m_2}{\Omega}\Lambda_1+\dfrac{\Delta_2}{m_1 m_2}\Big)\Big\}$	$-\dfrac{F\sqrt{\Omega}}{m_0}\Big\{-\epsilon_1\cdot\epsilon_2^*\Big(\dfrac{p_1\cdot p_2}{m_1 m_2}\Delta_2\Big)+$ $q\cdot\epsilon_1\, q\cdot\epsilon_2^*\Big(\dfrac{m_1 m_2}{\Omega}\Lambda_1-\dfrac{\Delta_2}{m_1 m_2}\Big)\Big\}$
$++\rightarrow 1^- 0^+$	$\dfrac{F}{\sqrt{\Omega}\,m_1^2 m_2}\Big\{\epsilon_1\cdot\epsilon_2^*\big[(\Omega-\Sigma)Y-$ $2\Delta_1\cdot p_1\cdot p_2\,\Omega\big]+q\cdot\epsilon_1\, q\cdot\epsilon_2\big[(p_1\cdot p_2-$ $2m_1^2)\Omega+p_1\cdot p_2\Sigma\big]\Big\}$	$\dfrac{F}{\sqrt{\Omega}\,m_1^2 m_2}\Big\{\epsilon_1\cdot\epsilon_2^*\big[-(\Omega+2m_2^2)Y$ $+2\Delta_1 p_1 p_2\,\Omega\big]+q\cdot\epsilon_1\, q\cdot\epsilon_2\big[-(p_1\cdot p_2$ $-2m_1^2)\Omega+2m_1^2 m_2^2\big]\Big\}$

Abbreviations:

$$\Lambda_i = \left[1+\left(\frac{m_0}{m_i}\right)^2\right]$$

$$\Delta_i = m_i^2 - p_1\cdot p_2$$

$$Y = \left[m_1^2 m_2^2 - (p_1\cdot p_2)^2\right]$$

$$\Sigma = m_1^2 + m_2^2 + m_3^2$$

$$p_1\cdot p_2 = (m_1^2 + m_2^2 - m_3^2)/2$$

$T^{2\alpha\beta}$ is a spin two wavefunction.

TABLE 15

Decay type	State	Mode	Γ (MeV)	Γ^{exp} (MeV)	M^{FKR} (MeV)
$1^- \to 0^- 0^+$	$\phi(1019)$	$K\bar{K}$	3.14	2.5 ± 0.3	9
		$\rho\pi$	0	< 0.6	0
	$\omega(784)$	$\pi\pi$	0	0.13 ± 0.03	0
	$K^*(892)$	$K\pi$	46.2	50.1 ± 1.1	59.5
		πK			144
	$\rho(765)$	$\pi\pi$	117	146 ± 10	142
$1^+ \to 1^- 0^+$	$B(1235)$	$\omega\pi$	66	120 ± 20	76.5
$1^{++} \to 1^- 0^+$	$K^*(1240)$	$K^*\pi$	47	~ 100	54
	$A_1(1070)$	$\rho\pi$	100	$200-400$	145
$2^{++} \to 0^- 0^+$	$f'(1514)$	$K\bar{K}$	62	40 ± 10	93
		$\pi\pi$	0	~ 0	0
	$f(1260)$	$K\bar{K}$	5.1	8 ± 5	12
		$\pi\pi$	153	130 ± 12	220
	$K^*(1420)$	$K\pi$	54.7	55 ± 6	78
		πK	54.7	55 ± 6	126
		$K\eta$	2	~ 2	4.5
		ηK	2	~ 2	3.6
	$A_2(1300)$	$\eta\pi$	13.8	15 ± 1.5	20
		$\pi\eta$	13.8	15 ± 1.5	40
		$K\bar{K}$	7.8	4.7 ± 1	15
$2^{++} \to 0^- 1^-$	$f'(1514)$	$\bar{K} K^* + K \bar{K}^*$	9.3	< 14	13.5
	$K^*(1420)$	$K^*\pi$	18.2	29.5 ± 6	20
		ρK	5.7	9.2 ± 3	7
		ωK	1.4	4.4 ± 2	1.8
	$A_2(1300)$	$\rho\pi$	53	72 ± 7	60

TABLE 16

Decay	T_{00}/T_{11}	$(T_{00}/T_{11})^{exp}$	$(T_{00}/T_{11})^{F.K.R.}$
$B \to \omega\pi$	1.0	$0.2 \to 0.7$	0.19
$A_1 \to \rho\pi$	1.0	$2.0 \to 1.1$	1.3

TABLE 17

Amplitudes for diffractive vertices

in the linearized oscillator model $J_\alpha = \varrho_\rho Q_\alpha F e^{q \cdot q^+/\sqrt{2}} e^{-q \cdot q/\sqrt{2}}$

Process $A \to A^*$	Amplitude $\langle A^* \vert J_\alpha \vert A \rangle = \langle A^* \vert J_\alpha^q \vert A \rangle + \langle A^* \vert J_\alpha^{\bar{q}} \vert A \rangle$
$0^{-+}(\pi, K) \to 0^{-+}(\pi, K)$	$-4 m_\rho \varrho_\rho Q_\alpha F \left(1 - t/4 m_\rho^2\right) \qquad m_0 = m_\rho$
$0^{-+}(\pi) \to 1^{-+}(B)$	0
$0^{-+}(\pi) \to 2^{-+}(A_3)$	$2\sqrt{2} m_{A_3} \varrho_\rho Q_\alpha Q_\mu Q_\nu T^{(2)* \mu\nu} F \left(3 + \left(\frac{m_\rho}{m_{A_3}}\right)^2 - \frac{t}{m_{A_3}^2}\right)$
$0^{-+}(\pi) \to J^{+-}$ J odd $N = J$	0
$0^{-+}(\pi) \to J^{-+}$ $J = N = $ even N^0	$\frac{\varrho_\rho (2)^J}{\sqrt{J!}} m_J F \left(3 + \left(\frac{m_\rho}{m_J}\right)^2 - \frac{t}{m_J^2}\right) Q_\alpha Q_{\mu_1} \cdots Q_{\mu_J} T^{(J)* \mu_1 \cdots \mu_J}$
$0^{-+}(\pi) \to 1^{-P}(\rho)$	0
$0^{-+}(\pi) \to 1^{++}(A_1)$	$\varrho_\rho F m_{A_1} \left(1 - \left(\frac{q_\rho \cdot q_A}{m_\rho m_A}\right)^2\right) Q_\alpha Q_\mu \epsilon_{A_1}^{* \mu}$
$0^{-+}(\pi) \to 2^{++}(A_2)$	0
$1^{--}(\rho) \to 1^{--}(\rho')$ cf $\gamma \to \rho$	$2 Q_\alpha \frac{\varrho_\rho F}{m_0} \left[\epsilon_1 \cdot \epsilon_2^* \left(m^2 + \left(\frac{m_0}{m}\right)^2 q_1 \cdot q_2 + \frac{\sqrt{2}}{m^2}(q_1 \cdot q_2)^2\right) - 4 q_1 \cdot \epsilon_1 q_2 \cdot \epsilon_2^* \left(\left(\frac{m_0}{m_1}\right)^2 - \frac{q_1 \cdot q_2}{m^2}\right)\right]$

Figure captions

1. Diffraction system.

2. Typical meson trajectory and possible pomeron trajectory.

3. (a) Typical multi-peripheral graph.

   (b) Multi-peripheral tree with resonances in some channels.

4. Diagrammatic representation of the unitarity equation.

5. Contributions to inelastic intermediate states.

6. (a) An A.F.S. cut   (b) A Mandelstam cut

7. Basic tower diagrams.

8. Some contributions to the itterated tower.

9. (a) Planar diagram.

   (b) Non planar diagram where partons pass each other but do not interact.

10. (a) Fishnet Feynman diagram.

    (b & c) Duality principal. A sum over all t-channel poles is equal to a sum over s-channel resonances.

11. Symbolic representation of Veneziano 4-point function in the analogue model.

12. Veneziano equivalent of the box diagram.

13. The quark quantum numbers.

14. Illustration of limiting fragmentation where target T and projectile P fragment into states T* and P* respectively.

15. Mass fragmentation spectrum for $p \rightarrow X$ under the impact of π^- [33]

16.   Diffractive resonance excitation of particle B into D.

17.   Deck mechanism for producing mass enhancement D.

18.   Peripheral model for dissociation $\pi \to 3\pi$

19.   Gauge invariant peripheral model for $\pi \to 3\pi$
fragmentation.

20.   Possible excited states of a composite object.

21.   Kinematics for spin J exchange.

22.   Pomeron fits to the $\pi N \to \pi N^*(5/2^+, 1688)$
date of reference [33]
The full line represents R.G.C., T.C.H.C. and
S.C.H.C. fits, dashed line is the γ- coupling fit
with S.F.P. mechanism, and the small circle line
the best γ- coupling fit with G.M. mechanism.

23.   Pomeron fits to the $\pi N \to \pi N^*(3/2^-, 1520)$ data [33].
Again the full line represents R.G.C., T.C.H.C. and
S.C.H.C. fits, dashed line is the γ- coupling fit
with either S.F.P. or sense mechanism, and the small
circle line the best γ- coupling fit with G.M.
mechanism.

24.   (a) Pomeron fits to the $\rho_{\frac{1}{2}\frac{1}{2}}$ data of [28]
for $N^*(5/2^+, 1688)$ in the helicity frame. Full
line represents R.G.C. and T.C.H.C., dashed
line is S.C.H.C.

        (b) Pomeron predictions for $\rho_{\frac{1}{2}\frac{1}{2}}$ for $N^*(3/2^-, 1525)$
in the helicity frame. Full line represents
R.G.C. and T.C.H.C., dashed line is S.C.H.C.
and the small circle line is the prediction of
the best γ- coupling fit to the differential
cross-section data.

incident →
wave
along
the →
direction
momentum $\vec{p}$
energy $\vec{E}$ →

dSn

n

$\tilde{x}'$

y

S

$\tilde{x}$

x

z = 0

z

Absorbing object.

FIG 1

$J = Re\alpha$
Spin

3

2

1

R meson

?

?

Pomeron

1   2   3 M^2 mass squared
                GeV^2

FIG 2

FIG. 3(a)

FIG. 3(b)

Disc

A $=$

Elastic
Ael

$+ \Sigma$

Inelastic
Ainel

$=$ $+$

FIG. 4

(a) Ladder diagram

(b)

(c)

FIG. 5

Regge Poles

(a)   (b)

FIG 6

+   +   +   +

FIG 7

FIG 8

(a)   (b)

FIG 9

(a)   (b)   (c)

FIG.IO

FIG.11

FIG.12

FIG.13

FIG14

FIG 15

Process $\pi^- p \longrightarrow \pi^- X$

Lab Energy = 8 Gev

$0.06 < t < 0.10$

D13 becomes visible at larger angles

FIG16

FIG17

IP or γ

IP or γ

π

π

π

π

=

IP or γ

π

π

π

ρ, f

π

π

} A₁, A₃ etc.

e

<u>FIG 18</u>

IP or γ

π

π

π

+

IP or γ

π

π

R

π

+

IP or γ

R

π

π

π

<u>FIG. 19</u>

J

3

2

1

$\sim \frac{1}{2}$

daughter trajectories

slope $\sim 1\cdot\ GeV^{-2}$

m^2

scattering region
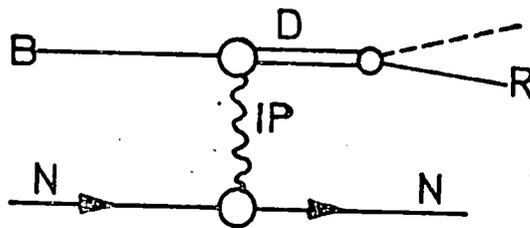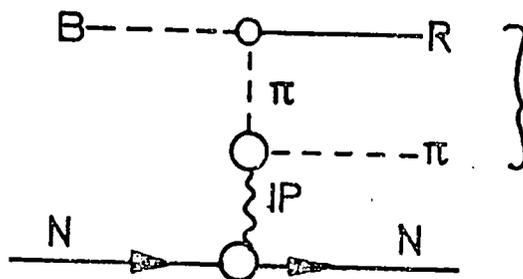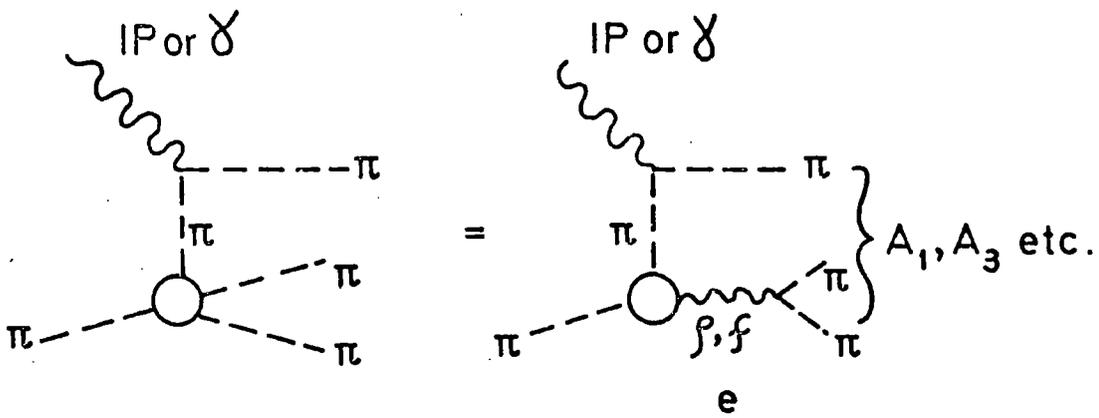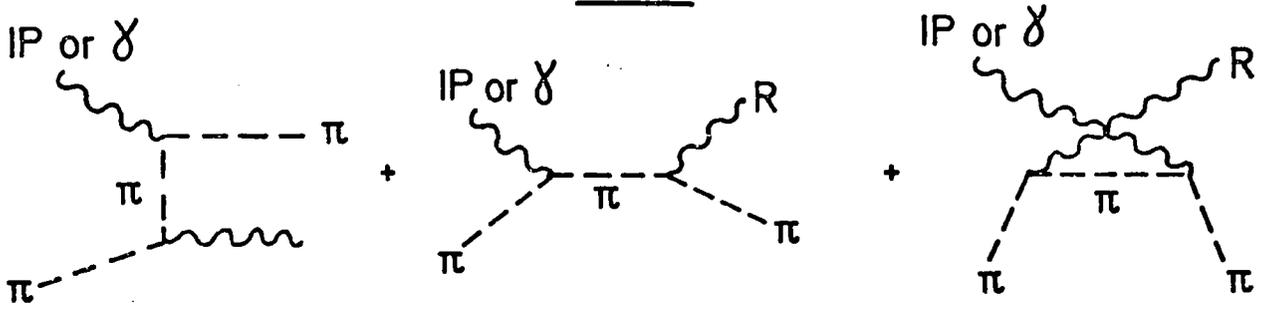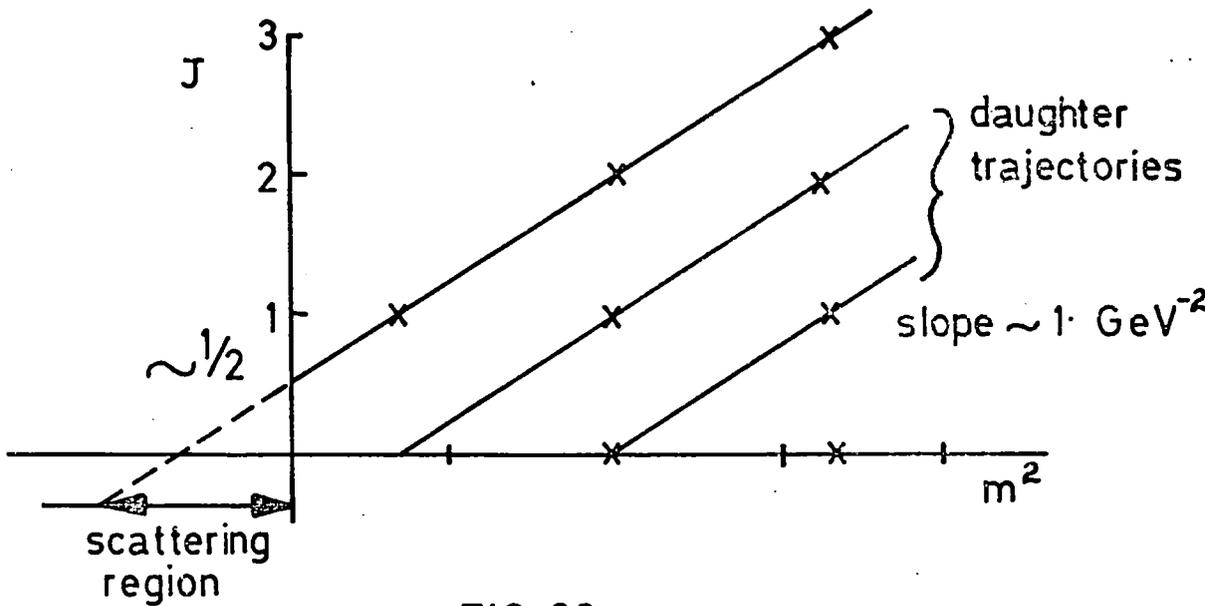
<u>FIG. 20</u>
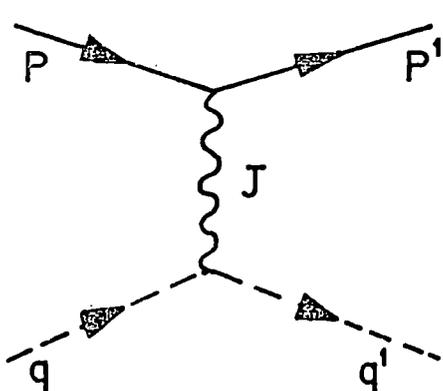
$P = \frac{1}{2}\ (p+p')$

$Q = \frac{1}{2}\ (q+q')$

$\Delta = (p'-p) = (q-q')$

$\Delta^2 = t$

<u>FIG. 21</u> $RQ = V = (s-u)/4$

P P'

J

q q'

Figure 22

$$\pi^- p \to \pi^- N^{*+}$$
$$N^* (1525) \tfrac{3}{2}$$
$$P\ LAB = 16\ GeV\!/\!c$$

$$\frac{d\sigma}{dt}$$

$$\frac{mb}{GeV^2}$$

Figure 23

FIG 24

Lorentz Contraction
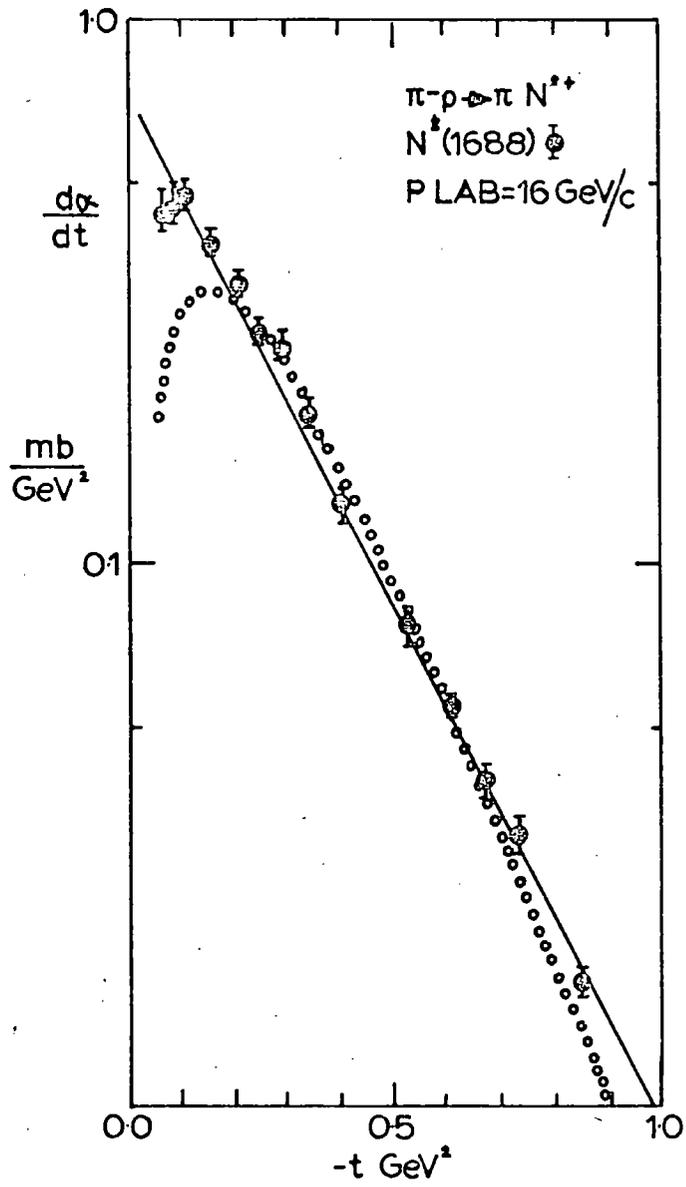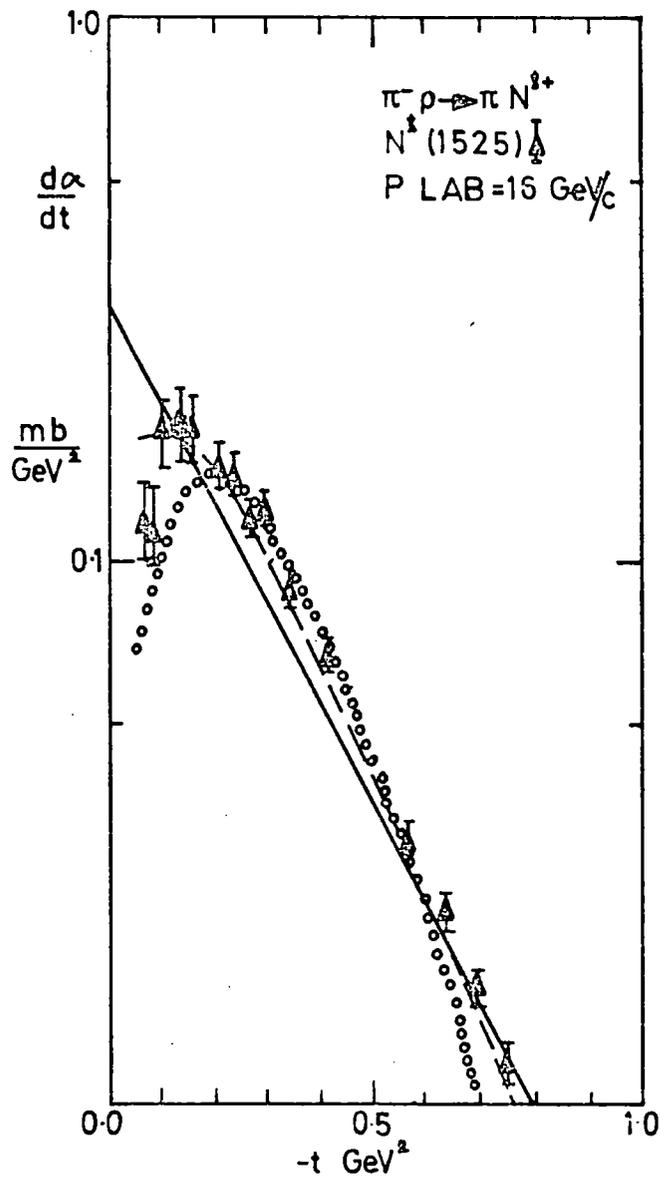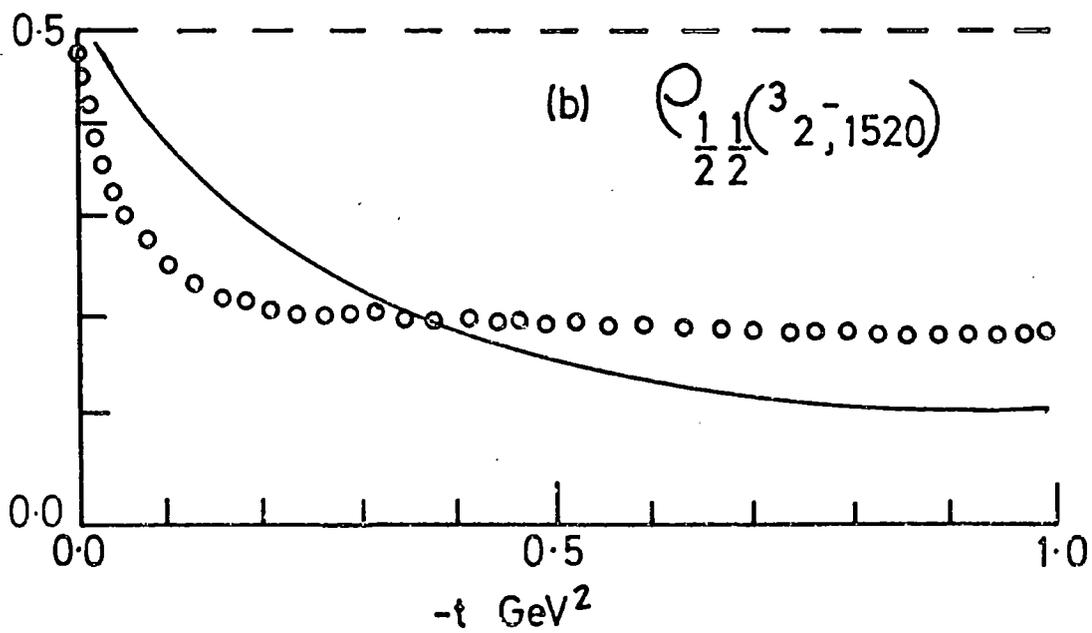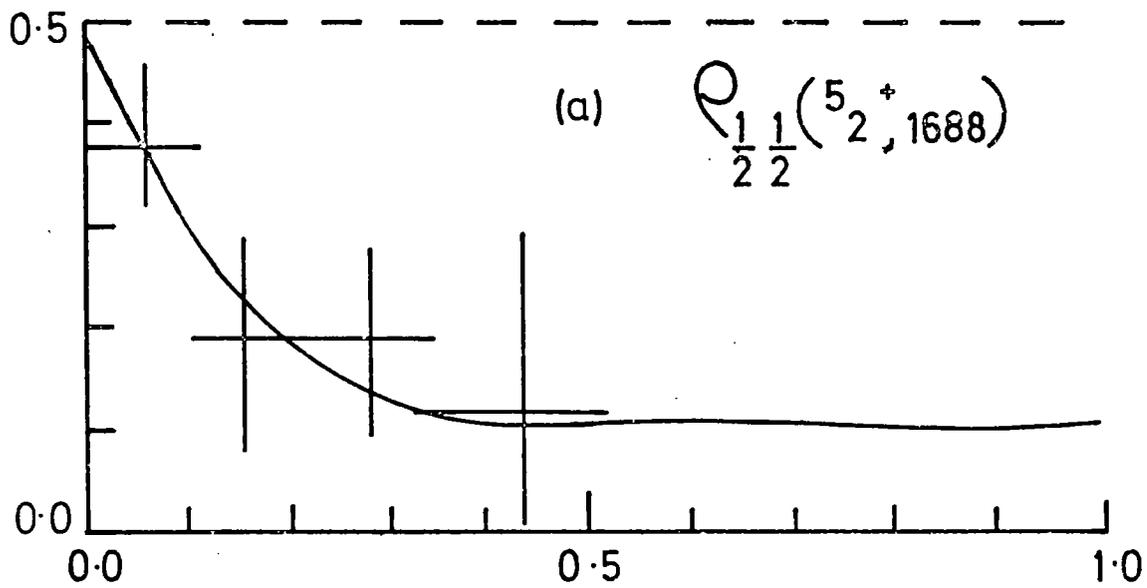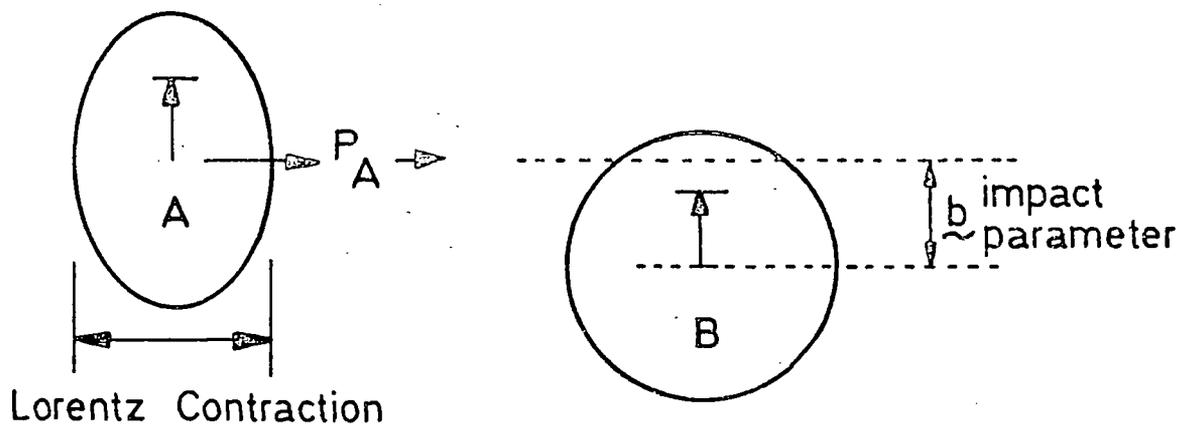
FIG. 25
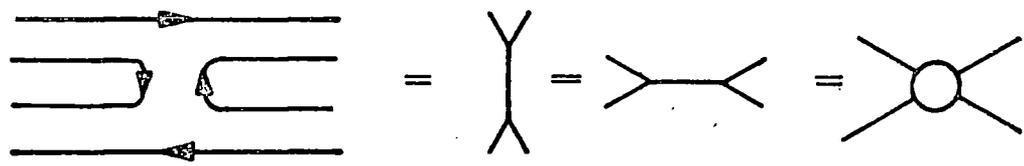
FIG. 26

FIG. 27

FIG. 28

FIG. 29

FIG 30

Bethe Salpeter Wave function $= \psi_{p(q)} =$

FIG 31

$V =$

FIG 32

FIG 33

FIG 34

FIG 35

Pi

Pf

FIG 36

P_A

k

P_B

A

B

$P_A + P_B + P_C = 0$

C

P_C

FIG 37

+

A

B

C

$$\frac{P/2-k}{}$$

P

$(P + q) \rightarrow P$

$P/2 + k$ $P/2 + k + q$

$q - 0$

FIG. 38

J

A_3

2^{-+}

B 1^+ 1^{+-}

π 0^{-+} 0^{-+}

0   1   2   3   4

$\frac{P^2 - m^2_0}{\Omega}$
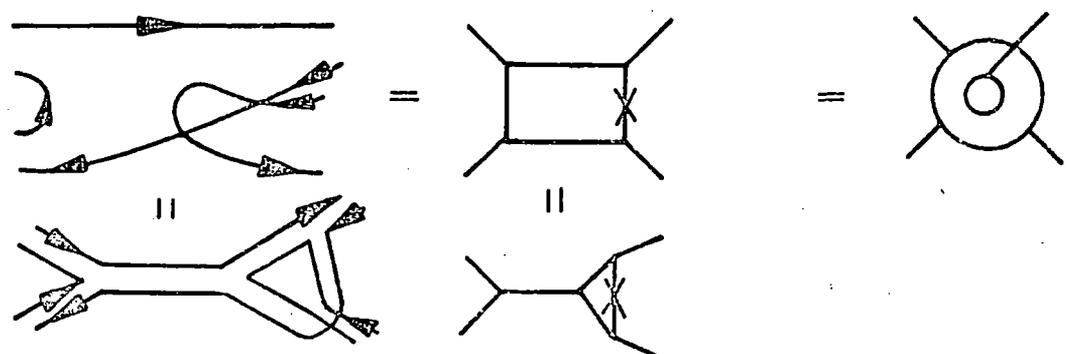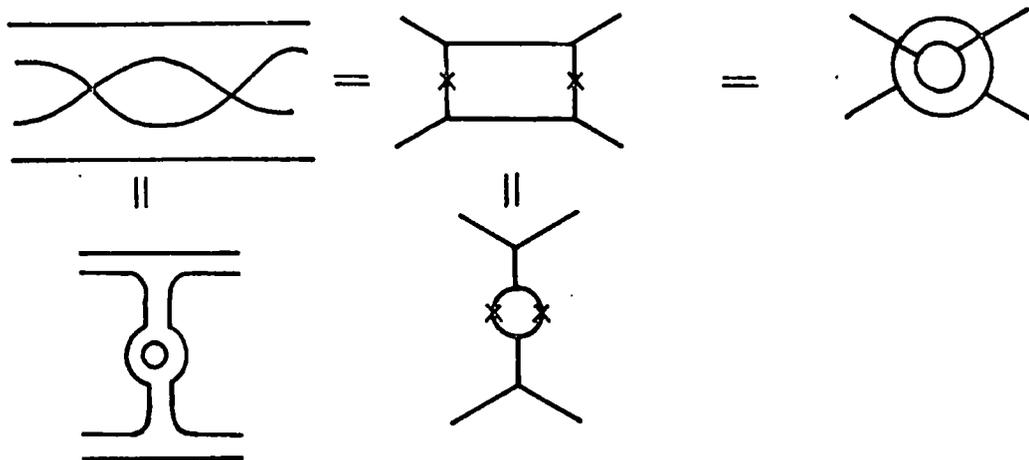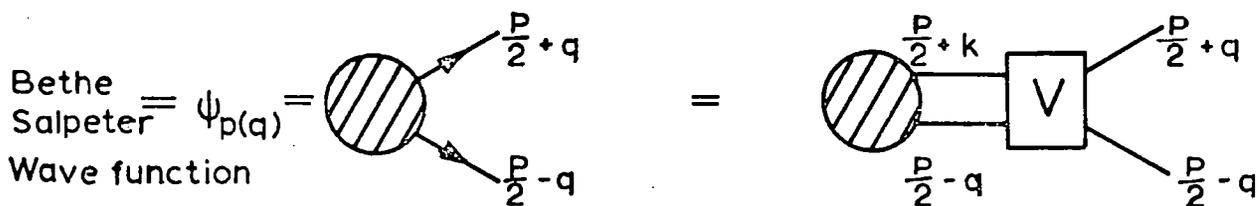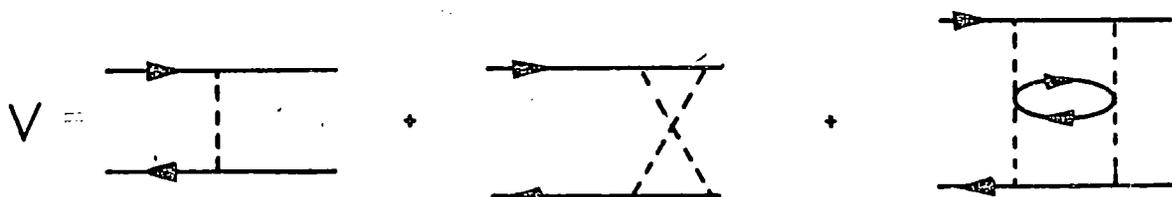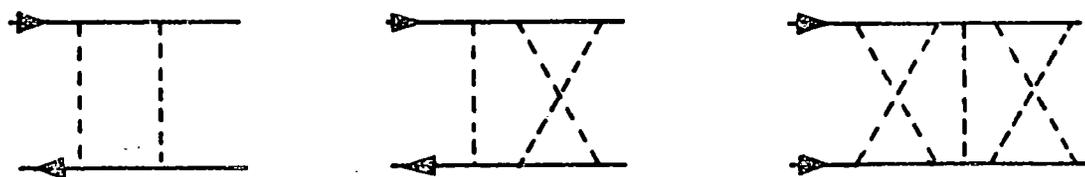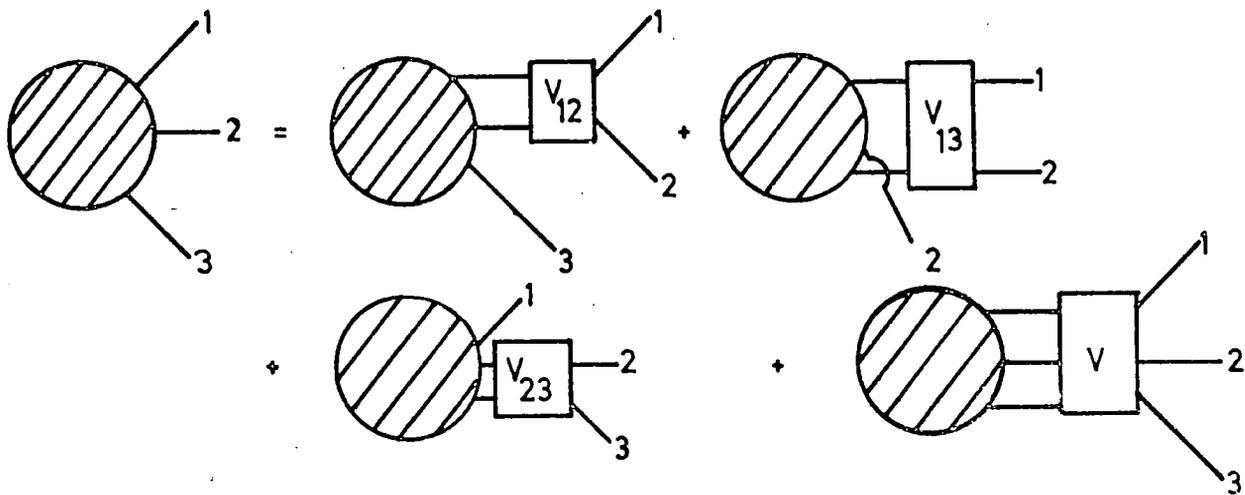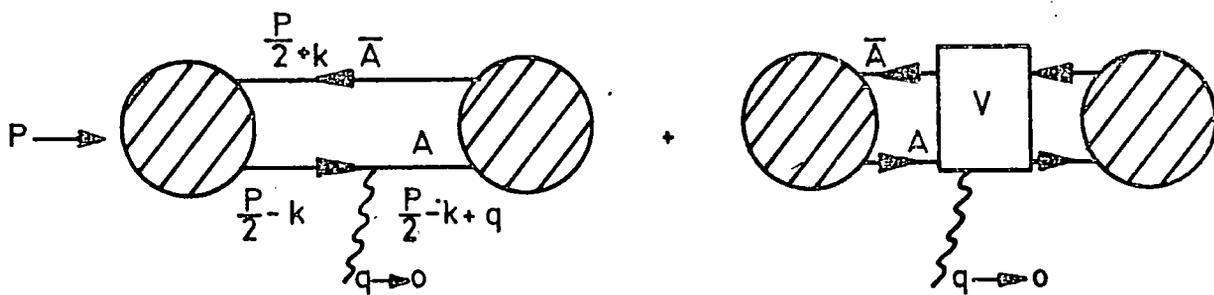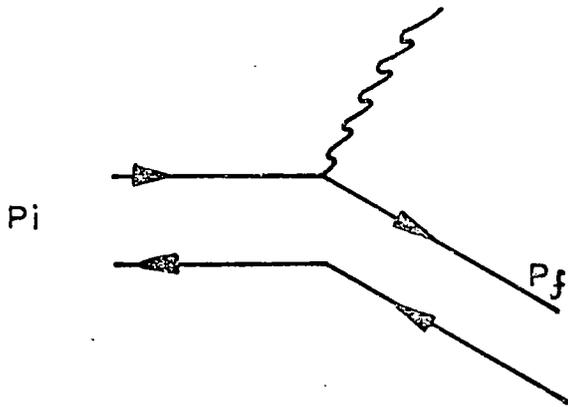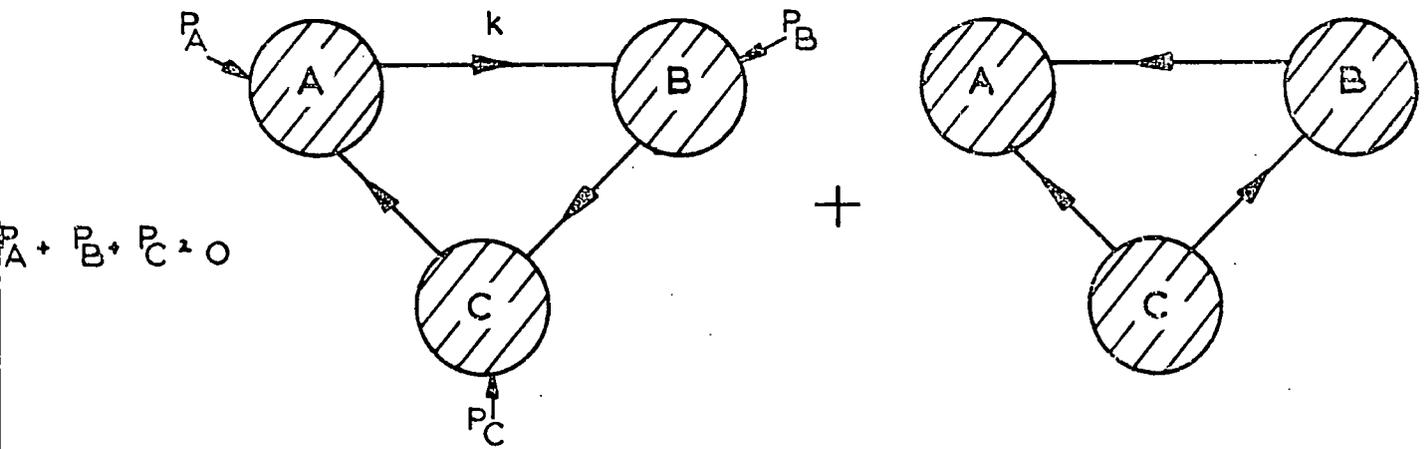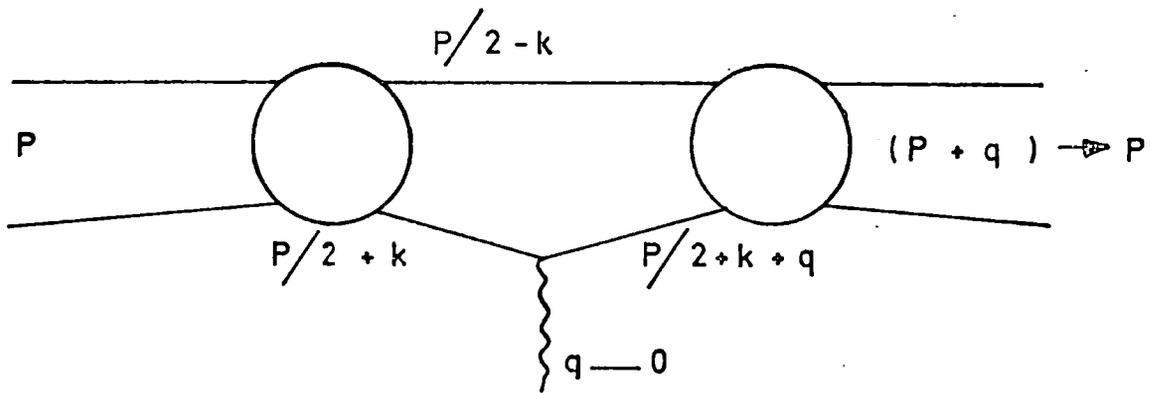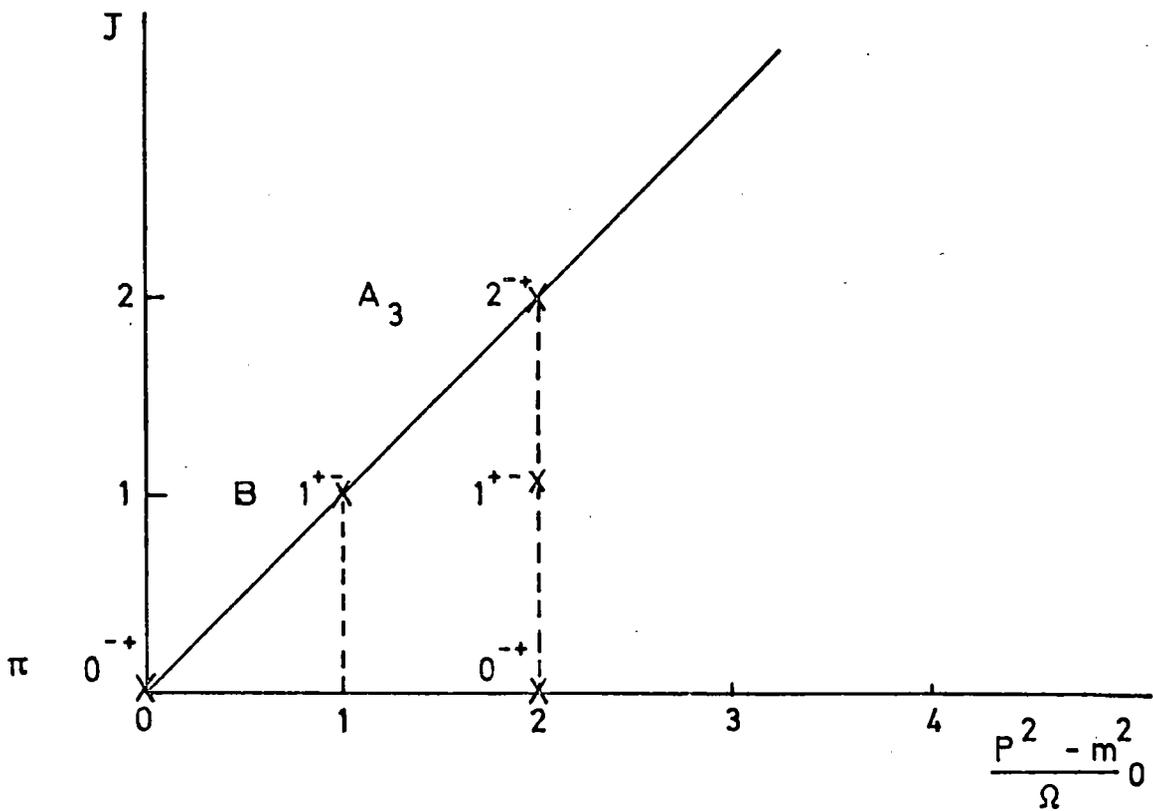
FIG. 39

FIG.40

FIG.41

FIG 42

FIG 43

$P_A^X = P_A + \Delta$

$P_B^X = P_B - \Delta$

$P_A + q + \Delta$
$\frac{}{2}$

$\frac{P_A}{2} - q$

$\frac{P_A}{2} + q + k$

$\frac{P_A}{2} + q$

P_A

P_B

FIG 44

P_A^X

P_B^X
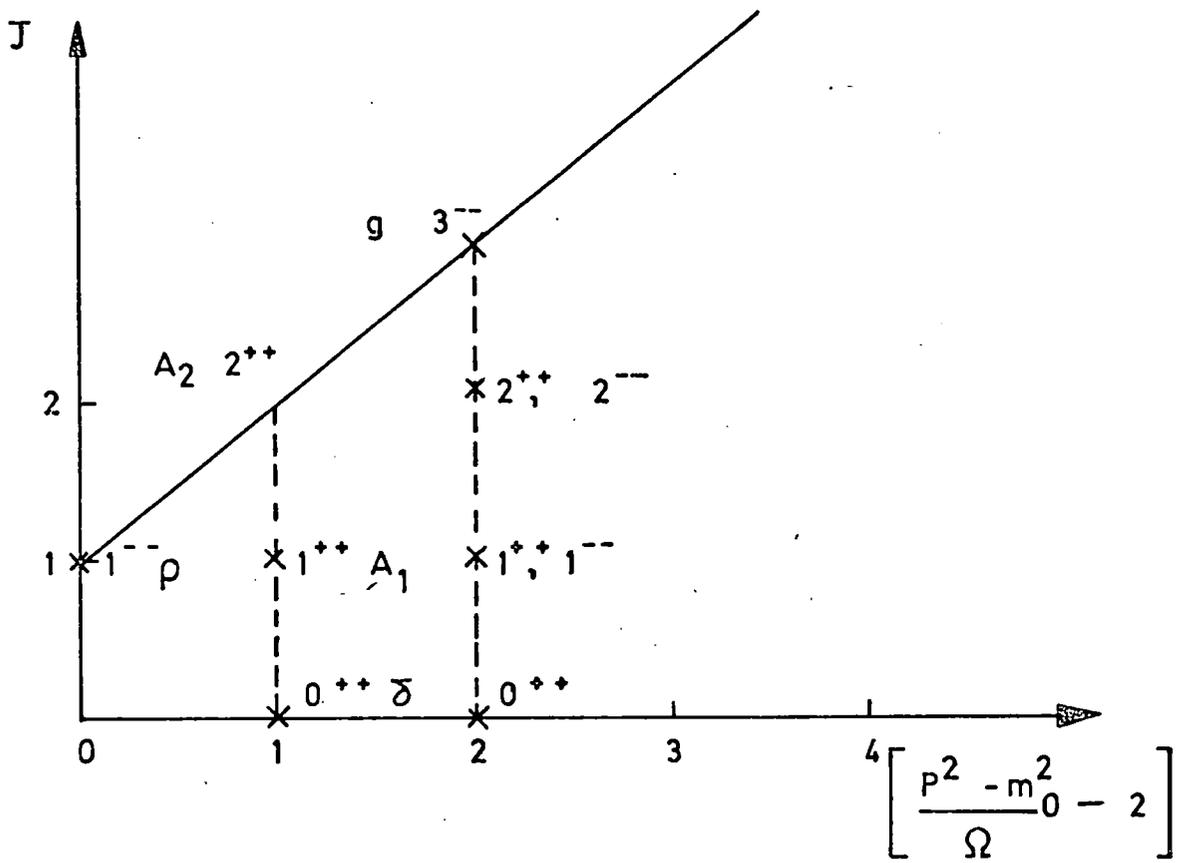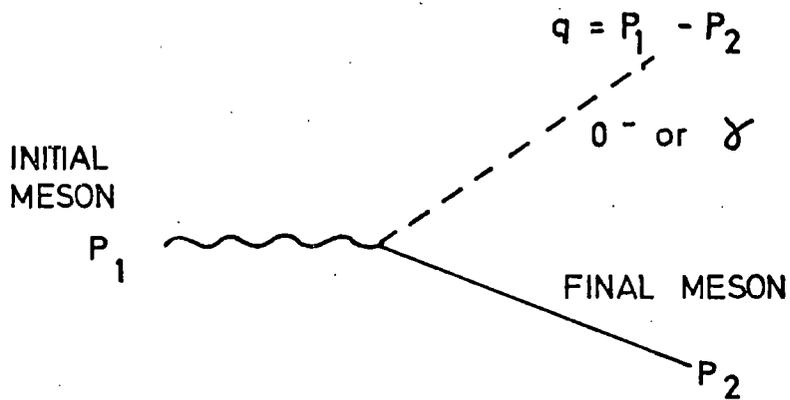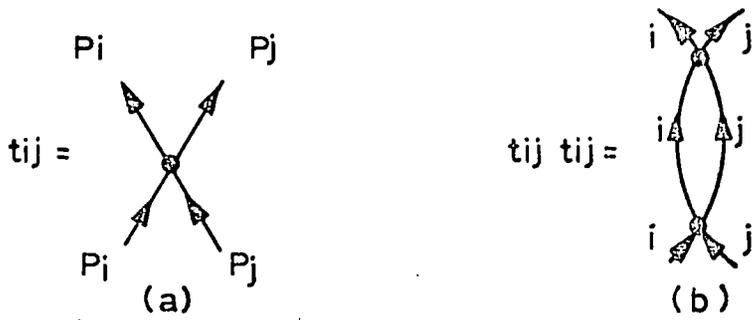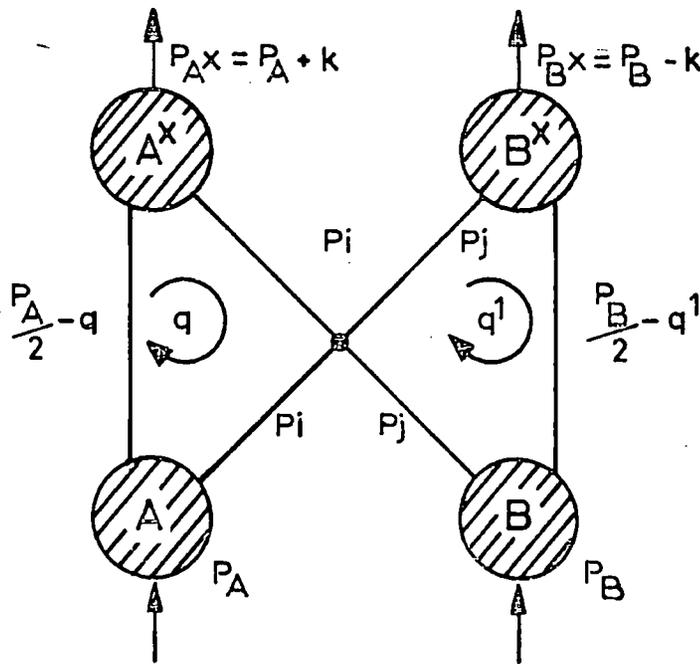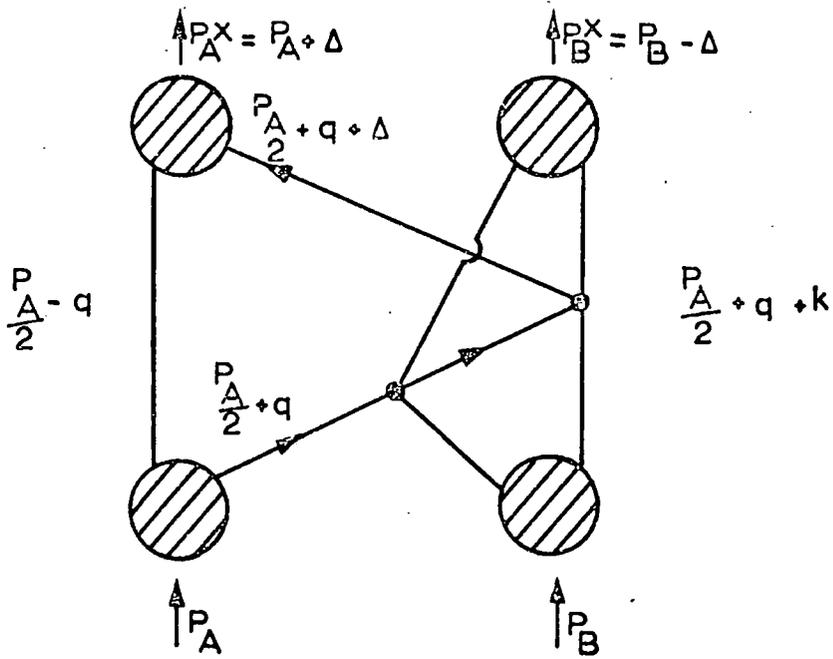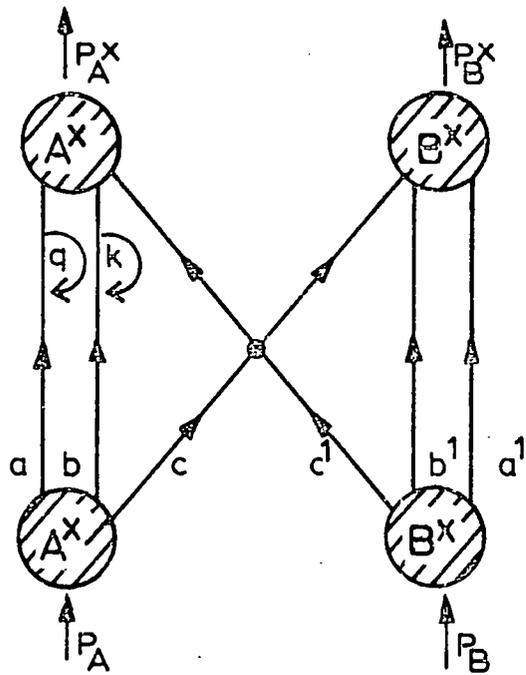
$P_a = \frac{1}{3} P_A + q + \frac{1}{\sqrt{3}} k$

$P_b = \frac{1}{3} P_A - q + \frac{1}{\sqrt{3}} k$
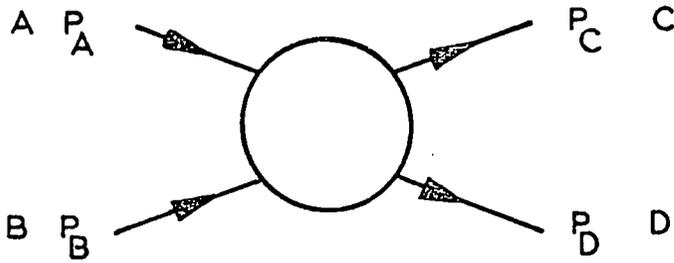
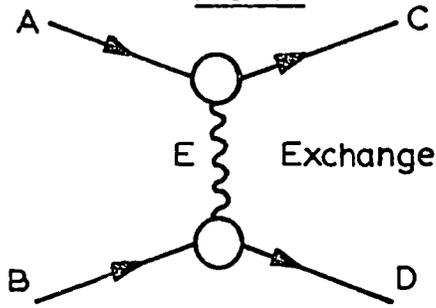$P_c = \frac{1}{3} P_A - \frac{2}{\sqrt{3}} k$
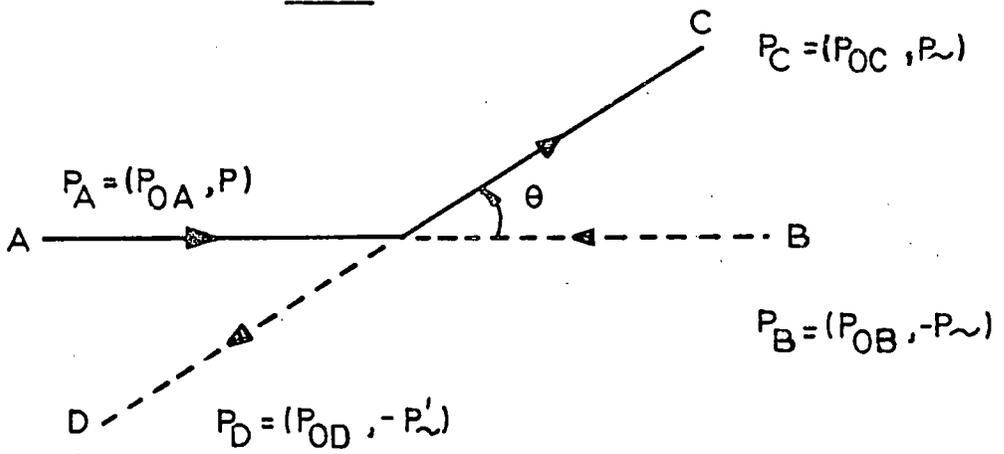
P_A

P_B

FIG 45

FIG 46

FIG 47

FIG 48